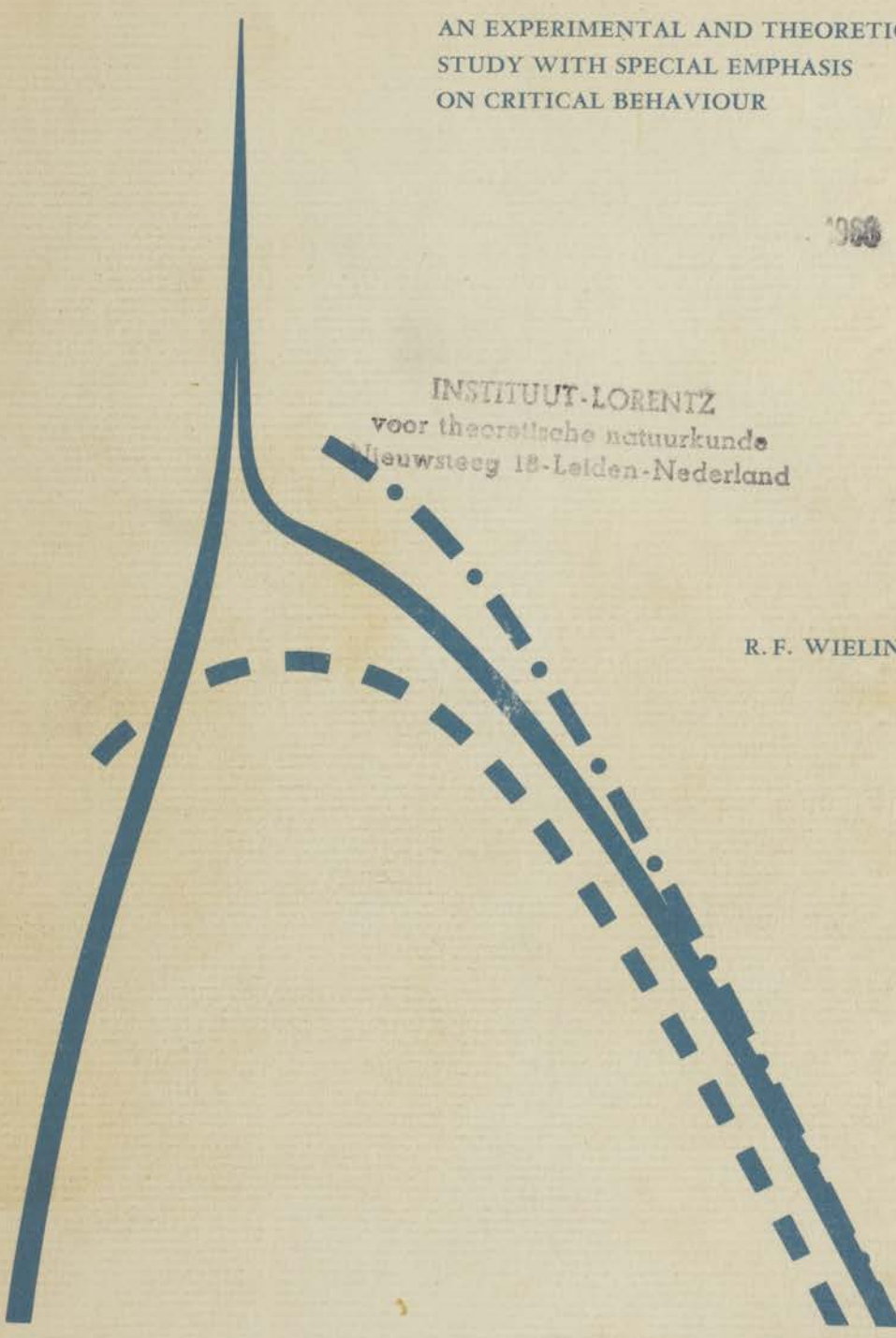


AN EXPERIMENTAL AND THEORETICAL  
STUDY WITH SPECIAL EMPHASIS  
ON CRITICAL BEHAVIOUR

1968

INSTITUUT-LORENTZ  
voor theoretische natuurkunde  
Nieuwsteeg 18-Leiden-Nederland

R. F. WIELINGA



CALORIC AND MAGNETIC INVESTIGATIONS  
NEAR 1 KELVIN

Universiteit Leiden



2 056 338 8

Bibliotheek  
Gorlaeus Laboratoria  
Universiteit Leiden  
Postbus 9502  
NL-2300 RA LEIDEN

16 OKT. 1968

# CALORIC AND MAGNETIC INVESTIGATIONS NEAR 1 KELVIN

AN EXPERIMENTAL AND THEORETICAL  
STUDY WITH SPECIAL EMPHASIS  
ON CRITICAL BEHAVIOUR

PROEFSCHRIFT

TER VERKRIJGING VAN DE GRAAD VAN DOCTOR IN  
DE WISKUNDE EN NATUURWETENSCHAPPEN AAN  
DE RIJKSUNIVERSITEIT TE LEIDEN, OP GEZAG VAN  
DE RECTOR MAGNIFICUS DR L. KUKENHEIM Ezn,  
HOGLERAAR IN DE FACULTEIT DER LETTEREN,  
TEN OVERSTAAN VAN EEN COMMISSIE UIT DE  
SENAAT TE VERDEDIGEN OP  
WOENSDAG 30 OKTOBER 1968 TE KLOKKE 15.15 UUR

door

**RIJNDER FOLKERT WIELINGA**

Geboren in 1940 te Palembang, Nederlands-Indië  
(thans Indonesië)

**INSTITUUT-LORENTZ**  
voor theoretische natuurkunde  
Nieuwsteeg 18-Leiden-Nederland

*kast dissertaties*

1968

Drukkerij J. H. Pasmans - 's-Gravenhage

Promotor: Prof. dr C.J. Gorter

Dit proefschrift is bewerkt  
onder toezicht van dr W.J. Huiskamp

This investigation is part of the research program of the  
"Stichting voor Fundamenteel Onderzoek der Materie (F.O.M.)",  
which is financially supported by the "Organisatie voor Zuiver  
Wetenschappelijk Onderzoek (Z.W.O.)".





## STELLINGEN

1. Het criterium, waarmee Friedberg de z.g. kritische temperatuur van een magnetische faseovergang bepaalt uit een afgeronde asymmetrische piek in de soortelijke-warmte curve, is aanvechtbaar.

S.A. Friedberg, *Phys.Rev.*164(1967)705.

2. De bewering van Sykes, Martin en Hunter, dat bij het vlak-gecentreerde rooster in het Ising model met spin  $\frac{1}{2}$  de theoretische soortelijke-warmte curve boven het overgangspunt, in het temperatuurgebied dat experimenteel toegankelijk is ( $T > 1,0001 T_c$ ), reeds voldoende nauwkeurig wordt beschreven door de eerste paar termen van de reeks in stijgende machten van  $J/kT$ , waarbij  $J$  de exchange constante voorstelt, is onjuist.

M.F.Sykes, J.L.Martin, en D.L.Hunter, *Proc.Phys.Soc.*91(1967)673. Dit proefschrift, hoofdstuk I.

3. De suggestie van Heller, dat de soortelijke warmte en de spontane magnetisatie van een magnetisch systeem in eenzelfde temperatuurgebied beneden het overgangspunt ( $1 - T/T_c < \epsilon$ , met b.v.  $\epsilon < 0,1$ ) zou kunnen worden beschreven door een functie van de vorm  $P(T) = A(1 - T/T_c)^a + B$ , heeft geen algemene geldigheid.

P.Heller, *Repts.Progr.Phys.* 30 dl. II(1967)791.  
Dit proefschrift, hoofdstuk I.

4. Het verdient aanbeveling theoretische resultaten voor modellen die een faseovergang beschrijven, te presenteren in een zodanige numerieke of gesloten vorm, dat zij getoetst kunnen worden aan experimentele resultaten over een ruim temperatuurgebied.

5. Het is van belang de soortelijke warmte van de dipolaire ferro-resp. antiferromagneet dysprosium ethylsulfaat en gadolinium trichloride hexahydraat niet alleen te meten als functie van de temperatuur, maar ook als functie van het magnetisch veld.

P.M.Levy, *Phys.Rev.* 170(1968)595.

D.T.Teaney, B.J.C. van der Hoeven Jr, en J.L.Moruzzi, *Phys.Rev.Letters* 20(1968)722.

B.E.Keen, D.P.Landau, B.Schneider en W.P.Wolf, *J.Appl.Phys.* 37(1966)1120.

6. Het ontwerp van een rotatiesymmetrische spoel, die bewikkeld wordt over een dikte die niet verwaarloosbaar is t.o.v. de straal, en die over een bepaalde afstand langs de as een homogeen veld levert, bevat minstens 4 parameters. Zelfs indien slechts één spoel wordt berekend is het efficiënter een tabel te ontwerpen, waarin slechts 2 parameters worden gevarieerd, en vervolgens de berekening uit te voeren in een klein, door inspectie gevonden, 4-parameter gebied, dan het probleem met brute-force op te lossen.

7. De geringe graad van circulaire polarisatie van gamma-straling uitgezonden na vangst van gepolariseerde neutronen in  $^{60}\text{Co}$ , zoals deze is gemeten door Kopecký, Kajfosz en Chalupa, is vermoedelijk te wijten aan depolarisatie-verschijnselen in het trefplaatje.

J.Kopecký, J.Kajfosz en B.Chalupa, *Nuclear Physics* 68(1965) 449.

8. Bij de berekening van de pompwerking van de supergeleidende dynamo door van Houwelingen en Volger is geen rekening gehouden met de wederkerige-inductie term.

D.van Houwelingen en J.Volger, *Philips Res.Repts.* 23(1968) 249.

9. Het is interessant de proeven over energie-dissipatie bij de stroming van superfluïde helium, zoals deze zijn verricht door van Alphen e.a. uit te breiden met verdere metingen aan een adiabatisch kanaal, bij welke metingen naast de geproduceerde hoeveelheid warmte ook de temperatuurgradient wordt gemeten in de richting van het kanaal.

W.M.van Alphen, J.F.Olijhoek, R.de Bruyn Ouboter en K.W. Taconis, *Physica* 32(1966)1901; R.de Bruyn Ouboter, K.W. Taconis en W.M.van Alphen, "Progress in Low Temperature Physics", dl. 5 p.76, red.C.J.Gorter, uitg. 'North-Holland Publ.Cy.'.

10. De bewering van Williams en Davies, dat de fout in de dynamische bepaling van de astronomische lengte-eenheid, zoals deze bepaling in 1950 door Rabe is gepubliceerd, onverklaard is gebleven, is onjuist.

E.Rabe, *Astron.J.*55(1950)112; E.Rabe, *Astron.J.*72(1967)852.  
D.Williams en R.D.Davies, *Monthly Notices of the Roy.Astron. Soc.* 140(1968)537.

11. Bij het uitvaardigen van een wet waarbij een recht wordt verleend, rust de verplichting op de wetgever middelen te verschaffen, die uitoefening van dit recht mogelijk maken.

Martin Luther King, "Chaos or Community" p.35, Hodder and Staughton, London 1968.

12. Vele moderne woonwijken zijn eerder ontworpen om naar te kijken, dan om in te wonen.

Godfried Bomans, "Pieter Bas", *Prisma*-reeks 20<sup>e</sup> druk (1967), p.173.

## Contents

INTRODUCTION AND SUMMARY	7
CHAPTER I	
THEORIES ON PHASE TRANSITIONS AND SOME APPLICATIONS	
1 Introduction and classification	11
2 Mean field theories	12
2.1 The Weiss molecular field	12
2.2 The Landau theory	14
3 Microscopic theories	15
3.1 The Hamiltonian	15
3.2 Series developments	17
3.3 The analysis of finite series	20
3.4 Check of the finite series analysis	23
3.5 Some numerical results on the specific heat, the susceptibility and the spontaneous magnetization	24
3.6 Some considerations on the rounding of specific heat curves of magnetic systems	35
References	40
CHAPTER II	
APPARATUS AND METHODS	
1 Introduction	42
2 The calorimeter	42
3 Temperature measurements and regulation	44
4 The heating circuit	47
5 Errors and calibration	48
References	50
CHAPTER III	
SPECIFIC HEAT SINGULARITIES OF THE ISING ANTIFERROMAGNETS $\text{CoCs}_3\text{Cl}_5$ AND $\text{CoCs}_3\text{Br}_5$	
1 Introduction	51
2 Crystal structure and paramagnetic resonance data	51
3 Experiment	54
4 Results	54
4.1 The determination of $T_N$	57
4.2 The critical behaviour	59
5 Discussion	61
5.1 $\text{CoCs}_3\text{Cl}_5$	61
5.2 $\text{CoCs}_3\text{Br}_5$	66
References	71

CHAPTER IV

EXPERIMENTAL STUDY OF THE BODY-CENTERED-CUBIC  
HEISENBERG FERROMAGNET

1	Introduction	72
2	Crystal structure	73
3	Experimental method	74
4	Heat capacity results	74
4.1	The singularity in $\text{CuK}_2\text{Cl}_4 \cdot 2\text{H}_2\text{O}$	76
4.2	The exchange constant	77
4.3	Comparison with spin-wave theory	78
5	Discussion	81
	References	84

CHAPTER V

THE SPONTANEOUS MAGNETIZATION OF THE B.C.C.  
HEISENBERG FERROMAGNET  $\text{Cu}(\text{NH}_4)_2\text{Br}_4 \cdot 2\text{H}_2\text{O}$

1	Introduction	85
2	Experimental method	86
3	The magnetization data	89
4	The anisotropy energy	91
5	The determination of the spontaneous magnetization and the critical temperature	95
6	Discussion	100
	References	107

CHAPTER VI

THE SPECIFIC HEAT OF TWO DIPOLAR ANTIFERROMAGNETS  
AND ONE FERROMAGNET BELOW 1 KELVIN

1	Introduction	109
2	Experimental method and determination of the critical temperature	112
3	Specific heat	112
3.1	Gadolinium sulphate octohydrate, $\text{Gd}_2(\text{SO}_4)_3 \cdot 8\text{H}_2\text{O}$	112
3.2	Gadolinium trichloride hexahydrate, $\text{GdCl}_3 \cdot 6\text{H}_2\text{O}$	116
3.3	Dysprosium ethylsulphate, $\text{Dy}(\text{C}_2\text{H}_5\text{SO}_4)_3 \cdot 9\text{H}_2\text{O}$	119
3.4	Singularities of the two gadolinium salts	122
4	Susceptibility	125
4.1	Gadolinium sulphate	125
4.2	Gadolinium trichloride	126
5	Summary and conclusions	128
	References	129

SAMENVATTING

131

CURRICULUM VITAE

135

## Introduction and summary

The subject of this thesis is the investigation of magnetic phase transitions in ionic crystals. From a theoretical point of view, ionic crystals belong to a relatively simple class of substances, a) because the interactions occur between *localized* spins, in contrast to the interactions between electrons in a metal or to the interactions between molecules in a liquid-gas transition, and b) because in those crystals in which exchange interactions predominate, the interaction is mainly confined to *nearest-neighbours*, which facilitates the calculations considerably.

From an experimental point of view, ionic crystals are attractive for the study of phase transitions, as a large number of magnetic substances can be prepared. Depending on the crystal structure, the interactions may occur in a predominantly one-dimensional structure (refs. 1 and 2; chapter VI dysprosium ethylsulphate), a two-dimensional structure (chapter III section 5.2,  $\text{CoCs}_3\text{Br}_5$ ; ref. 3), or a three-dimensional structure (numerous examples, see e.g. refs. 4 and 5;  $\text{CoCs}_3\text{Cl}_5$  in chapter III, and e.g.  $\text{CuK}_2\text{Cl}_4 \cdot 2\text{H}_2\text{O}$  in chapter IV).

The temperatures at which the experiments were performed lie in the region of 1 Kelvin. Thermal expansion effects in this temperature region are very small compared to the magnetic interactions, so that usually the magnetic phase transition is not accompanied by a latent heat production. Another advantage of performing experiments at very low temperatures is the small value of the lattice contribution to the specific heat, which can be easily estimated. The experimental equipment is described in chapter II.

In recent years considerable progress has been made in the theory of lattice statistics<sup>6,7</sup>). Accurate numerical predictions for a number of thermodynamic quantities have been obtained for the Ising  $s=1/2$  model, both below and above the critical temperature (see also chapter I section 3.5). The calculations for the Heisenberg model are far more difficult to perform, so that up to now relatively few predictions have been made for this model. For the long-range dipolar interaction, both theoretical and experimental results are scarce, so that much work remains to be done.

In chapter I a survey is given of phenomenological and microscopic theories on phase transitions. In particular we have considered the methods of analysis of finite series, derived e.g. for the susceptibility and specific heat. By means of a computer program based on the analysis of series by the ratio-method, we have obtained new closed-form expressions describing the temperature dependence of the quantity

considered in the whole temperature region above the critical point. With the help of these closed-form expressions, the experimental results can be compared with the theory in any desired temperature region. Chapter I ends with some considerations on the rounding of the specific heat curve observed in many crystals. Calculations based on a simple model using a Gaussian distribution of transition points indicate that the temperature at which the maximum of the specific heat curve occurs, does not coincide with the transition temperature in the case the specific heat curve is asymmetric.

In chapter III the measurements of the thermal properties of the crystals  $\text{CoCs}_3\text{Cl}_5$  ( $T_N = 0.527\text{K}$ ), and  $\text{CoCs}_3\text{Br}_5$  ( $T_N = 0.282\text{K}$ ) are analysed. From paramagnetic resonance and calorimetric data it is concluded that at very low temperatures  $\text{CoCs}_3\text{Cl}_5$  is a fair representative of the cubic  $s = \frac{1}{2}$  Ising system. The specific heat singularity is excellently described by the theoretical predictions for the cubic Ising model, if the transition temperature is chosen in conformity with the suggestions given in chapter I. The properties of  $\text{CoCs}_3\text{Br}_5$  are well described by a two-dimensional Ising model. Characteristic features are the large specific heat above  $T_N$ , which corresponds to an appreciable short-range ordering, and a logarithmic temperature dependence for the specific heat near the transition point.

In chapter IV specific heat measurements are reported for two isomorphous copper salts having a positive exchange interaction, viz.  $\text{CuK}_2\text{Cl}_4 \cdot 2\text{H}_2\text{O}$  ( $T_c = 0.88\text{K}$ ) and  $\text{Cu}(\text{NH}_4)_2\text{Br}_4 \cdot 2\text{H}_2\text{O}$  ( $T_c = 1.74\text{K}$ ). Earlier evidence on the first salt indicated that the three-dimensional  $s = \frac{1}{2}$  Heisenberg model was applicable<sup>8</sup>). In this chapter it is shown that the calorimetric measurements on  $\text{Cu}(\text{NH}_4)_2\text{Br}_4 \cdot 2\text{H}_2\text{O}$  are well described by spin-wave theory for temperatures up to  $0.5T_c$ , which confirms the applicability of the b.c.c. Heisenberg model. In the light of recent calculations on the extent to which the next-nearest neighbour (n.n.n.) interaction modifies the predictions made for nearest-neighbour (n.n.) coupling only, the data were reanalysed. For a b.c.c. structure we derive  $J_2/J_1 = +0.25 \pm 0.1$  for the ratio of the n.n.n. to n.n. exchange coupling, indicating that small n.n.n. interactions are present. The specific heat singularity was measured for  $\text{CuK}_2\text{Cl}_4 \cdot 2\text{H}_2\text{O}$  as close to  $T_c$  as  $|1 - T/T_c| = 10^{-3}T_c$ . A logarithmic temperature dependence was found of equal amplitude for temperatures above and below  $T_c$ .

Measurements on the spontaneous magnetization of the Heisenberg  $s = \frac{1}{2}$  b.c.c. ferromagnet  $\text{Cu}(\text{NH}_4)_2\text{Br}_4 \cdot 2\text{H}_2\text{O}$ , performed in the temperature region  $0.05 < T/T_c < 0.997$  are reported in chapter V. A small anisotropy energy persisting even above  $T_c$  is observed. In view of the strong spin-spin correlation it is interpreted in terms of slightly

anisotropic exchange coupling between pairs of copper ions. The experimental data up to  $T/T_c=0.7$  are well described by spin-wave theory. Recent Green's functions calculations fit the data up to  $T/T_c=0.98$ . Close to the critical temperature,  $3 \cdot 10^{-3} < 1 - T/T_c < 10^{-1}$ , the spontaneous magnetization is described by the relation  $M(T)/M(0) = 1.33(1 - T/T_c)^{0.38}$ . The behaviour of the critical isotherm is described by  $H \sim M^\delta$ , where  $\delta$  has the fairly low value: 3.9.

Finally, in chapter VI specific heat and susceptibility measurements are reported of three dipolar salts. Gadolinium sulphate octohydrate  $Gd_2(SO_4)_3 \cdot 8H_2O$ , and gadolinium trichloride hexahydrate  $GdCl_3 \cdot 6H_2O$  become antiferromagnetic at  $T_N=0.182$  and  $0.185K$ , respectively. Dysprosium ethylsulphate,  $Dy(C_2H_5SO_4)_3 \cdot 9H_2O$ , becomes ferromagnetic at  $T_c=0.115K$ . The relatively high specific heat of the first two salts is related to the population of the low-lying crystalline field doublets. The behaviour of dysprosium ethylsulphate may be described approximately by a linear-chain interaction. In the three salts the onset of long-range order is very abrupt, which is illustrated best by the gadolinium salts. Another remarkable feature of the experimental result is the hunch closely above the critical temperature, which may be described by negative terms (in  $T^{-3}$  or in higher order of the inverse temperature) in the series development of the high-temperature specific heat.

Summarizing, it may be concluded that the extension of the well-known techniques of calorimetry and magnetization measurements to temperatures lower than 1 Kelvin has yielded experimental data, which can be compared directly to numerical results of recent theoretical work. Such a comparison is fruitful if the magnetic compounds are carefully chosen with respect to the applicability of theoretical models of magnetic interactions.

### References

1. HASEDA, T. and MIEDEMA, A.R., *Physica* 27(1961)1102.
2. WITTEKOEK, S., Thesis, Leiden, 1967.
3. BREED, D.J., *Physica* 37(1967)35.
4. KADANOFF, L.P., GÖTZE, W., HAMBLEN, D., HECHT, R., LEWIS, E.A.S., PALCIAUSKAS, V.V., RAYL, M., SWIFT, J., ASPNES, D., and KANE, J., *Rev. Mod. Phys.*, 39(1967)395.
5. HELLER, P., *Rep. Progr. Phys.* 30, pt. II(1967)790.
6. DOMB, C., 'Magnetism' vol. IIA ch. I, eds. RADO, G.T. and SUHL, H., Ac. Press New-York and London 1965.
7. FISHER, M.E., 'The theory of equilibrium critical phenomena', *Rep. Progr. Phys.* 30, pt. II(1967)615.
8. MIEDEMA, A.R., VAN KEMPEN, H., and HUISKAMP, W.J., *Physica* 29(1963) 1266; *Commun. of the Kamerlingh Onnes Lab.*, No. 336a.



## Chapter I

## THEORIES ON PHASE TRANSITIONS AND SOME APPLICATIONS

## 1 Introduction and classification

An interesting subject of experimental and theoretical physics is formed by the phenomena of phase transitions. If the temperature or another suitable thermodynamic parameter is varied, the difference between the phases often vanishes at a certain *critical point*, beyond which only one equilibrium phase exists. The following examples may be mentioned: 1) the point that terminates the coexistence curve of a liquid and its vapour characterized by a critical pressure, density and temperature,  $p_c$ ,  $\rho_c$  and  $T_c$ ; 2) the critical temperature of a binary metallic alloy, above which the components mix homogeneously in any proportion; 3) the Curie-point of a ferromagnetic crystal above which the spontaneous magnetization vanishes; 4) the lambda point of liquid  $^4\text{He}$ , below which part of the fluid shows superfluidity; 5) the critical point in a superconductor, below which the electrical resistance vanishes.

If the phases on both sides of a transition point are thermodynamically stable, the corresponding phase transition can formally be classified by means of the Gibbs free energy function. If e.g. the first derivative of this function with respect to one of the usual thermodynamic variables changes discontinuously at the critical point, the transition is called *first-order*. The phenomena of boiling and melting e.g. are first-order transitions.

A discontinuity in the specific heat,  $c_v$ , of  $^4\text{He}$  at the critical point, called lambda-point, was observed by Keesom and Keesom<sup>1)</sup>. In view of this experimental result Ehrenfest<sup>2)</sup> introduced the class of *second-order* transitions, defined by the existence of a discontinuous change of a second derivative of the Gibbs free energy function at the critical point.

However, more precise measurements, closer to  $T_c$ , performed by Buckingham and Fairbank<sup>3)</sup> and Kellers<sup>4)</sup>, indicate that the specific heat of liquid  $^4\text{He}$  close to  $T_c$  diverges to infinity logarithmically on both sides, so that one should not speak of a discontinuity in the specific heat. In view of the temperature resolution experimentally obtainable, the only transitions that can be classified as a second order transition are those of a superconductor from the superconducting or superconducting-mixed state to the normal state.

However, transitions characterized by logarithmic or power-law

singularities in the behaviour of some thermodynamic variable as a function of another suitable variable can be classified in the scheme of Ehrenfest. This has recently been done by Gorter<sup>5)</sup> for a class of transitions involving logarithmic singularities. The scheme proposed by Gorter may be extended so that it includes power-law singularities as well.

In a phase-transition a very large number of particles cooperate. Macroscopically observable quantities such as pressure and magnetization as a function of the temperature must therefore be derived by means of statistical mechanics. Since the particles interact, the system is essentially a many-body system. An exact solution for such a system is notoriously difficult, even if the simplest interaction is assumed and the positions are fixed on a lattice.

Two methods of tackling this problem will be briefly described. The first method assuming that on each particle a mean field is acting will be used in various theories, called mean-field theories. In the second approach a Hamiltonian for the interaction is assumed and the macroscopic observables are calculated exactly or approximately in the framework of statistical thermodynamics. Several exact results have been derived (see section 3.4). These results can furthermore be used as a check on approximation techniques used for problems defying an exact solution. Results obtained with the second method show that the mean-field theories become the more realistic, the larger the range of interaction<sup>6,7)</sup>.

## 2 Mean field theories

In this section we shall summarily describe the molecular field theory and Landau's phenomenological theory of second order phase transitions. By grouping both theories together we emphasize their common assumption of the existence of a mean-field acting on the constituent parts of the system. The theory of Landau in the form sketched below, however, can be extended by introducing a term describing the fluctuations. We omit the description of the Van der Waals theory of condensation because this theory involves the same essential approximation as the molecular field theory.

### 2.1 The Weiss molecular field

A coherent qualitatively correct description of the magnetic properties of a ferromagnetic substance is furnished by the molecular field model. The essential features are shown in the derivation of the expression of the magnetization as a function of the temperature, the internal field and the interaction between the spins.

Let us consider a system of spins for this purpose, each spin  $i$  having two orientations, denoted by  $\mu_i = +1$  or  $-1$  respectively, and an interaction energy  $-v_{ij} \mu_i \mu_j$  with spin  $j$ . If  $H$  denotes the applied field, expressed in units of energy and  $H_i$  the field acting on spin  $i$ , we may write

$$H_i = \sum_j v_{ij} \mu_j + H, \quad (1)$$

The average magnetization is given by

$$\langle \mu_i \rangle = \frac{\text{Tr } \mu_i \exp(\beta \mu_i H_i)}{\text{Tr } \exp(\beta \mu_i H_i)}. \quad (2)$$

The molecular field approximation consists in assuming that the field acting on each ion is the same. Formula (2) is accordingly simplified to

$$\langle \mu_i \rangle = \frac{\text{Tr } \mu_i \exp(\beta \mu_i \langle H_i \rangle)}{\text{Tr } \exp(\beta \mu_i \langle H_i \rangle)}, \quad (3)$$

which takes the simple form

$$\langle \mu_i \rangle = \frac{\exp(\beta \langle H_i \rangle) - \exp(-\beta \langle H_i \rangle)}{\exp(\beta \langle H_i \rangle) + \exp(-\beta \langle H_i \rangle)} \quad (4)$$

for  $\mu_i = +1$  or  $-1$ .

With the help of eq.(1) the molecular field may be denoted by

$$\langle H_i \rangle = v(0) \langle \mu_j \rangle + H.$$

Using this notation eq.(4) is given by

$$\langle \mu_i \rangle = \tanh [\beta(v(0) \langle \mu_i \rangle + H)]. \quad (5)$$

For  $H = 0$ , a solution  $\langle \mu_i \rangle = 0$  is found for every value of  $v(0)$ . A non-trivial solution is only found, if  $\beta v(0) > 1$ . In this case a solution is also formed by  $-\langle \mu_i \rangle$ . If  $\beta v(0) > 1$  the only solution is  $\langle \mu_i \rangle = 0$ . The temperature defined by the relation  $1/\beta (\equiv kT) = v(0)$  may therefore be called the critical temperature.

Other properties such as entropy and specific heat according to this simple model of ferromagnetism may also be easily derived.

## 2.2 The Landau theory

An elegant formalism describing the essential features of a second-order phase transition is given by Landau<sup>8)</sup>. The Gibbs free energy function,  $G$ , containing all macroscopic information is used as a starting point. The central assumption of the theory is, that below the critical point an order parameter may be defined that is non-zero, but vanishes at the critical point. Secondly it is assumed that the Gibbs function near  $T_c$  may be developed into a double Taylor series of the order parameter and  $\Delta T = T - T_c$ . If furthermore fluctuations are neglected, we may write the Gibbs free energy in the form

$$G(T, M) = G(T_c, 0) + c(T)M^2 + e(T)M^4 + \dots, \quad (6)$$

where

$$c(T) = c_0 + c_1 \Delta T + c_2 (\Delta T)^2 + \dots, \quad (7)$$

and

$$e(T) = e_0 + e_1 \Delta T + e_2 (\Delta T)^2 + \dots. \quad (8)$$

By symmetry odd powers in  $M$  vanish. Noting that

$$H = \left( \frac{\partial G}{\partial M} \right)_T, \text{ and } \frac{1}{\chi} = \left( \frac{\partial H}{\partial M} \right)_T,$$

we obtain

$$H = 2 c(T)M + 4 e(T)M^3 + \dots, \quad (9)$$

and

$$\frac{1}{\chi} = 2 c(T) + 12 e(T)M^2 + \dots. \quad (10)$$

Since  $1/\chi \rightarrow 0$ , if  $T \rightarrow T_c$  and  $M = 0$ , the coefficient  $c_0$  from eq.(7) equals zero. Substituting  $e(T)$  from eq.(8) into eq.(10) and neglecting terms of higher order than  $\Delta T$  and  $M^2$  we derive

$$\frac{1}{\chi} \approx \frac{1/2 c_1}{T - T_c + 6(e_0/c_1)M^2}. \quad (11)$$

According to relation (9),  $M = 0$  in zero field, so that (11) reduces to

the Curie-Weiss law in this case. Below  $T_c$  and in zero field, eq.(9) has two thermodynamically stable solutions, namely

$$M_0^2 \approx \frac{c_1}{2e_0} (T_c - T). \quad (12)$$

Besides, we see from (9) that the critical isotherm has the simple form

$$H \approx 4e_0 M^3.$$

It is also an easy matter to calculate the discontinuity in the specific heat at  $T_c$  in this model.

### 3 Microscopic theories

In the first part of the preceding section statistical mechanical methods have been explicitly used for the calculation of macroscopic quantities. At the very beginning, however, a drastic simplification has been made, namely the assumption that fluctuations are absent, the consequence of which cannot be assessed beforehand. A more rigorous treatment of the interactions would reveal the nature of the simplifications involved in the mean-field theory. Up to this time an exact statistical mechanical derivation of the macroscopic quantities has only been obtained for a few types of interaction hamiltonians. As an example we mention the exact solution for the two-dimensional Ising model in zero field, obtained by Onsager. The specific heat in this model tends to infinity, if the temperature approaches the critical temperature. This result is in violent disagreement with the molecular-field prediction of a finite specific heat below and a zero-specific heat above the critical temperature.

In the following subsections we shall briefly describe some methods to obtain approximate predictions of macroscopic quantities. The approximations will consist in the calculation (and asymptotic analysis) of only a finite number of terms in a series development for the quantity investigated.

#### 3.1 The Hamiltonian

The static dipolar interaction between two spins — although best known theoretically — cannot account for the magnitude of most magnetic interactions. Since the range of interaction is infinite and the directional dependence is quite complicated, this Hamiltonian has thus far not been considered as a basis for theories on phase transitions. Recently, however, calculations of the magnetic susceptibil-

ity at high temperatures have been performed with the use of the spherical model<sup>10</sup>). In this model the interaction energy between the sites  $i$  and  $j$  varies in proportion to  $1/r^{d+\sigma}$ , where  $r$  denotes the distance between the sites  $i$  and  $j$ ,  $d$  the dimension of the lattice and  $\sigma$  a positive constant. In this model the exponent,  $\gamma$ , of the singularity in the susceptibility near and above  $T_c$ , defined by the relation

$$\frac{\chi T_c}{C} \simeq \left(1 - \frac{T_c}{T}\right)^{-\gamma} \quad (14)$$

takes the molecular-field) value 1 for  $0 < \sigma < 3/2$ , and the values  $\sigma(3 - \sigma)$  for  $3/2 < \sigma < 2$ , and 2 for  $\sigma > 2$ .

The Hamiltonian that has proved to be most successful in describing phenomena related to magnetic ordering, especially in insulators, is

$$H = -2J \sum_{\substack{i,j \\ i < j}} \mathbf{s}_i \cdot \mathbf{s}_j - g \mu_B H \sum_i s_{iz} \quad (15)$$

where  $J$  is a constant,  $\mathbf{s}_i$  and  $\mathbf{s}_j$  are spin operators. The summation is taken over all pairs of nearest-neighbours. This spin-dependent interaction is called *exchange* interaction, since historically, this expression originates from the direct exchange of two electrons<sup>11,12,13,14</sup>,  $J$  being the exchange integral. The expression (15) is commonly called the *Heisenberg* Hamiltonian.

The observation of the occurrence of exchange interaction between magnetic ions surrounded by a group of diamagnetic ions led Kramers<sup>15</sup> to the idea of *superexchange*. Slater<sup>16</sup>), however, pointed out that generally the derivation of (15) was not valid in solids. For the case that the electron orbitals are only slightly non-orthogonal, Herring<sup>17</sup>) has recently derived (15). Another recent development in the field was the presentation by Anderson<sup>18</sup>) of a new theory of superexchange. This theory could explain why most exchange interactions were of the antiferromagnetic type ( $J < 0$ ).

In view of the theoretical justification of (15) for real solids, a thorough statistical mechanical derivation of its properties is very attractive. However, since the spin operators do not commute, the calculations are rather difficult. If only one component of the spins in (15) is supposed to interact with that of another spin, a substantial simplification of the calculations will result, since in this case the spin operators commute. This Hamiltonian has the form

$$H = -2J \sum_{\substack{i,j \\ i < j}} s_{iz} s_{jz} - g \mu_B H \sum_i s_{iz} \quad (16a)$$

and is called after Ising<sup>19</sup>). An alternative form of this Hamiltonian, yielding the same maximum internal energy and magnetization, independent of  $s$ , for a given value of  $J'$  and  $g\mu_B H$ , is

$$H = -\frac{J'}{s^2} \sum_{\substack{i,j \\ i < j}} s_{iz} s_{jz} - \frac{g\mu_B H}{s} \sum s_{iz}. \quad (16b)$$

From the definitions (16a) and (16b) it follows that  $J' = 2Js^2$ . For a  $s = \frac{1}{2}$  system, therefore,  $J' = \frac{1}{2}J$ . The Ising interaction might be regarded as realistic for those cases in which axial spin orientation is strongly preferred. This phenomenon may occur in a solid, if for example, the lowest level is twofold degenerate with very anisotropic  $g$  values that favour orientation along an axis ( $g_{\parallel} \gg g_{\perp}$ ).

By using the Heisenberg and Ising Hamiltonians, a wealth of results has been obtained in the last few decades, notably by the London group<sup>20</sup>.

An interesting practical extension of (15) is formed by the model taking account of *next-nearest-neighbour* interaction. Some results for three-dimensional lattices have been obtained<sup>21</sup>), which agree very well with the experiment<sup>21</sup>). Another model of practical interest is found by a type of interaction intermediate to (15) and (16) which might be called the *anisotropic Heisenberg model*. A few results have recently been obtained<sup>22</sup>) viz. the variation of the critical temperature, as a function of the anisotropy parameter and the value of  $\gamma$  as a function of this parameter.

The properties of the models using the Hamiltonians (15) and especially (16) have furthermore been calculated as a function of the variation of the parameters spin quantum number<sup>23</sup>), dimensionality<sup>24</sup>) and coordination number<sup>25</sup>). If the dimension or the coordination number increases, the results approach those of the molecular field model, as might have been anticipated.

We conclude this section on Hamiltonians and models (which is not exhaustive) by mentioning the Heisenberg model in the limit of infinite spin, called the *classical Heisenberg model*. In the limit of infinite spin, the spin may be considered as a classical vector of length  $[s(s+1)]^{1/2}$ , so that the calculations are simplified considerably. Various properties have been derived<sup>25,26</sup>), some of which will be more fully analysed in section 3.5.

### 3.2 Series developments

In this section we shall give an example of the way in which the partition function,  $Z_N$ , for a canonical ensemble may be expressed in

the form of a series development in a parameter, which depends on the temperature region considered. We specialize to the simplest case, e.g. the Ising model with spin  $\frac{1}{2}$ , the method being quite general. We shall firstly consider the low-temperature region, in which the deviations from the fully ordered state are small. Secondly we consider the high-temperature region, in which the exchange energy is small compared to the thermal energy.

a) *Low-temperature expansions*

For the Ising model with  $s = \frac{1}{2}$  in zero field, the partition function may be written in the form

$$Z_N = 2 \sum g(N, N_{++}, N_{--}, N_{+-}) \exp [K(N_{++} + N_{--} - N_{+-})], \quad (17)$$

where  $N$  is the total number of spins considered,  $N_{++}$ ,  $N_{--}$ ,  $N_{+-}$ , the number of pairs of spins having spins up, spins down, and spins antiparallel respectively,  $K$  stands for  $\frac{1}{2}J/kT$ , and  $g$  is the combinatorial factor counting the numbers  $N_{++}$ ,  $N_{+-}$ ,  $N_{--}$  that can be formed in a lattice of  $N$  sites and  $q$  nearest-neighbours for each site (the lattice must be closed in itself for this situation to occur). One easily verifies that the relation

$$N_{++} + N_{+-} + N_{--} = \frac{1}{2}qN \quad (18)$$

holds. Expression (17) may now be written in the form

$$\begin{aligned} Z_N &= 2 \sum_{N_{+-}=0}^{\frac{1}{2}qN} g(N, N_{+-}) \exp [K(\frac{1}{2}qN - 2N_{+-})], \\ &= 2 [\exp(\frac{1}{2}qNK)] \sum_{N_{+-}=0}^{\frac{1}{2}qN} g(N, N_{+-}) [\exp(-2K)]^{N_{+-}}, \quad (19) \end{aligned}$$

which may be compactly written as

$$Z_N = 2 [\exp(\frac{1}{2}qNK)] \sum_{n=0}^{\frac{1}{2}qN} a_n(q) z^n. \quad (20)$$

The coefficients  $a_n(q)$  contain the information of the lattice and can be evaluated in principle by counting procedures. The first two non-zero coefficients in the expansion (20) may be easily evaluated as 1 and  $N$  respectively. Each successive term in the calculation is exact. The approximation made, when using the development, only

consists in the evaluation of the asymptotic behaviour of the coefficients.

*b) High-temperature expansions*

The partition function for an ensemble of  $N$  particles with a Hamiltonian  $H$  may be compactly written in the form

$$Z_N(\beta) = \langle \exp(-\beta H) \rangle, \quad (21)$$

where  $\langle \rangle$  denotes the trace taken with respect to a set of  $(2s + 1)^N$  orthonormal states, spanning the space of  $H$ , and  $\beta$  denoting  $1/kT$ . In the high-temperature limit  $Z_N(\beta)$  can be developed in powers of  $\beta$  according to

$$Z_N(\beta) = 1 - \beta \langle H \rangle + \frac{\beta^2}{2!} \langle H^2 \rangle + \dots \frac{(-\beta)^r}{r!} \langle H^r \rangle + \dots, \quad (22)$$

where the coefficient of  $\beta^r$  will be a polynomial of order  $r$  in  $N$ . In order to evaluate  $\langle H^r \rangle$ , basically two calculations have to be performed. The first, a combinatorial problem, involves the grouping of the various contributions according to the type of graph, and counting the number of independent graphs of each type for the lattice considered. The second consists in the calculation of the mean value of the spin operators for the particular type of graph.

In this section we take the Ising model with spin in zero field as an example. Denoting the spin variables by  $\sigma_i, \sigma_j$ , which take the values  $\pm 1$ , and denoting  $\frac{1}{2} \beta J$  by  $K$ , the partition function for  $N$  particles takes the form

$$Z_N(\beta) = \sum_{\sigma_i, \sigma_j = \pm 1} \exp(K \sum_{\langle ij \rangle} \sigma_i \sigma_j), \quad (23)$$

where  $\langle ij \rangle$  denotes a summation over nearest-neighbours  $i$  and  $j$ . Since the spin variables commute, we may write the summation as a product

$$Z_N(\beta) = \sum_{\sigma_i, \sigma_j = \pm 1} \prod_{\langle ij \rangle} \exp(K \sigma_i \sigma_j). \quad (24)$$

Noting that the  $\sigma_i \sigma_j$  satisfy the relation

$$(\sigma_i \sigma_j)^2 = (\sigma_i \sigma_j)^4 = \dots = 1, \text{ and } (\sigma_i \sigma_j) = (\sigma_i \sigma_j)^3 = (\sigma_i \sigma_j)^5 = \dots,$$

the exponential may be written in the form

$$\begin{aligned}
 \exp(K\sigma_i\sigma_j) &= 1 + K\sigma_i\sigma_j + \frac{K^2}{2!}(\sigma_i\sigma_j)^2 + \dots \\
 &= \cosh K + \sigma_i\sigma_j \sinh K \\
 &= (\cosh K)(1 + \sigma_i\sigma_j \tanh K),
 \end{aligned} \tag{25}$$

so that eq.(24) becomes

$$Z_N(\beta) = \sum_{\sigma_i, \sigma_j = \pm 1} \prod_{\langle ij \rangle} (\cosh K)(1 + \sigma_i\sigma_j \tanh K). \tag{26}$$

The product may be expanded<sup>27)</sup>, so that eq.(26) takes the form

$$\begin{aligned}
 Z_N(\beta) &= (\cosh K)^{\frac{1}{2}qN} \sum_{\sigma_i, \sigma_j = \pm 1} [1 + (\tanh K) \sum_{\langle ij \rangle} \sigma_i\sigma_j + \\
 &\quad + (\tanh K)^2 \sum_{\langle ij \rangle \neq \langle kl \rangle} \sum \sigma_i\sigma_j\sigma_k\sigma_l + \dots],
 \end{aligned} \tag{27}$$

where  $\frac{1}{2}qN$  is the total number of nearest-neighbour pairs, and where the summations are taken over non-identical neighbouring pairs. Equation (27) may be written compactly in the form

$$Z_N(\beta) = [2(\cosh K)^{\frac{1}{2}q}]^N \sum_{r=0}^{\infty} b_r (\tanh K)^r, \tag{28}$$

where the coefficients  $b_r$ , which denote the combinatorial factors defined by eq.(27), contain the information of the lattice structure.

### 3.3 The analysis of finite series

The series derived by the methods indicated in the previous sections are necessarily truncated, as the labour involved in deriving each successive term roughly increases exponentially fast.

Within the radius of convergence an (infinite) power series

$$F(z) = \sum_{n=0}^{\infty} a_n z^n,$$

where  $z$  denotes a complex variable, is bounded. The power series diverges for certain  $z$  on the radius of convergence, called *singular points*. The singular point lying closest to the origin is called *dominant singular point*,  $z_0$ . In general the physical domain of  $z$  is the positive real axis. The series may now be divided into two classes:

- 1) that in which  $z_0$  lies on the positive real axis. This case will occur, if all  $a_n$ 's are positive. This class of functions can be simply analysed by the *ratio-method* (see below).

- 2) that in which  $z_0$  can be written as  $z_0 = r_0 \exp(i\theta_0)$ , with  $r_0$  real and positive, and  $\theta_0$  real and unequal to zero. A series belonging to this class cannot be analysed by the ratio method, since the magnitudes and signs of the coefficients are quite irregular. The *Padé-approximant* method, to be discussed in section 3.3.2, however, is suited for this class of series. Moreover, weaker singularities (lying farther from the origin) on the positive real axis can also be analysed. The only drawback of this method is that rigorous knowledge of the convergence of the Padé-approximants to the function  $F(z)$  is not complete<sup>28)</sup>.

### 3.3.1 The ratio-method

This method of determining the critical point and singular behaviour near the critical point stems from the following considerations. Let  $F(z)$  be a function of the form

$$F(z) = A(z)(1 - \mu z)^{-(1+g)}, \quad (29)$$

where  $A(z)$  is a smoothly varying function of  $z$  for  $z$  near  $z_{c-} = 1/\mu$ , and  $g > -1$ . The order,  $\lambda$ , of the singularity of  $F(z)$  for  $z \rightarrow z_{c-}$  defined by

$$\lambda \equiv \lim_{z \rightarrow z_{c-}} \left[ \frac{\ln F(z)}{\ln(1 - \mu z)} \right], \quad (30)$$

has the value  $\lambda = -(1+g)$ . If  $A(z)$  is a function that diverges logarithmically to some power  $\alpha \neq 0$ , for  $z \rightarrow z_{c-} = 1/\mu$ , according to

$$A(z) = [\ln(1 - \mu z)]^\alpha, \quad (31)$$

the order of the singularity of  $F(z)$  has still the value  $-(1+g)$  according to the definition (30).

For  $|z| < |z_c|$  the function  $F(z)/A(z)$  may be developed around  $z$  according to the binomial expansion

$$\frac{F(z)}{A(z)} = 1 + (1+g)\mu z + \frac{(1+g)(2+g)}{2!} \mu^2 z^2 + \frac{(1+g)(2+g)(3+g)}{3!} \mu^3 z^3 + \dots, \quad (32)$$

which may equivalently be noted as

$$\frac{F(z)}{A(z)} = \sum_{n=0}^{\infty} a_n z^n. \quad (33)$$

From eqs.(32) and (33) it is easy to see that the ratio of successive coefficients, to be denoted as  $\mu_n$ , is given by

$$\mu_n \equiv \frac{\alpha_n}{\alpha_{n-1}} = (1 + \frac{g}{n})\mu. \quad (34)$$

If the plot of  $\mu_n$  as a function of  $1/n$  is linear for large  $n$ , we can obtain  $\mu = 1/z_c$  from the intersection of this line with the axis  $1/n = 0$ , while the slope yields us the value of  $g$ . This procedure is commonly called the *ratio-method*.

In the limit  $n \rightarrow \infty$  a factor  $A(z)$  of the form shown in eq.(31) does not alter the convergence. Even for  $n$  in the order of 10, however, such a factor may alter the behaviour of the  $\mu_n$ 's significantly, especially, if  $(1+g) \simeq 0$ . In this case even a slowly varying function of the temperature, like  $A(z) = z^2$ , influences the  $\mu_n$ 's appreciably. Most of the series of section 3.5.2, however, have  $1+g \gg 0$ , so that the convergence may be determined from the available number of terms, even if slowly varying functions of temperature,  $A(z)$ , are considered.

### 3.3.2 The Padé-approximant method

Expansions having a dominant singularity off the real axis can be analytically continued by means of Padé-approximants<sup>30,31)</sup> beyond the circle of convergence up to the physical singularity on the real axis. Therefore, this method can also be used for the analysis of finite series in those cases, where the ratio-method fails.

We are interested in the series of the form

$$F(x) = 1 + \alpha_1 x + \alpha_2 x^2 + \dots + \alpha_n x^n + \dots, \quad (35)$$

of which only the first  $n$  coefficients are known. Let us consider the ratio of polynomials  $P(x)/Q(x)$

$$\frac{P(x)}{Q(x)} = \frac{1 + \alpha_1 x + \dots + \alpha_N x^N}{1 + \beta_1 x + \dots + \beta_D x^D}. \quad (36)$$

For  $N+D = k \leq n$ , the coefficients  $\alpha_1, \dots, \alpha_N$  and  $\beta_1, \dots, \beta_D$  are uniquely determined by the requirement that the series expansion of (36) shall coincide with (35) for the first  $k$  coefficients. Relation (36) is called  $[D, N]$  Padé-approximant to the function  $F(x)$ . For  $N+D \leq n$  the coefficients  $\alpha_1, \dots, \alpha_N, \beta_1, \dots, \beta_D$ , are determined by equating like powers of  $x$  in the following equations:

$$F(x) \cdot Q(x) - P(x) = O(x^{N+D+1}). \quad (37)$$

The Padé-approximant is particularly suitable for the representation of functions, whose only singularities are simple poles. These can be located as the  $D$  zeros of  $Q(x)$ . If we expect the singularity of  $F(x)$  to be of the type

$$F(x) \sim A/(x - x_c)^p, \quad (38)$$

where  $\sim$  stands for: asymptotically proportional to, and  $p$  and  $x_c$  are positive constants, the logarithmic derivative of  $F(x)$ ,

$$(d/dx) \ln F(x) \sim -p/(x - x_c), \quad (39)$$

will have a simple pole at  $x_c$  with residue  $-p$ . By the following procedure the value of  $A$  may be determined. If  $p$  is known, the Padé-approximants to

$$[F(x)]^{1/p} \sim A^{1/p}/(x - x_c), \quad (40)$$

having a simple pole at  $x_c$ , will yield us both  $x_c$  and  $A$ .

Summarizing, the Padé-approximant method consists of inspecting the convergence of the tabulated values of the critical quantities found by means of the successive approximants  $[D, N]$  (with  $D + N \leq n$ ) to the function  $F(x) = 1 + \sum_{i=1}^n \alpha x^i$ .

### 3.4 Check of the finite series analysis

The results obtained by applying the methods given in sections 3.3.1 and 3.3.2 to the high-temperature series found by (3.2) may be checked in several ways. Many numerical results show that the results obtained by both procedures are consistent<sup>28,31)</sup>. In this section we shall restrict ourselves to two special examples.

a) *A comparison with some exact results.* In the Ising model Kramers and Wannier<sup>32)</sup> derived the exact value of the transition temperature for a quadratic lattice, namely

$$v_c = \tanh(J/k T_c) = \sqrt{2} - 1 = 0.4142135 \dots$$

A second exact result for this lattice, viz.  $\gamma = 7/4$  may be obtained by applying an exact argument<sup>28)</sup> to Onsagers result<sup>9)</sup>. By forming the  $[7,7]$  Padé-approximant to the susceptibility series for the qua-

dratic lattice<sup>33)</sup>, Baker<sup>31)</sup> obtained the values  $v_c = 0.4142106$  and  $\gamma = 1.7496$ , respectively.

For the triangular lattice the transition temperature in the Ising model has been derived by Houtappel<sup>34)</sup> and has the value

$$1/v_c = 3.73205 \dots$$

On using the ratio-method, Domb and Sykes<sup>33)</sup> obtained the value  $3.731 \pm 0.002$ . This agrees remarkably well with the exact value.

b) *A comparison of critical temperatures derived from series for two physical quantities*

An internal check of the procedures used can be found in certain cases. We mention the determination of  $J/kT_c$  for the spin- $\frac{1}{2}$  Ising model in three dimensions. Baker<sup>30)</sup> has applied the Padé-approximant technique to the susceptibility series<sup>33)</sup> and the series for the spontaneous magnetization<sup>33,30)</sup> for the three cubic lattices. Expressing the critical temperature by the parameter  $u_c = \exp(-4J/kT_c)$ , the results for both series,  $u_c^X$  and  $u_c^m$ , as given by the highest approximants available, are:

$$\text{f.c.c. : } u_c^X = 0.664658, u_c^m = 0.6637;$$

$$\text{b.c.c. : } u_c^X = 0.53266, u_c^m = 0.5316;$$

$$\text{s.c. : } u_c^X = 0.41194, u_c^m = 0.4109.$$

One may notice that the results agree within a few parts of  $10^{-3}$ . It may further be mentioned that the most precise results, viz. those obtained for  $u_c^X$ , agree within the quoted error with the results found by Domb and Sykes<sup>33)</sup> using the ratio-method.

### 3.5 Some numerical results on the specific heat, the susceptibility and the spontaneous magnetization

In the sections 3.5.1 and 3.5.2 we shall present some new results obtained from finite series given in the literature, by a method related to the ratio-method. The idea<sup>35)</sup> is the following. Let us assume that the series

$$F(x) = \sum_{i=0}^n a_i x^i + a_{n+1} x^{n+1} + \dots, \quad (41)$$

of which only the first  $n$  coefficients are known, has an asymptotic behaviour described by

$$F(x) \sim A(1 - \mu x)^{-\alpha}, \quad (42)$$

where  $\alpha$  is a positive constant. If  $\alpha$  and  $\mu \equiv 1/x_c$  are known, the function  $(1-\mu x)^{-\alpha}$  can be expanded (see eq.(32)) in powers of  $x$  according to

$$(1-\mu x)^{-\alpha} = \sum_{i=0}^{\infty} \beta_i x^i. \quad (43)$$

The constant  $A$  from eq.(42) can easily be obtained approximately by forming the ratio's  $A_i = \alpha_i/\beta_i$  for the last few known terms of the series (41). The function  $F(x)$  can now be represented over the whole interval  $0 < x < 1/\mu$  by the following closed expression:

$$F(x) = A(1-\mu x)^{-\alpha} + \sum_{i=0}^n (\alpha_i - A \beta_i) x^i, \quad (44a)$$

or equivalently by

$$F\left(\frac{x}{x_c}\right) = A\left(1 - \frac{x}{x_c}\right)^{-\alpha} + \sum_{i=0}^n (c_i - A d_i) \left(\frac{x}{x_c}\right)^i, \quad (44b)$$

$$\text{where } c_i \equiv \alpha_i (x_c)^i \text{ and } d_i \equiv \beta_i (x_c)^i. \quad (44c)$$

It is convenient to introduce the notation

$$\sum_{i=0}^n (c_i - A d_i) \equiv C_0. \quad (44d)$$

A plot of  $F(x/x_c)$  versus  $(1-x/x_c)$  on a logarithmic scale yields the value  $\alpha$  only, if  $C_0$  is small compared to the first right-hand term of (44b), for the temperature region (region of  $x$ ) considered.

In the case of the specific heat of the three-dimensional Ising model with  $s = 1/2$ , the expression (44b) is given by

$$c/R = 1.1 \left(1 - \frac{T}{T_c}\right)^{-1/8} - 1.2, \quad (45)$$

for  $x \sim 1/\mu$ . One may notice that the second right-hand term is not small compared to the first one. This will be the case for the specific heat, calculated according to any model, because the terms  $\alpha_0$  and  $\alpha_1$  are zero, whereas  $\beta_0$  and  $\beta_1$  are non-zero (see the first two terms on the right-hand side of (32)). It is clear that in this case the asymptotic behaviour cannot be deduced from the usually made logarithmic plot of  $c/R$  vs.  $(1-T_c/T)$ , where  $1-T_c/T > 10^{-4}$ .

The asymptotic behaviour (42) of the susceptibility however, may be easily observed experimentally, since in relation (44b) the second

right-hand term is small compared to the first right-hand term. One may see this from the following considerations: a) that the susceptibility series is calculated in the form of a correction to the Curie law, so that  $\alpha_0$  and  $\alpha_1$  do not vanish, and b) that the exponent  $\alpha$  is large ( $> 1$ ), so that the contribution of the first right-hand term of eq. (44b) is large, even for  $1 - T/T_c = 0.01$ !

### 3.5.1 Specific heat

a) *the Ising model  $s=1/2$ - f.c.c. and s.c. lattices.* For the f.c.c. lattice we have calculated the values of  $c/R$ , given by the expression<sup>35)</sup>

$$c/R = 1.091(1-t)^{-1/8} - 1 - 1/8t - 0.0142t^2 - 0.0032t^3 - 0.0001t^4 + 0.0005t^5 + 0.0002t^6, \quad (46)$$

where  $t = T_c/T$ , for the temperature region  $10^{-4} < 1-t < 0.6$ .

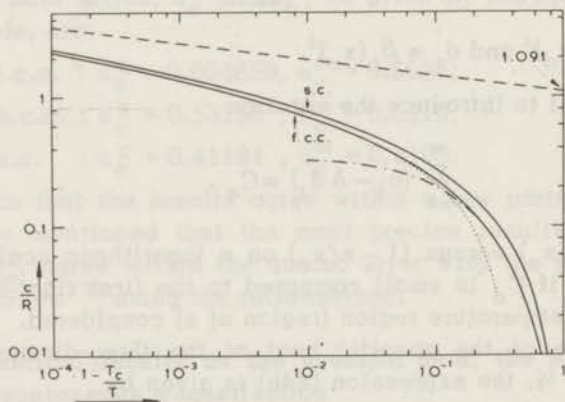


Fig. 1. The curves represent specific heat values,  $c/R$ , for the s.c. and f.c.c. Ising  $s=1/2$  lattice, plotted versus  $(1-T_c/T)$  on a logarithmic scale. The upper lying drawn curve gives the result for the s.c. lattice, calculated from eq. (47). The lower lying drawn curve, representing the result for the f.c.c. lattice, is calculated from eq. (46). The other curves represent several approximations to (46), see the text.

The results are shown by the lowest of the two drawn curves in fig. 1. The *dashed line* represents the asymptotic behaviour of the first term of the right-hand side of eq.(46) only. The *dotted curve* is obtained by inserting  $t = 1$  in all but the first right-hand terms of (46). The *dash-dotted curve* is calculated by the use of the finite series (41)

for  $n = 12$ . From inspection of the curves we may notice a) that the asymptotic behaviour is not even approximately reached in the temperature region that can be covered experimentally, b) that the specific heat curve experimentally observable ( $1-t < 10^{-4}$ ), can only be described accurately by the 12 term series (41) for the fairly high temperature region  $1-t > 0.2$ , and c) that the dotted curve describes the full temperature dependence (46) quite well for  $0 < 1-t < 0.05$ .

The highest of the two drawn curves, representing the specific heat of the s.c. lattice, has been calculated by means of the expression<sup>36)</sup>

$$c/R = 1.2337(1-t^2)^{-1/8} - 1.2337 - 0.0068t^2 - 0.0070t^4 + 0.0029t^6 \\ + 0.0001t^8 - 0.0001t^{10}. \quad (47)$$

The asymptotic behaviour for the s.c. lattice is similar to that of the f.c.c. lattice.

b) *planar classical spin model, f.c.c. lattice.* The specific heat series of a model of classical spins constrained to lie in a plane (planar model), containing 7 non-zero terms<sup>37)</sup>, have been analysed by two methods. The first method was described in 3.5, and results in the asymptotic expression

$$c/R = 11.64(1-t)^{-0.03} - 12.06. \quad (48)$$

It is clear that the asymptotic behaviour (48) cannot be found from a logarithmic plot of  $c/R$  vs.  $(1-t)$  for  $(1-t) > 10^{-4}$ .

However, we may note, that the asymptotic temperature dependence of eq.(48) is nearly logarithmic. Therefore we extended the method described in section 3.5 by considering the coefficients obtained from the expansion of  $\log(1-\mu x)$  in powers of  $x$ , analogous to the expansion (43). The values of  $A$ ,  $c_i/d_i$ , and  $C_0$  (see eq.(44)) for the planar classical spin model are given in table I. The entries  $c_i/d_i$  for the last few terms are nearly constant so that the method appears to be correct. In fig. 2 the specific heat, calculated from the data of table I for the whole temperature region above  $T_c$ , is plotted versus  $(1-T_c/T)$  on a semilogarithmic scale as a drawn curve. The dashed line represents the asymptotic behaviour of the series, described by

$$c/R = -0.380 \ln(1-T_c/T) - 0.469. \quad (49)$$

TABLE I

Specific heat, $c/R$ , of the f.c.c. planar "classical" spin model, derived from the series of ref. 37. The symbols are defined in sections 3.5 and 3.5.1.					
$x \equiv J/kT$ ; $x_c = 0.10367$ ; singularity: log.					
$i$	$a_i$	$\beta_i$	$a_i/\beta_i$	$A$	$c_i - Ad_i$
1	0	9.64600 E+0	0		- 0.38000
2	12	4.65226 E+1	0.25794		- 0.06103
3	96	2.99171 E+2	0.32089		- 0.01970
4	774	2.16435 E+3	0.35761		- 0.00560
5	6240	1.67018 E+4	0.37361		- 0.00128
6	50600	1.34254 E+5	0.37689		- 0.00052
7	418992	1.11004 E+6	0.37746		- 0.00036
8	3543500	9.36883 E+6	0.37822	↓	- 0.00022
9	30446813	8.03303 E+7	0.37902	0.380	- 0.00011
					$C_0 = -0.4688$

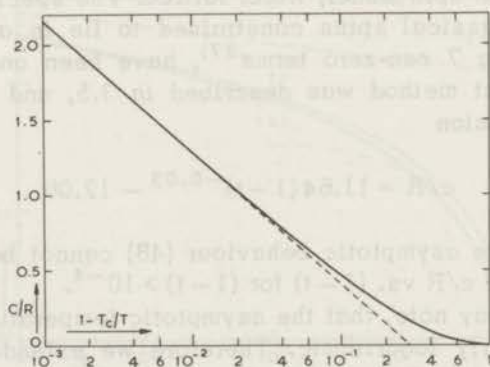


Fig. 2. The specific heat,  $c/R$ , of the f.c.c. planar, classical-spin model is plotted versus  $(1 - T_c/T)$  on a semilogarithmic scale. The drawn curve represents the closed form result given by eq. (44b) (see the text), derived from the series (42) of ref. 37. The dashed line represents the approximation (49).

We notice that the asymptotic logarithmic behaviour can be easily reached experimentally. This result favours the asymptotic representation (49) to that given by eq. (48).

## 3.5.2 Susceptibility

The susceptibility series for the three-dimensional cubic lattices published in the literature have been analysed by the method described in section 3.5. The models dealt with are: The *Heisenberg*  $s = \frac{1}{2}$ , *Ising*  $s = \frac{1}{2}$ , *classical-spin* and *planar classical-spin* models. The symbols used in the tables are defined in section 3.5. The temperature  $T$  is given in units  $T_c$ . The values for the parameters  $x_c$  and  $\alpha$  were taken from the cited publications.

The results of the analysis have been presented in the tables II to V. We may notice the following two points:

a) The convergence of the ratio's  $a_i/\beta_i$  for large  $i$  is very good (a few parts in a thousand) for nearly all Hamiltonians and lattices considered. For the s.c. lattice in the Heisenberg model however, the convergence is somewhat erratic (see table II) but the amplitude may nevertheless be estimated with an error of only about  $\frac{1}{2}\%$ .

The only amplitudes,  $A$ , calculated in the literature viz. those for the Ising  $s = \frac{1}{2}$  and Heisenberg  $s = \frac{1}{2}$  Hamiltonians, are shown in the tables II and III for comparison. In table II the values for  $A$ , given in the second row, have been taken from ref. 38. Agreement with our

TABLE II

Reduced susceptibility, $\chi T / (\text{Curie-const.})$ , of the cubic Heisenberg $s = \frac{1}{2}$ ferromagnets, derived from the series of ref. 38. The symbols are defined in section 3.5; $x \equiv J/kT$ , $\alpha = 1.43$ .						
$x_c$	s.c.		b.c.c.		f.c.c.	
	0.5962		0.3973		0.2492	
$i$	$a_i/\beta_i$	$c_i - Ad_i$	$a_i/\beta_i$	$c_i - Ad_i$	$a_i/\beta_i$	$c_i - Ad_i$
1	1.25077	0.07260	1.11133	0.03360	1.04560	-0.03633
2	1.22750	0.04779	1.09020	0.00382	1.07227	0.00221
3	1.17350	-0.05264	1.09442	0.01275	1.07507	0.00809
4	1.18449	-0.03411	1.08533	-0.00587	1.07148	0.00105
5	1.23039	0.07262	1.08841	0.00099	1.06936	-0.00390
6	1.20701	0.01797	1.08756	-0.00114	1.06933	-0.00428
7	1.17665	-0.06346	1.08852	0.00142	1.07003	-0.00265
8	1.20495	0.01418	1.08648	-0.00435	1.07054	-0.00130
9	1.22812	0.08437	1.08791	-0.00028	1.07074	-0.00079
10	1.19363	-0.01993	1.08765	-0.00109		
$A$	1.20	the present calculation	1.088	the present calculation	1.071	the present calculation
	1.10	ref. 38	1.04	ref. 38	1.07	ref. 38
	1.204	ref. 38, corrected	1.092	ref. 38, corrected	1.075	ref. 38, recalculated
$C_0$		-0.0606		-0.0484		-0.1089

values (first row) is only found for the f.c.c. lattice. By inspecting the calculation of A in ref. 38, the error can be easily located. The amplitude is calculated from the formula for the reduced susceptibility

$$\frac{\chi T}{C} \sim \left( \frac{R}{x_c - x} \right)^a = \frac{A}{(1 - T_c/T)^a}, \quad (50)$$

where the residue R at  $x = x_c$  to the function  $(\chi T/C)^{1/a}$ ,  $a$  and  $x_c$  are given. In ref. 38, the amplitude for the f.c.c. lattice has indeed been calculated according to (50). For the s.c. and b.c.c. lattices, however, the values  $1/a$  have been used, instead of  $a$ . Using (50), the values for the amplitudes (presented in the third row for A in table II) agree remarkably well with our results for all three lattices.

The two entries for A in table III, cited from ref. 39, have been calculated by the ratio-method, the other ones by the Padé-approximant method. As one may notice the agreement in table III between our results and those cited from the literature is excellent. The amplitudes, however, as listed in ref. 40 seem to be erroneously quoted from refs. 30 and 31.

TABLE III

Reduced susceptibility, $\chi T/\text{Curie-const.}$ , of the cubic Ising $s=1/2$ ferromagnets, derived from the series of refs. 33 and 39. The symbols are defined in section 3.5; $x \equiv \tanh J/kT$ ; $\alpha = 1.250$ .						
$x_c$	s.c.		b.c.c.		f.c.c.	
	0.21815		0.15617		0.10175	
$i$	$a_i/\beta_i$	$c_i - Ad_i$	$a_i/\beta_i$	$c_i - Ad_i$	$a_i/\beta_i$	$c_i - Ad_i$
1	1.04712	0.03640	0.99949	0.03186	0.97680	0.01013
2	1.01524	-0.00388	0.97123	-0.00390	0.97181	0.00437
3	1.02219	0.00639	0.98006	0.00924	0.97084	0.00325
4	1.01579	-0.00358	0.97309	-0.00147	0.97024	0.00250
5	1.02033	0.00396	0.97639	0.00406	0.96971	0.00171
6	1.01727	-0.00129	0.97316	-0.00149	0.96925	0.00098
7	1.01932	0.00241	0.97491	0.00168	0.96890	0.00038
8	1.01765	-0.00066	0.97319	-0.00154	0.96863	-0.00013
9	1.01887	0.00169	0.97430	0.00059		
10	1.01787	-0.00027				
11	1.01868	0.00139				
A	1.018	the present calculation	0.974	the present calculation	0.9687	the present calculation
	1.018	ref. 39	$0.973 \pm 0.001$	ref. 39		
	1.018	ref. 30	0.973	ref. 30	0.9688	ref. 30
$C_0$		0.0246		0.0650		0.0545

The close agreement between our values of  $A$  and those published in the literature up to now, combined with the smooth convergence of the ratios  $a_i/\beta_i$  for large  $i$  in all series considered, suggest that the values of  $A$  for the *classical*- and *planar classical*-Heisenberg models (tables IV and V) are also correct to a few parts in thousand.

TABLE IV

Reduced susceptibility, $\chi T$ /(Curie-const.), of the cubic classical Heisenberg ferromagnets, derived from the series of ref. 25. The symbols are defined in section 3.5; $x \equiv J/kT$ .						
	s.c.		b.c.c.		f.c.c.	
$x_c$	0.3475		0.2435		0.1577	
$\alpha$	1.42		1.38		1.38	
$i$	$a_i/\beta_i$	$c_i - Ad_i$	$a_i/\beta_i$	$c_i - Ad_i$	$a_i/\beta_i$	$c_i - Ad_i$
1	0.97887	0.09638	0.94106	0.08703	0.91420	0.06514
2	0.93707	0.04480	0.89862	0.03387	0.88844	0.03521
3	0.92929	0.03583	0.89523	0.03189	0.87727	0.01900
4	0.91825	0.01570	0.88460	0.01338	0.87167	0.00095
5	0.91691	0.01387	0.88354	0.01207	0.86869	0.00369
6	0.91289	0.00475	0.87945	0.00337	0.86722	0.00052
7	0.91239	0.00370	0.87926	0.00308	0.86669	-0.00075
8	0.91089	-0.00030	0.87752	-0.00123	0.86679	-0.00055
9	0.91121	0.00062	0.87773	-0.00073		
$A$	0.911		0.878		0.867	
$C_o$	0.3044		0.3047		0.2647	

TABLE V

Reduced susceptibility, $\chi T$ /(Curie-const.), of the cubic planar classical Heisenberg ferromagnets, derived from ref. 37. The symbols are defined in section 3.5; $x \equiv J/kT$ , $\alpha = 1.32$ .						
	s.c.		b.c.c.		f.c.c.	
$x_c$	0.2265		0.1603		0.10367	
$i$	$a_i/\beta_i$	$c_i - Ad_i$	$a_i/\beta_i$	$c_i - Ad_i$	$a_i/\beta_i$	$c_i - Ad_i$
1	1.03582	0.02863	0.97579	0.05090	0.94820	0.03241
2	1.01477	0.01162	0.94558	0.01302	0.93538	0.01802
3	1.02014	0.01029	0.94968	0.02122	0.93026	0.01132
4	1.01485	0.00154	0.94181	0.00867	0.92764	0.00748
5	1.01809	0.00784	0.94306	0.01163	0.92602	0.00484
6	1.01544	0.00291	0.93951	0.00506	0.92494	0.00290
7	1.01604	0.00430	0.93993	0.00618	0.92418	0.00144
8	1.01404	0.00009	0.93787	0.00190	0.92362	0.00027
$A$	1.014		0.937		0.9235	
$C_o$	0.0427		0.1816		0.1552	

b) The correction series (i.e. the second right-hand term of eq.(44b)) evaluated at  $T_c$ , denoted by  $C_0$ , is small compared to  $A$ , especially for the Ising and Heisenberg models (see table II and III). Since furthermore  $\alpha$  is large, the simple asymptotic relation (42) describes the temperature dependence in the large temperature region:  $1 - T_c/T < 0.3$  quite well. In other words, the critical behaviour for these models may be observed at temperatures as high as  $1.3 T_c$ , and it can be measured accurately in the temperature region  $10^{-2} < 1 - t < 10^{-1}$ . Since the values of  $A$  may be considered reliable, the values of  $c_1 - A d_1$  and  $C_0$  can be calculated equally reliably. Above  $T_c$  the temperature dependence of the reduced susceptibility can now be easily calculated by means of eq.(44b). In the temperature region  $T_c < T < 1.3 T_c$ , which is of interest for critical behaviour, the plot of the precise values of  $\chi T/C$  vs.  $1 - T_c/T$  hardly departs from the plot of the asymptotic expression (42). For this reason we have preferred to present some of the calculated values in the form of a table (table VI). We only tabulate the results for the three most important models: the *classical*- and *spin 1/2 - Heisenberg* models and the Ising  $s=1/2$  model. The values for temperatures between  $T_c$  and  $1.01 T_c$  are omitted as they can be easily calculated from eq. (44b) by substituting  $C_0$  (given in the tables II to V) for the second term on the right-hand side.

In conclusion, we may remark that the method described in section 3.5 to analyse series expected to diverge according to a simple power law is simple. It has the advantage over the Padé-approximant method that it is easy to estimate the temperature region in which the behaviour is described by the asymptotic temperature dependence with a specified accuracy.

### 3.5.3 The spontaneous magnetization

Using the Ising  $s=1/2$  model, an exact expression for the temperature dependence of the spontaneous magnetization has been deduced for several two-dimensional lattices<sup>41,42</sup>). On approaching  $T_c$  the reduced spontaneous magnetization for the square lattice (s.q.) may be represented asymptotically by the expression

$$m(t) \simeq B(1-t)^\beta, \quad (51)$$

where  $t$  stands for  $T/T_c$ , the amplitude  $B = 1.242$  and  $\beta = 1/8$ . In the three-dimensional case one must take recourse to series expansions. By means of Padé-approximant analysis of long series for the three cubic lattices, Essam and Fisher<sup>43</sup>) concluded that eq.(51) describes the asymptotic behaviour of  $m(t)$  quite well. The value of  $\beta$  is  $5/16$

TABLE VI

Values of the reduced susceptibility,  $\chi T/C$ , as a function of  $1-t$  for three models, calculated by eq. (44b) and the constants from tables II to IV;  $t = T_c/T$ .

	$\chi T/C$								
	Heisenberg $s = \frac{1}{2}$			Ising $s = \frac{1}{2}$			classical Heisenberg		
$1-t$	s.c.	b.c.c.	f.c.c.	s.c.	b.c.c.	f.c.c.	s.c.	b.c.c.	f.c.c.
0.0099	881.7	799.4	786.9	333.1	318.7	313.1	639.5	512.5	506.1
0.0157	454.0	411.7	405.2	187.7	178.3	175.3	331.0	270.3	266.9
0.0215	290.4	263.3	259.1	127.4	120.6	118.6	212.5	175.7	173.4
0.0291	188.4	170.8	168.1	87.45	82.66	81.25	138.4	115.8	114.4
0.0403	118.4	107.3	105.6	58.33	55.06	54.14	87.36	74.09	73.13
0.0521	81.90	74.28	73.06	42.31	39.92	39.26	60.71	52.03	51.35
0.0610	65.35	59.28	58.30	34.75	32.78	32.24	48.58	41.91	41.36
0.0826	42.38	38.46	37.81	23.81	22.47	22.11	31.72	27.71	27.34
0.103	30.80	27.97	27.48	18.02	17.02	16.75	23.19	20.45	20.17
0.123	23.97	21.78	21.39	14.48	13.69	13.47	18.15	16.12	15.90
0.149	18.16	16.51	16.21	11.36	10.76	10.59	13.85	12.41	12.23
0.200	11.86	10.81	10.60	7.84	7.45	7.33	9.18	8.33	8.21
0.248	8.67	7.93	7.76	5.98	5.69	5.61	6.80	6.24	6.15
0.301	6.55	6.01	5.88	4.69	4.48	4.42	5.22	4.83	4.76

for all lattices, and the amplitudes are 1.570 and 1.488 for the s.c. and f.c.c. lattices respectively.

In order to investigate in which temperature region the behaviour of the magnetization in the above-mentioned model may be described by the asymptotic relation (51b) (viz. to an accuracy of say 1%), we have explicitly calculated the temperature dependence for  $t < 0.999$ . The results for the s.q., s.c. and f.c.c. lattices are shown in fig. 3. The drawn curve for the s.q. lattice has been calculated with the formula given in ref. 51. The values of  $m(t)$  for the cubic lattices have been calculated from the Padé-approximants listed in ref. 53. The dashed lines represent the asymptotic behaviour given by eq.(51). We may notice, that the deviation of the asymptotic expression (51) from the calculated values of the full expression is less than 1%, if  $1-t < 10^{-2}$  for the s.q. lattice, and for the cubic lattices, if  $1-t > 3 \cdot 10^{-2}$ . This result indicates that the critical behaviour of this model can be reached under experimental conditions.

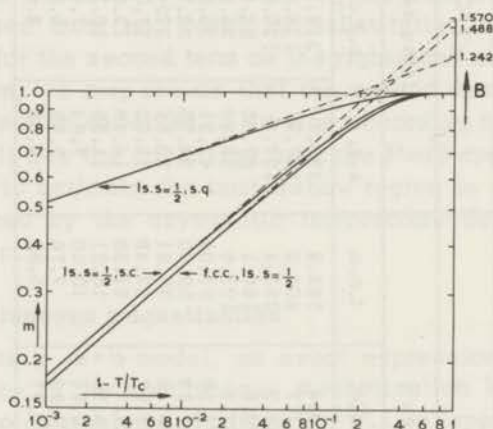


Fig. 3. The reduced spontaneous magnetization,  $m(t)$ , of the Ising  $s=1/2$ , s.q., s.c. and f.c.c. lattices as a function of  $1-T/T_c$ . The drawn curve for the s.q. lattice is calculated from the formula given in ref. 41, those for the cubic lattices have been evaluated with the help of the Padé-approximants listed in ref. 43. The dashed lines are represented by  $m(t) = B(1-t)^\beta$ , with  $B=1.242$  and  $\beta=1/8$  for the s.q. lattice. For the s.c. and f.c.c. lattices  $\beta=5/16$ , with  $B=1.570$  and  $1.488$ , respectively.

### 3.6 Some considerations on the rounding of specific heat curves of magnetic systems

#### 3.6.1 Imperfections

Specific heat measurements on magnetic systems, performed with high temperature resolution ( $\Delta T \sim 0.0002 T_c$ ) often reveal a rounding of the specific heat curve over a temperature interval ranging between  $0.001 T_c$  and  $0.01 T_c$  (see refs. 44, 45 and Ch. III). This effect is commonly attributed to imperfections of physical or chemical origin. Large regions of imperfections may divide the sample into effectively many independent structures. This effect may be considered as a size effect. Another possible cause of the rounding of the specific heat peak might be formed by a region of stress in the neighbourhood of an imperfection. A calculation of the variation of the transition point with stress has been performed in the simple case of the influence of uniaxial anisotropy on the transition point for a ferromagnet. These two effects arising from imperfections will be considered quantitatively.

a) *Finite size effect.* The imperfection may consist in cracks dividing the sample into small parts containing a relatively small number of interacting spins. From statistical mechanics it follows that in a finite system the thermodynamic variables do not exhibit discontinuities. In particular the specific heat of such a system has a finite maximum. For the two dimensional rectangular Ising  $s = \frac{1}{2}$  model Onsager<sup>9)</sup> has derived the expression

$$c/R \approx -0.4945 \ln M \quad (52)$$

for the specific heat maximum at  $T_c$  of an infinitely long strip of width  $M$  spins. For the infinite s.q. lattice the expression has the asymptotic form

$$c/R \approx -0.4945 \ln |1 - T/T_c| \quad (53)$$

for  $T$  near  $T_c$ . From the relations (52) and (53) it follows that size effects will occur if

$$M < \frac{1}{|1-t|}, \quad (54)$$

where  $t = T/T_c$ .

Let us consider the specific example that the crackfree regions are 0.1 mm in diameter and that the spacing of the spins is  $7 \text{ \AA}$ . We then obtain  $M = 1.5 \cdot 10^{+5}$ , so the temperature interval in which size

effects determine the specific heat is given by  $|1-t| < 10^{-5}$ . However, measurements performed on the optically and chemically very pure sample  $\text{CoCl}_2 \cdot 6\text{H}_2\text{O}$  of Skalyo et al.<sup>44)</sup>, which is considered to represent a s.q. Ising antiferromagnet, show a rounded specific heat peak for  $|1-t|$  as large as  $2 \cdot 10^{-3}$ .

In the three dimensional Ising  $s = \frac{1}{2}$  model no exact results have been obtained. Domb<sup>46)</sup>, however, has obtained the following estimate for the specific heat maximum

$$c/R \approx \frac{D}{\alpha} [(bM)^\alpha - 1]. \quad (55)$$

$D$  specifies the dimension,  $\alpha$  the power by which the specific heat in  $D$  dimensions diverges, and  $b$  is a constant of order unity. Taking  $M = 10^5$ , and  $\alpha = 1/8$ <sup>35)</sup> for  $T > T_c$  in three dimensions, we obtain  $c/R = 75$  from eq.(55). This value is about 30 times as high as the maximum observed for the salt  $\text{CoCs}_3\text{Cl}_5$ , which we consider a fair representation of the cubic Ising model (Ch. III).

From these results we infer that this size-effect is no plausible interpretation for the experimentally found rounding of the specific heat peak.

*b) The influence of the domain structure.* By the use of a variational technique, it has recently been pointed out<sup>47)</sup> that in a ferromagnet having uniaxial anisotropy the transition point for spins in a domain,  $T_{c,\text{domain}}$ , differs from that for spins in a wall,  $T_{c,\text{wall}}$ . The proposed expression has the form

$$T_{c,\text{domain}}/T_{c,\text{wall}} = 1 + \frac{2K}{J} \quad (56)$$

where  $K$  denotes the uniaxial anisotropy constant and  $J$  the exchange parameter. Let us consider the case that  $2K/J = 0.01$ . Even if the domains are supposed to be very small (0.2 mm length), the ratio of the numbers of spins present in a wall and in the domains, respectively, is only 0.05. The resulting spread in  $T_c$  predicted by eq.(56) is only  $0.0005 T_c$ . This spread is about a factor 10 higher than observed, so that it also fails to account for the experimentally found broadening.

### 3.6.2 Effect of the volume-dependence of the exchange interaction

As the exchange integral  $J$  is strongly dependent on the lattice parameter, and the energy gain in a phase-transition depends on the value of the exchange parameter, one may suppose that the thermal expansion is anomalous in the temperature region close to the phase

transition. This phenomenon has been observed by several experimentalists<sup>48,49</sup>. Theoretically, for the Heisenberg model below  $T_c$ , Pytte<sup>50</sup> has derived an expression for this anomalous expansion, which is a linear function of the specific heat of the spin system. Using the molecular field approximation Bean and Rodbell<sup>51</sup> have derived the specific heat of a spin system having a volume-dependent exchange interaction. They derived that the specific heat near  $T_c$  rises steeply, if the parameter  $\beta$ , describing the volume-dependence  $J(v) = J(v_0) \times [1 + \beta(v_0 - v)/v_0]$ , is increased. If  $\beta$  is larger than a critical value  $\beta_c$ , the transition changes into a first order transition. The latter result has also been obtained by Rice<sup>52</sup>, who has used general thermodynamic arguments.

On the basis of the Ising model, Domb<sup>53</sup> has elegantly derived the expression

$$\left(\frac{\partial P}{\partial v}\right)_T = \left(\frac{\partial P}{\partial v}\right)_{\text{solid}} - \frac{E_{\text{order}}}{J} \left(\frac{\partial^2 J(v)}{\partial v^2}\right)_T + c_v T \left(\frac{\partial J(v)/\partial v}{J}\right)_T^2, \quad (56)$$

which may be used to estimate the value of  $c_v$  required to change the transition from second order into first order ( $(\partial P/\partial v)_T = 0$ ). In eq.(56),  $v(\partial P/\partial v)_{\text{solid}}$  denotes the reciprocal compressibility for the solid in the absence of volume-dependent exchange,  $J(v)$ ; the left-hand side multiplied by  $v$  denotes the same quantity for the complete system, and  $c_v$  is the specific heat at constant volume. As both  $E_{\text{order}}$ , the energy gained at  $T$  by the ordering process, and the third right-hand term evaluated at  $T_c$  are proportional to  $T_c$ , the third term outweighs the second term, independently of  $T_c$ , if  $c_v$  is sufficiently large. Let us consider the specific case of an ionic crystal at very low temperatures, with a molar weight of 500 gr. and a molar volume of 250 cc. Let us assume  $J(v)$  to be strongly dependent on volume,  $J(v) = J(v_0) \times (v_0/v)^4$ ;  $T = T_c \sim 1$  K;  $E_{\text{order}} = NkT_c$ ,  $c_v = 10Nk$ ,  $k$  denoting the Boltzmann constant; and  $v(\partial P/\partial v)_{\text{solid}} = -10^{11}$  [cm<sup>-2</sup> dyne], which is of the order of magnitude observed in the salt  $\text{KMnF}_3$ <sup>54</sup>. After insertion of the numerical values in eq.(56) the second right-hand term appears to be negligible with respect to the third right-hand term. The expression (56) may now be simplified to

$$\left(\frac{\partial P}{\partial v}\right)_T \approx \frac{(v \frac{\partial P}{\partial v})_{\text{solid}}}{v} + \frac{16 c_v T}{v^2}. \quad (57)$$

Substituting the numerical values we obtain

$$\left(\frac{\partial P}{\partial v}\right)_T \approx -4.10^8 + 2.5 \cdot 10^5 [\text{erg/cc}^2].$$

We conclude that the system would be unstable if  $c_v/R$  was of the order  $10^4$ . This value is not nearly reached under experimental conditions ( $|T - T_c| > 10^{-4}$ ). This result indicates that near 1 Kelvin the volume-dependence of the exchange energy has a negligible influence on the stability of the lattice, and consequently on the sharpening of the specific heat peak.

### 3.6.3 Calculation of the rounding of the specific heat peak in the s.c. Ising $s = \frac{1}{2}$ model

In spite of the absence of a plausible mechanism to interpret the rounding of the specific heat peak, it is worthwhile to consider a simple mathematical model that gives a finite maximum for any singularly divergent function. In the model it is assumed a) that the specimen contains regions,  $R(i)$ , that have slightly different transition points,  $T_c(i)$ , centered round  $T_c$ , and b) that the regions,  $R(i)$ , have an abundance, given by a distribution function,  $d$ . The specific heat curve,  $c(T)$ , in this model may be found from

$$c(T) = \sum_i d(i) c(T, T_c(i)). \quad (58)$$

Hitherto, the only three-dimensional model for which  $c(T)$  close to  $T_c$  has been published, is the Ising  $s = \frac{1}{2}$  model. In order to perform the calculation we have chosen the s.c. lattice, since the temperature-dependence of the specific heat for  $T$  close to  $T_c$  ( $0.9 < T/T_c < 1$ ) can be evaluated from ref. 55. We have obtained the simple expression

$$c(T, T_c)/R = -0.556 \ln(1 - T/T_c) + 0.03. \quad (59)$$

The asymptotic form of  $c(T, T_c)$  for  $T > T_c$ , ( $0.9 < T_c/T < 1$ ), has been provided by Sykes<sup>56)</sup> as

$$c(T, T_c)/R = 1.2337 (1 - (T_c/T)^2)^{-1/8} - 1.2445. \quad (60)$$

Eq.(59) obtains for  $T < T_c(i)$ , while eq.(60) obtains for  $T > T_c(i)$ . We have chosen a Gaussian distribution function for  $d$ , viz.

$$d(i) = \frac{\exp - \left(\frac{i \times \text{step}}{F}\right)^2}{\sum_{i=-120}^{i=120} \exp - \left(\frac{i \times \text{step}}{F}\right)^2}. \quad (61)$$

where the integer  $i$  runs from  $-120$  to  $120$ ,  $F$  is the half-width in units  $T_c$  and  $\text{step} \equiv 0.05 F$  denotes the partition. The critical temperature  $T_c(i)$  is given by

$$T_c(i) = T_c \exp(i \times \text{step}). \quad (62)$$

By using eqs.(59),(60),(61) and (62), the specific heat, given by eq.(58) may be evaluated as a function of the temperature.

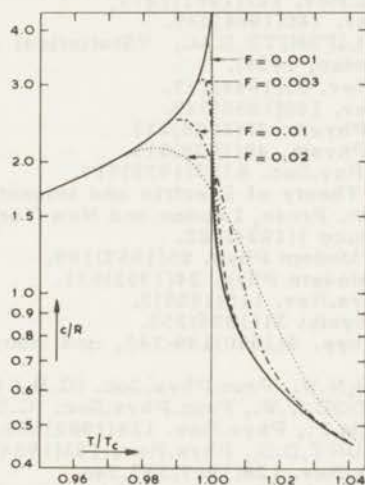


Fig. 4. The specific heat,  $c/R$ , as a function of  $T/T_c$  for the Ising  $s = \frac{1}{2}$  model. The drawn lines represent the theoretical values (see the text). Specific heat curves of systems having a Gaussian distribution of transition points of half width  $0.001 T_c$ ,  $0.003 T_c$ ,  $0.01 T_c$  and  $0.02 T_c$ , respectively, are represented by (from top to bottom) the dotted, dashed, chain- and dotted curves.

Fig. 4 shows the s.c. Ising  $s = \frac{1}{2}$  curves ((59), and (60)), and the curves (58) calculated with  $F = 0.001 T_c$ ,  $0.003 T_c$ ,  $0.01 T_c$ , and  $0.02 T_c$ , respectively. We may notice firstly that the broadened curves fit smoothly to the theoretical curves, if  $|T_c - T| > F$ , and are rounded for  $|T_c - T| < F$ . Secondly fig. 4 shows that the maximum of  $c(T)$  does not occur at  $T_c$ , but at a temperature  $T = 1 - F$  for all the curves with  $F > 0.01 T_c$ . This result is not surprising, as the s.c. Ising  $s = \frac{1}{2}$  specific heat curve is strongly asymmetric (see the plot of (59) and (60)). Therefore, the temperature at which the maximum of the broadened peak occurs, will be shifted by an amount  $F$  in the direction of the region in which  $c(T)$  is largest for a fixed value of  $|T_c - T|$ . It is clear that the maximum of the broadened peak will only occur at  $T_c$  if the specific heat curve is symmetric with respect to  $T_c$ .

## References

1. KEESOM, W.H. and KEESOM, A.P., Proc. Roy. Acad. of Amsterdam, 35 (1932)736; Communications from the Kamerlingh Onnes Lab., Leiden, No. 221d.
2. EHRENFEST, P., Proc. Roy. Acad., Amsterdam, 36(1933)153; Commun., Leiden, suppl. 75b.
3. BUCKINGHAM, M.J. and FAIRBANK, W.M., "Progress in Low Temperature Physics", vol. III, p. 80, ed. C.J. Gorter (North-Holland Publishing Co., Amsterdam, 1961).
4. KELLERS, C.F., Bull. Am. Phys. Soc., Ser. II, 2(1957)183.
5. GORTER, C.J., Physica 34(1967)220.
6. BAKER, G.A. Jr., Phys. Rev. 122(1961)1477.
7. JOYCE, G.S., Phys. Rev. 146(1966)349.
8. LANDAU, L.D. and LIFSHITZ, E.M., "Statistical physics", chap. 14 (Pergamon Press, London, 1958).
9. ONSAGER, L., Phys. Rev. 65(1944)117.
10. JOYCE, G.S., Phys. Rev. 146(1966)349.
11. HEISENBERG, W., Z. Physik. 38(1926)411.
12. HEISENBERG, W., Z. Physik. 49(1928)619.
13. DIRAC, P.A.M., Proc. Roy. Soc. A123(1929)714.
14. VAN VLECK, J.H., "Theory of Electric and Magnetic Susceptibilities", Chapt. XI, Oxford Univ. Press, London and New York, 1932.
15. KRAMERS, H.A., Physica 1(1934)182.
16. SLATER, J.C., Revs. Modern Phys. 25(1953)199.
17. HERRING, C., Revs. Modern Phys. 34(1962)631.
18. ANDERSON, P.W., Phys. Rev. 115(1959)2.
19. ISING, E., Zeits. f. Physik. 31(1925)253.
20. DOMB, C., Adv. in Phys. 9(1960)149-245, and many subsequent publications of the group.
21. WOOD, D.W., DALTON, N.W., Proc. Phys. Soc. (G.B.) 87(1966)755.
22. DALTON, N.W. and WOOD, D.W., Proc. Phys. Soc. (G.B.) 90(1967)459.
23. DOMB, C. and SYKES, M.F., Phys. Rev. 128(1962)168.
24. FISHER, M.E. and GAUNT, D.S., Phys. Rev. 133(1964)A224.
25. STANLEY, H.E., Phys. Rev. 158(1967)537, 546.
26. BOWERS, R.G. and JOYCE, G.S., Phys. Rev. Letters, 19(1967)630.
27. VAN DER WAERDEN, B.L., Z. Physik., 118(1941)473.
28. FISHER, M.E., "The theory of equilibrium critical phenomena", Rep. on Progr. in Phys. vol. 30, pt. II(1967)688.
29. DOMB, C. and SYKES, M.F., Proc. Roy. Soc. A240(1957)214.
30. BAKER, G.A. Jr., Phys. Rev. 124(1961)768.
31. BAKER, G.A. Jr., "Advances in theoretical physics", vol. I, Ch. 1, ed. K.A. Brueckner (Ac. Press New-York-London)1965.
32. KRAMERS, H.A. and WANNIER, G.H., Phys. Rev. 60(1941)252, 263.
33. DOMB, C. and SYKES, M.F., J. Math. Phys. 2(1961)63.
34. HOUTAPPEL, R.M.F., Physica 16(1950)425.
35. SYKES, M.F., MARTIN, J.L. and HUNTER, D.L., Proc. Phys. Soc. 91(1967) 671.
36. SYKES, M.F., private communication.
37. BOWERS, R.G. and JOYCE, G.S., Phys. Rev. Lett. 19(1967)630.
38. BAKER, G.A. Jr., GILBERT, H.E., EVE, J. and RUSHBROOKE, G.S., Phys. Rev. 164(1967)800.
39. FISHER, M.E. and SYKES, M.F., Physica 28(1962)939.
40. FISHER, M.E., "The theory of equilibrium critical phenomena", Rep. on Progr. in Phys. vol. 30, pt. II(1967)p671, p.692.
41. YANG, C.N., Phys. Rev. 85(1952)808.
42. POTTS, R.B., Phys. Rev. 88(1952)352.
43. ESSAM, J.W. and FISHER, M.E., J. chem. Phys. 38(1963)802.
44. SKALYO, J. Jr., COHEN, A.F., FRIEDBERG, S.A. and GRIFFITHS, R.B., Phys. Rev. 164(1967)705.
45. TEANEY, D.T., "Critical Phenomena", Misc. Publ. No. 273(1966) p.50, (Nat. Bur. of St., eds. Green M.S. and Sengers, J.V.).

46. DOMB, C., Proc. Phys. Soc. 86(1965)933.  
 47. KLAMUT, J., KOZŁOWSKI, G., Proc. Phys. Soc. (G.B.) 92(1967)517.  
 48. GIBBONS, D.F., Phys. Rev. 115(1959)1194.  
 49. DONALDSON, R.H. and LANCHESTER, P.C., J. Phys. C. (Proc. Phys. Soc. (G.B.) 1(1968)364.  
 50. PYTTE, E., Ann. Phys., N.Y., 32(1965)377.  
 51. BEAN, G.P. and ROBBELL, D.S., Phys. Rev. 126(1962)104.  
 52. RICE, O.K., J. Chem. Phys. 22(1954)1535.  
 53. DOMB, C., J. Chem. Phys. 25(1956)783.  
 DOMB, C., Proc. Phys. Soc. (G.B.), 88(1966)260.  
 54. HEEGER, A.J., BECKMANN, O., PORTIS, A.M., Phys. Rev. 123(1961)1652.  
 55. BAKER, G.A. Jr., Phys. Rev. 129(1963)99.  
 56. SYKES, M.F., has kindly provided us with this information.

## Chapter II

## EXPERIMENTAL APPARATUS AND METHODS

## 1 Introduction

Temperatures below 1 Kelvin can easily be obtained by the method of adiabatic demagnetization. In the Kamerlingh Onnes Laboratory, this method has been investigated and applied by several workers<sup>1,2,3,4,5</sup>. The experimental apparatus, consisting of a  $^4\text{He}$  system, a large electromagnet, a Hartshorn mutual inductance bridge and a simple detection circuit has been described extensively by the above-mentioned authors. Since the measurements of the singularity in the specific heat, and those of the magnetization as a function of the temperature and field, necessitate a high temperature resolution, the detection and recording had to be improved drastically. In the following sections we shall describe the sample-holder, and the new experimental devices and methods used.

## 2 The calorimeter

The apparatus, used for measurements between 0.05 and 2 K, is shown in fig. 1. The sample, S, is in close thermal contact with the magnetic thermometer, T, and the eddy current heater, H. The sample-heater-thermometer system may be cooled via a superconducting thermal switch, H.S., which forms a link with the chromium-alum cooling salt. The guard-salt, G, which is demagnetized because it is in the strong stray-field of the magnet, serves to reduce the heat input to the inner glass tube.

The sample may consist of one or two slabs (1 to 2 cms large) of single crystal or of fine powder. Good thermal contact with the heater-thermometer is realized by Apiezon-N grease. The single crystals are tied by thin cotton threads to brass-plates. Powdered samples were mixed with grease. Thermal contact with the calorimeter is established by a brush of about 100 enamelled copper wires of 0.3 mm diameter. As in most cases the coefficients of thermal expansion of the brass plates and crystals are different, fairly hard crystals are apt to crack on cooling. In this case, the thermal conduction below 0.25 K may become very poor and heat capacity measurements become difficult. Therefore, below this temperature, most experiments have been performed on powdered crystals. Typical quantities used were: half a gram of powder for  $T < \frac{1}{2} T_c$ , 10 grams of single crystal or powder for  $0.8 < T/T_c < 1.4$ , and about 4 grams of single crystal for  $T > 1.4 T_c$ .

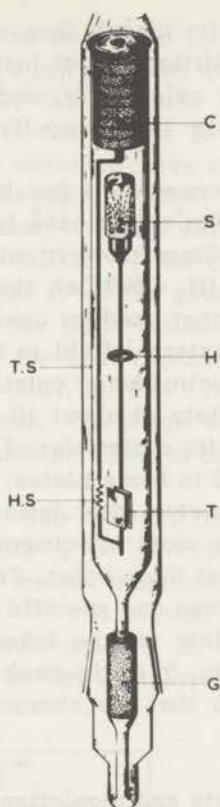


Fig. 1. Apparatus for measuring heat capacity between 0.03 and 2 K.

- |                              |                        |
|------------------------------|------------------------|
| C chromium alum cooling salt | T magnetic thermometer |
| S sample                     | H.S. heat switch       |
| H heater, copper ring        | G guard salt (Cr-alum) |
|                              | T.S. thermal shield    |

At temperatures above 0.8 K the heat capacity of the grease becomes disturbingly large ( $325 T^3$  ergs  $K^2/\text{gr.}^6$ ), so that single crystals are to be preferred. However, the bounds indicated depend somewhat on the value of  $T_c$ .

The heater is made of a copper ring of 12 mm diameter, in which eddy currents are generated by a coil wound on the outer glass tube. The inhomogeneity of the field is less than 0.2% for a distance of 1 cm along the axis of the coil. The heat generated by the coil per sec and per unit current depends on the frequency used. The advantage

of this heater over a resistor clearly lies a) in the absence of leads that would introduce an additional heat leak, and would increase the heat capacity of the empty calorimeter, and b) the simplicity of construction. A disadvantage is the necessity for calibration, which is discussed in section 5.

The thermal switch is formed by a few lead or tin wires of 0.1 mm diameter and 1 cm length. Tin was chosen for the measurements in the lowest temperature region. Since the critical field for tin ( $H_c \approx 300$  Oe) is lower than that for lead ( $H_c \approx 800$  Oe), the stray field at the sample position, caused by the magnet used for operating the switch, is lower for tin than for lead. The external field is formed either by a Nb-coil in the  $^4\text{He}$  bath or by an electromagnet outside the cryostat.

The cooling salt<sup>5)</sup> consists of about 10 disks of single crystal of chromium-potassium-alum with a diameter of 20 mm and a thickness of 5 mm. The crystals are glued to brass plates, which are tightly screwed to a copper rod of 3 mm diameter. After demagnetization only 10 minutes were needed for precooling most specimens. If no switch is used a run of measurements can last three hours. Since at temperatures above 0.15°K the time needed to take one specific heat point does not exceed 5 minutes, at least 30 points can be taken. The observed rounding (see Ch. III fig. 4, Ch. VI fig. 5) of the peak in the specific heat facilitates the measurement, so that the character of the singularity can be determined in one run.

### 3 Temperature measurements and regulation

a) *The magnetic thermometer.* The specific heat data have been obtained by magnetic thermometers. At temperatures much higher than the transition temperature  $\chi''/\chi' \ll 1$ , so that  $\chi_0$ , forthwith denoted as  $\chi$ , may be set equal to  $\chi'$ . In this temperature region the temperature-dependence of the susceptibility of a normal paramagnetic substance obeys the Curie-Weiss law

$$\chi = C/T^*, \quad (1)$$

with

$$T^* = T - \theta. \quad (2)$$

In these formulae,  $C$  and  $T^*$  denote the Curie-constant and the Curie-Weiss temperature respectively. Since for cerium magnesium nitrate ( $\text{Ce}_2\text{Mg}_3(\text{NO}_3)_{12} \cdot 24\text{H}_2\text{O}$ , CMN)  $\theta$  is smaller than  $2\text{mK}$ <sup>9)</sup>, and as the specific heat above about 0.1 K is very small, this salt has been used as a thermometer for nearly all experiments. The difference

between  $T^*$  and  $T$  may be neglected for temperatures above 0.15 K. Doping of the CMN with a few per cent of  $\text{Cu}^{2+}$  ions reduces the spin-lattice relaxation time of the Ce-spins to about one fourth<sup>10)</sup>. Such  $\text{Cu}^{2+}$ -doped crystals have been used for nearly all the experiments.

A thermometer that is about ten times as sensitive as CMN is cobalt-cesium-tutton-salt ( $\text{CoCs}_2(\text{SO}_4)_2 \cdot 6\text{H}_2\text{O}$ , called CoCs-sulphate). The  $g$  value in the  $K_3$  direction<sup>4)</sup> of this salt is about  $5.5^{10)}$ . Since  $\theta$  in the  $K_3$  direction is only  $0.03\text{K}^{10)}$ , the CoCs-salt may be useful as a thermometer. We have used it for the determination of the character of most singularities. For the CoCs-tutton-salt we have determined the magnetic contribution to the heat capacity per gram to be about 1000 times as high as that of CMN, so that CoCs-sulphate cannot generally be used as a thermometer. The large thermal relaxation time found below about 0.3 K puts another limit to the applicability of this thermometer.

b) *The bridge circuit.* The real and imaginary parts,  $\chi'$  and  $\chi''$ , of the dynamic susceptibility  $\chi_\omega = \chi' - i\chi''$ , have been determined by means of a Hartshorn<sup>11)</sup> mutual inductance bridge that has been modified by several workers<sup>12,1)</sup>. A set-up, showing the essential parts, and including recent improvements in the detection and recording system, is drawn in fig. 2. The sample,  $S$ , is placed in one of the two

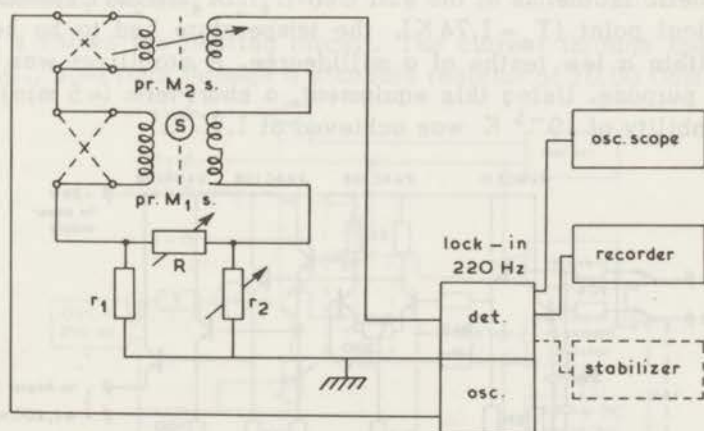


Fig. 2. Schematic diagram of the Hartshorn bridge and detection system.

- $M_1$  mutual inductance formed by the coil system  
 $M_2$  variable mutual induction  
 $S$  sample  
 $R, r_1, r_2$  network for compensation of a.c. losses in  $M_1$ .

(oppositely wound) secondary coils forming a mutual inductance,  $M_1$ , with the primary coil. The voltage of the secondary of  $M_1$  can be resolved into two components, one of which is in-phase with the voltage of the secondary of the variable mutual inductance,  $M_2$ , the other differing  $\pi/2$  radians from that of the former. The first component can therefore be compensated by setting  $M_2 = M_1$ , the second by tapping a suitable voltage from a resistive network ( $r_1, r_2, R$ ) carrying the primary current. The two components can be visualized independently by phase-sensitive detection and displaying the two components on an oscillograph.

If  $M_0$  denotes the value of  $M_1$  in the absence of a specimen, and if  $R_{\text{eff}}$  stands for  $r_1 r_2 / (r_1 + r_2 + R)$ , then the dynamic susceptibility,  $\chi_0'$ , is found from:  $\chi' = (M_2 - M_0) / q$  (3), and  $\chi'' = R_{\text{eff}} / \omega q$  (4), where  $M_2$  denotes the value of  $M_1$  in units of  $3.100 (\pm 0.003) \mu\text{H}$ .  $M_0$  and  $q$  can be derived from a plot of  $M_2$  vs.  $1/T$ . The frequency used was 220 Hz, which enabled us to maintain a fast response ( $\approx 1$  sec), while using a high Q-factor ( $\approx 300$ ), without undue heating the calorimeter by eddy currents. If the Hartshorn bridge is replaced by an a.c. Wheatstone bridge, a resistive thermometer can be used. Resistive thermometry has been used in the magnetization experiment on  $\text{Cu}(\text{NH}_4)_2\text{Br}_4 \cdot 2\text{H}_2\text{O}$  (Ch. V).

c) *The stabilizer.* In chapter V measurements will be reported on the magnetic isotherms of the salt  $\text{Cu}(\text{NH}_4)_2\text{Br}_4 \cdot 2\text{H}_2\text{O}$ . Especially near the critical point ( $T_c \approx 1.74$  K), the temperature had to be kept constant within a few tenths of a millidegree. A stabilizer was built<sup>13)</sup> for this purpose. Using this equipment, a short-term ( $\approx 5$  min) temperature stability of  $10^{-5}$  K was achieved at 1.75 K.

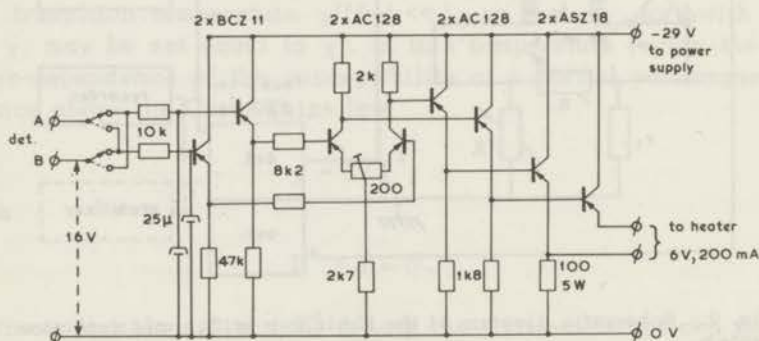


Fig. 3. Diagram of the unit used for the temperature stabilization. The input d.c. voltage varying between +0.5 to -0.5 V is derived from the detector. The maximum output current is 200 mA, the voltage being 6V.

The principle of operation is straightforward. In a heater resistor (near the specimen) heat is produced by a current that is proportional to the off-balance d.c. voltage (of the proper sign), derived from the detector. Fig. 3 shows the diagram. The signal,  $V_{AB}$  varies between  $-0.5\text{ V}$  and  $+0.5\text{ V}$ . The commutator,  $C$ , chooses the proper sign. The first stage ( $2 \times \text{BC211}$ ) serves to transform the impedance. The second stage ( $2 \times \text{AC128}$ ) amplifies the signal to about  $6\text{ V}$ . The final two stages ( $2 \times \text{AC128}$ , and  $2 \times \text{ASZ18}$ ) amplify the current, available for heating, to  $200\text{ mA}$ , the maximum voltage still being  $6\text{ V}$ . If  $V_{AB} > 0$ , a current runs through the heater; if  $V_{AB} < 0$ , no current passes the heater.

A variable a.c. current proportional to the available d.c. current may in some cases be welcome for temperature regulation, because no leads are needed in the former method. Such an a.c. current can be easily obtained, if the varying d.c. current is used to light an electric bulb. The light of this bulb may vary the resistance of a photosensitive resistor. If this resistor is placed in a circuit containing the heating coil and an oscillator, a.c. heating can be used for temperature stabilization. This device can be used for any isothermal measurement performed in a apparatus that makes use of adiabatic demagnetization, e.g. for susceptibility measurements near a critical point below  $1\text{ K}$ .

#### 4 The heating circuit

Fig. 4 shows the heating circuit. The current through the heating coil, H.C., also runs through a standard resistor of  $10.00\text{ Ohms}$ , which

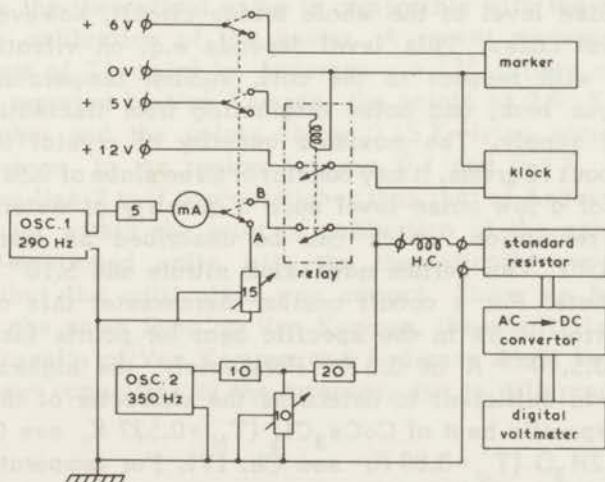


Fig. 4. The diagram of the heating circuit and block-diagram of the measuring system. H.C. denotes the heating coil.

is doubly wound in order to reduce the self-inductance. The a.c. voltage across this resistor is converted to a d.c. voltage by means of a Solartron a.c.-d.c converter (LM 1219). This d.c. voltage is displayed on a Solartron digital voltmeter (4 digits, type LM 1520). The primary oscillator, denoted as osc. 1, operating at 290 Hz, only produces a current through H.C., if the switch is in position B. The relay switch, activated by the manual switch, closes the heating circuit of osc. 1 and starts the mechanical clock (Jaquet, type 309d) nearly simultaneously (error about 1 msec). The reading accuracy is a hundredth of a second. The over-all inaccuracy is about 0.02 sec, which has been checked by means of a 100 kHz oscillator and an electronic counter. If the variable resistor of 15 Ohms matches the impedance of the heating coil plus standard resistor, and if the switch is in position A, the current can be adjusted before the heating period is started.

The secondary oscillator, osc. 2, operating at 350 Hz, maintains a constant current through H.C., which serves to compensate the heat leak through the switch. If we use this procedure, the temperature range of operation of the thermal switch is considerably extended.

## 5 Errors and calibration

The main source of random errors lies in the inaccuracy of the temperature determination. The noise level of the amplifier is  $10^{-7}$  V across an input impedance of 100 kOhms, corresponding in our coil system to 0.2% of the signal of 1 gr. of cerium magnesium nitrate at 1 K. The noise level of the whole bridge circuit, however, is much larger in most cases. This level depends e.g. on vibrations of the thermometer with respect to the coil, sudden temperature changes caused by gas leak, and noise originating from fluctuations in the mains power supply. The maximum quantity of crystal that can be mounted is about 12 grams. It may consist of three slabs of  $0.5 \times 1.5 \times 2.5 \text{ cm}^3$ . In the case of a low noise level such a quantity of material gives a temperature resolution, which can be described as fractional and amounts to  $5 \cdot 10^{-4}$  for cerium magnesium nitrate and  $5 \cdot 10^{-5}$  for cobalt cesium sulphate. For a cobalt cesium thermometer this corresponds e.g. to an error of 5% in the specific heat for points taken over an interval of  $0.5 \cdot 10^{-3}$  K at 0.5 K. Fortunately, the highest accuracy obtainable was sufficient to determine the character of the singularities in the specific heat of  $\text{CoCs}_3\text{Cl}_5$  ( $T_N = 0.527$  K, see Ch. III), and of  $\text{CuK}_2\text{Cl}_4 \cdot 2\text{H}_2\text{O}$  ( $T_c = 0.88$  K, see Ch. IV). For temperatures below 0.3 K, a thermometer with a higher temperature resolution might provide us with a better analysis of the specific heat singularities namely

for  $\text{GdCl}_3 \cdot 6\text{H}_2\text{O}$  with  $T_N = 0.185$  K. Outside the peak region, however, a smaller amount of thermometer crystal has to be used, as in this case the heat capacity of the thermometer becomes important. Generally at temperatures below 0.1 K for cerium magnesium nitrate, and below 0.5 K for cobalt cesium sulphate, the magnetic contribution becomes large. At temperatures above 0.8 K the contribution of the lattice to the specific heat becomes important. Therefore we have to deduce the size and type of thermometer from a preliminary experiment.

A second source of errors is the inaccuracy of the extrapolations of the temperature curves before and after the heating, which strongly depend on the thermal relaxation time of the specimen, and on the heat leak. At temperatures below 0.15 K and above 0.6 K these errors may become the most important ones. Random errors, arising from inaccuracies of the clock and the measurement of the current, are negligible as they amount to less than 0.5%.

Finally, a systematic error may be introduced by the calibration of the eddy current heater. As a calibration, the heat capacity of 100 mg of Tb metal was measured in the temperature region between 0.1 and 0.4 K, where the heat capacity of the empty calorimeter is smallest. This measurement was compared with the measurement of Van Kempen et al.<sup>14)</sup>, the accuracy of the latter being a few percent. The entropy change per gramion calculated from the measurements of the magnetic specific heat of e.g. the salts gadoliniumsulphate octohydrate and gadoliniumtrichloride hexahydrate (see Ch. VI) amounted to 98,5% and 103% of  $R \ln(2s+1)$ , respectively. The deviation of the experimental values from the theoretical value is compatible with the quoted accuracy of the calibration of the heater. A recent measurement of the specific heat of Tb metal by Anderson e.a.<sup>15)</sup>, differs a few percent from those reported by Van Kempen, the points at 0.05 K lying a few percent higher and the points above 0.15 K lying somewhat lower. On the average, in the region between 0.1 and 0.3 K, the curve of Van Kempen lies 2 to 3 percent higher than that of Anderson. However the agreement within the error of calibration of the entropy yield in the above-mentioned salts with the theoretically expected values indicates that the calibration was correct. Since we have used Tb metal from the same lump as Van Kempen, the small discrepancy between the results of Van Kempen and Anderson might be attributed to different heat capacities of the samples, due to differences in purity.

## References

1. DE KLERK, D., Thesis, Leiden (1948).
2. STEENLAND, M. J., Thesis, Leiden (1952).
3. BEUN, J. A., Thesis, Leiden (1957).
4. MIEDEMA, A. R., Thesis, Leiden (1960).
5. VAN KEMPEN, H., Thesis, Leiden (1965).
6. SCHEFFER, J., private communication.
7. EDELSTEIN, A. S. and MESS, K. W., *Physica*, 31(1965)1707, Commun. No. 344c, Leiden.
8. CLEMENT, J. R. and QUINNELL, E. H., *Rev. Sci. Instr.*, 23(1952)213.
9. MESS, K. W., LUBBERS, J., NIESEN, L. and HUISKAMP, W. J., to be published in *Physica*.
10. LUBBERS, J., private communication.
11. HARTSHORN, L., *J. Sci. Instr.*, 2(1925)145.
12. CASIMIR, H. B. G., DE HAAS, W. J. and DE KLERK, D., *Physica* 6(1939)241.
13. We are much indebted to Mr. R. Hulstman for the design and construction of the temperature stabilizing unit.
14. VAN KEMPEN, H., MIEDEMA, A. R. and HUISKAMP, W. J., *Physica*, 30 (1964)229, Communication No. 336c, Leiden.
15. ANDERSON, A. C., HOLMSTRÖM, B. and KRUSIUS, H., *Phys. Rev. Letters* 20(1968)154.

## Chapter III

SPECIFIC HEAT SINGULARITIES OF THE ISING  
ANTIFERROMAGNETS  $\text{CoCs}_3\text{Cl}_5$  AND  $\text{CoCs}_3\text{Br}_5$ 

## 1 Introduction

$\text{CoCs}_3\text{Cl}_5$  and  $\text{CoCs}_3\text{Br}_5$  are attractive for studying thermodynamic and magnetic<sup>1)</sup> properties for the following reasons:

1. the crystallographic structure is known<sup>2,3)</sup> to be relatively simple and shows that all Co ions are equivalent. When the tetragonal structure is simplified in one detail concerning Cs ions, one may view the Co ions as being arranged in a simple Bravais lattice, which is a slightly elongated cube.
2. electron paramagnetic resonance data<sup>4,5,6)</sup> show in both salts that the Co ion has, as far as its lowest doublet is concerned, a very anisotropic  $g$ -value and consequently these salts are probably fair examples for the Ising model. In this case one has effective spin  $\frac{1}{2}$  and a uniaxial  $g$ -tensor.
3. these compounds are chemically stable and single crystals can be grown relatively easily.

When it was reported by Van Stapele<sup>7)</sup> that these compounds obey Curie's law at temperatures as low as a few Kelvin we initiated an investigation on the properties of these salts below 1 K<sup>8)</sup>. In view of the interest in the properties of the three-dimensional Ising model<sup>9)</sup>, we studied in particular the critical behaviour of these salts in the vicinity of the transition point. Since the Ising model provides a relatively large amount of numerically accurate predictions<sup>10)</sup> on thermodynamic quantities, like the short-range ordering entropy and energy, it is interesting to apply this model to various substances. In this chapter we will be mainly concerned with the heat capacity, energy and entropy of  $\text{CoCs}_3\text{Cl}_5$  and  $\text{CoCs}_3\text{Br}_5$ . Experimental results on the magnetic properties of these crystals have been described by Mess et al.<sup>1)</sup>, which will be used extensively throughout this chapter.

## 2 Crystal structure and electron paramagnetic resonance data

The crystal structure of  $\text{CoCs}_3\text{Cl}_5$  has been determined by Powell et al.<sup>2)</sup> and in more detail by Figgis et al.<sup>3)</sup>. The dimensions of the tetragonal unit cell are at room temperature  $9.219 \pm 0.005 \text{ \AA}$  in the  $a$  and  $b$  directions and  $14.554 \pm 0.007 \text{ \AA}$  along the  $c$  axis; the unit cell contains four molecules of  $\text{CoCs}_3\text{Cl}_5$  and this corresponds to a density of 3.411 at room temperature.

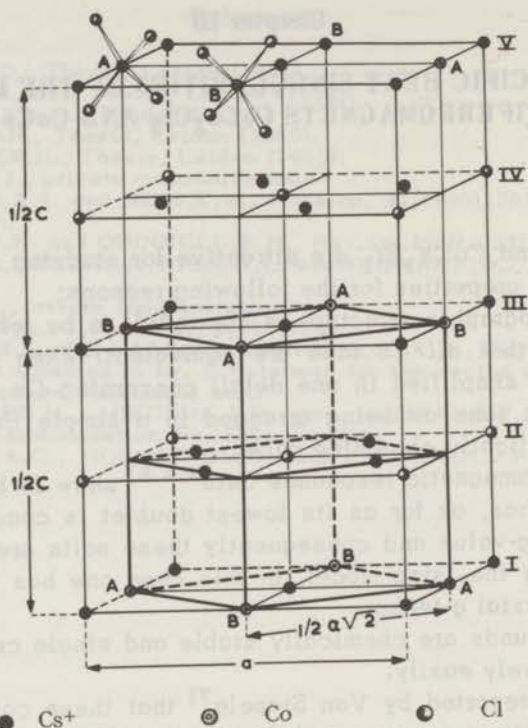


Fig. 1. Crystal structure unit cell of  $\text{CoCs}_3\text{Cl}_5$

The chlorine tetrahedra at position A and B are rotated around the  $c$  axis with respect to each other. Plane II differs from plane IV by a mirror reflection. The parallelepiped indicated by thick lines is the simple Co-Bravais lattice mentioned in the text.

$$\frac{1}{2}c = 7.277 \text{ \AA} \quad a = 9.219 \text{ \AA} \quad \frac{1}{2}a\sqrt{2} = 6.52 \text{ \AA}$$

One may divide the unit cell into two halves (fig.1) by a plane parallel to the  $ab$  axes (III in fig.1). The halves are equal except for a rotation of the  $\text{CoCl}_4$  group and mirror reflection of  $\text{ClCs}_4$  groups. Since the Cs ions will probably not participate significantly in the exchange interaction between Co ions we will henceforth consider the parallelepiped, indicated in fig.1, as the simple Bravais lattice for the Co ions. The positions of all Co ions can be obtained from translational operations of this Bravais lattice which has the dimensions  $\frac{1}{2}a\sqrt{2} = 6.519 \text{ \AA}$  and  $c/2 = 7.277 \text{ \AA}$  and contains one  $\text{CoCs}_3\text{Cl}_5$  molecule. This Bravais parallelepiped, therefore, is not very different from a cube and for our discussion we will regard the Co ion as having six nearest Co neighbours in a simple cubic (s.c.) environment. It may be

noted that the immediate surroundings of the Co ion consists of a tetrahedron of chlorine ions, having predominantly cubic symmetry. The structure of the  $\text{CoCs}_3\text{Br}_5$  is isomorphous to that of the chloride, while the unit cell dimensions are  $a = 9.619 \pm 0.003 \text{ \AA}$  and  $c = 15.163 \pm 0.003 \text{ \AA}$ , which gives  $\frac{1}{2}a\sqrt{2} = 6.801 \text{ \AA}$  and  $c/2 = 7.582 \text{ \AA}$  at room temperature and a specific density of 4.06.

E.P.R. measurements<sup>5)</sup> on both  $\text{CoCs}_3\text{Cl}_5$  and  $\text{CoCs}_3\text{Br}_5$  were obtained at 77K and, using pulsed fields, also at 4K<sup>6)</sup>. Temperature variation did not yield any significant change in the results of measurements on the constants in the spin-hamiltonian, which implies the absence of a phase transition to a lower symmetry when cooling the crystals. The spin-hamiltonian for the Co ion ( $S' = \frac{3}{2}$ ) is given by the expression:

$$H = D \left\{ (S'_z)^2 - \frac{S'(S'+1)}{3} \right\} + g_{//} \beta H_z S'_z + g_{\perp} \beta (H_x S'_x + H_y S'_y) + AS'_z I_z + B(S'_x I_x + S'_y I_y). \quad (1)$$

From the results it can be deduced that the fourfold degeneracy of the  $^4A_2$  ground state<sup>11)</sup> of the Co ion in a cubic field is removed by a tetragonal distortion due to a small elongation of the chlorine tetrahedron along the  $c$  axis. Further, it is found that the  $S'_z = \pm \frac{3}{2}$  doublet is lowest, where  $z$  coincides with the crystalline  $c$  axis for all ions, both in the chloride and in the bromide.

The experimental values for the constants of the spin-hamiltonian are given in table I<sup>6,12)</sup>. From the values of  $D$  (for instance  $2D/k = -12.4 \text{ K}$  in the chloride) we conclude that at temperatures of about 1K

TABLE I

	$D [\text{cm}^{-1}]$	$g_{//}$	$g_{\perp}$	$A [10^{-4} \text{cm}^{-1}]$	$B [10^{-4} \text{cm}^{-1}]$
$\text{CoCs}_3\text{Cl}_5$	$-4.30 \pm 1\%$	$2.40 \pm 1\%$	$2.30 \pm 1\%$	$23.6 \pm 0.4^{12)}$	$10.0 \pm 0.4$
$\text{CoCs}_3\text{Br}_5$	$-5.34 \pm 2\%$	2.42	2.32	$32.0 \pm 0.6$	$21.7 \pm 1.8$

one deals practically exclusively with the  $S'_z = \pm \frac{3}{2}$  doublet; henceforth we will assign an effective spin  $S = \frac{1}{2}$ ,  $g_{//} = 7.29$  and  $g_{\perp} = 0$  to this doublet.

The fact that the ground doublet is fairly accurately described by  $S'_z = \pm \frac{3}{2}$  wave functions (implying  $g_{\perp} = 0$ ) is also corroborated by observations on  $S'_z = \pm \frac{3}{2} \rightarrow S'_z = -\frac{1}{2}$  transitions. Such transitions were observed if the external field made a small angle with the  $c$  axis, but vanished for  $\vec{H} // c$ .

The occurrence of  $g_{\perp}=0$  in combination with uniaxial symmetry for all (equivalent) Co ions makes these salts very interesting for low temperature investigations. Anticipating that exchange interactions are small compared to the energy difference,  $\Delta \approx 2D$ , between the two doublets, we may consider the exchange to be confined to the z-components of the spin. Denoting the maximum and minimum energies for a pair of interacting spins by  $+J'$  and  $-J'$ <sup>10</sup>, the Hamiltonian for this system takes the form

$$H = -\frac{J'}{S^2} \sum_{\substack{i,j \\ i < j}} S_i^z S_j^z \quad (S = \frac{1}{2}). \quad (2)$$

If the exchange interaction energy were much larger than  $\Delta$ , we would consider a Heisenberg hamiltonian e.g.

$$H = -\sum_{\substack{i,j \\ i < j}} 2JS_i \cdot S_j \quad \text{for} \quad S = \frac{3}{2}. \quad (3)$$

This gives the relation  $J = \frac{2}{9}J'$ .

### 3 Experiment

The experimental arrangement is described in Chapter II, section 2. The crystals used for the preliminary measurements were drawn from the melt. Those used for the more precise measurements have been obtained from an aqueous solution of  $\text{CoCl}_2$  and  $\text{CoBr}_2$  respectively, with an excess of moles  $\text{CsCl}$ .

A single crystal of  $\text{CoCs}_3\text{Cl}_5$  mounted between brass plates is liable to fracture on cooling, which deteriorates the thermal contact. Therefore, we have preferred to measure the specific heat singularity on a powdered sample. The sizes of the crystals are estimated to be of the order of 0.1 mm.

### 4 Results

The specific heat,  $C_{\text{magn}}$  of purely magnetic origin, is plotted for  $\text{CoCs}_3\text{Cl}_5$  in fig. 2a and for  $\text{CoCs}_3\text{Br}_5$  in fig. 3. It is seen that sharp lambda type anomalies occur at  $T_N \approx 0.52 \text{ K}$  for the chloride and at  $T_N \approx 0.28 \text{ K}$  for the bromide. While the maxima in the two curves are approximately equal, the forms of the curves differ appreciably. In order to obtain  $C_{\text{magn}}$  and to deduce values for the entropy,  $S$ , and energy,  $E$ , a few corrections and approximations have to be applied.

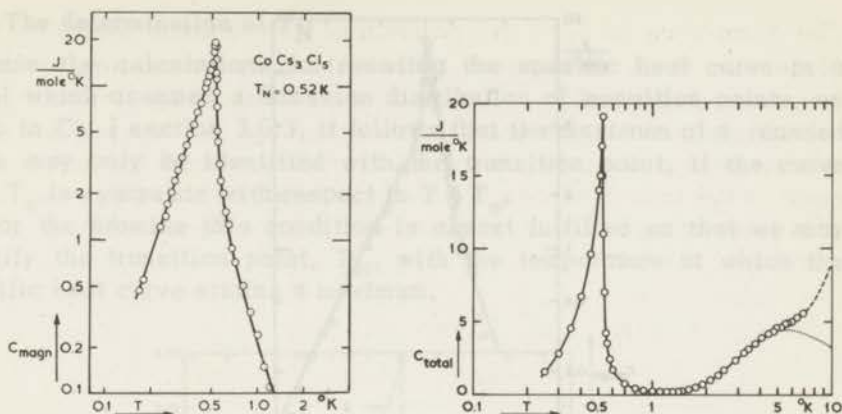


Fig. 2a. Heat capacity  $C_{\text{magn}}$  of  $\text{CoCs}_3\text{Cl}_5$  in joules/mole K versus temperature  $T$ .

Fig. 2b. Curve of fig. 2a plotted on a linear  $C$ -scale and including the Schottky anomaly (dotted) due to doublet  $2D/k = -12.4$  K. The  $T^3$ -contribution of the lattice is given by the difference of the dashed and the dotted curves.

a. At temperatures above 1 K, particularly for the chloride, contributions to the specific heat of the next higher doublet (at 12.4 K) and also of the lattice have to be subtracted. These contributions were determined in a calorimetric experiment<sup>13)</sup> between 1.5 K and 7 K, and were found to amount to 5% at 1 K and are insignificant for our data below 1 K (fig. 2b).

The results in the chloride at about 1 K must be considered to be relatively imprecise, due partly to inaccuracy in our measurements and also to the applied corrections. It is therefore appropriate to compare these results with the  $b/T^2$  heat capacity at temperatures between 1.3 and 4 K determined by means of adiabatic susceptibility measurements at high frequencies (as mentioned in ref. 1). A value of  $b = 0.163$  joule K/mole is found for the chloride and we will use this value for extrapolation of  $C_{\text{magn}}$  starting at  $T = 1.1$  K. This portion of  $C_{\text{magn}}$  contributes only 1½% to the total entropy.

b. A possible contribution to the heat capacity may arise from hyperfine structure (h.f.s.) interaction at low temperatures. This contribution,  $C_{\text{hfs}}$ /mole, can be calculated in the magnetically ordered state according to

$$C_{\text{hfs}}/R = \frac{1}{3} I(I+1) \frac{9A^2}{4k^2 T^2} \quad (4)$$

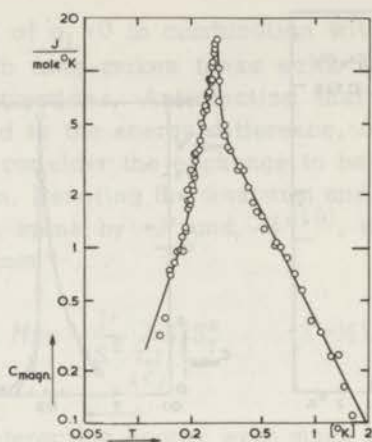


Fig. 3. Heat capacity  $C_{\text{magn}}$  of  $\text{CoCs}_3\text{Br}_5$  in joules/mole K versus temperature  $T$ .

where  $A/k$  is  $0.0034 \text{ K}$  in the chloride. This leads to  $C_{\text{hfs}}/\text{mole} = 1.13T^{-2} \text{ mJ/K}$  and may therefore be neglected except at the very lowest temperatures where, however, nuclear spin-lattice relaxation times may become very long.

c. Evidence for lack of temperature equilibrium between lattice and electron spin system is found at the far end of the low temperature side of the peak in both salts, particularly in the bromide. Thus the lowest two isolated points in the curve of fig. 2a have to be considered as relatively inaccurate. Hence we have extrapolated the curve for the chloride downwards starting at  $T = 0.23 \text{ K}$  with the aid of a molecular field approximation for the specific heat. For this purpose we find that the specific heat at  $T = 0.23 \text{ K}$  would require a molecular field,  $H_m$ , at this temperature of about  $2500 \text{ Oe}$ . On the basis of this value of  $H_m$  we calculate for the entropy yield below  $T = 0.24 \text{ K}$  a value of  $0.018 R$ .

Using the above extrapolations we find for the total entropy yield in the chloride  $\Delta S = 0.698 R$ , compared to  $R \ln 2 = 0.693 R$ . A similar procedure may be applied to the bromide. Here the  $T^{-2}$ -dependence at the high temperature side of the peak is much more clearly established. Further, at the low temperature side the specific heat has been measured to low values, so that contributions from the extrapolated portions of the curve are small. We find for  $\Delta S$  in the bromide  $0.678 R$ , which is 2% less than  $R \ln 2$ , and this has probably to be attributed to the mentioned lack of spin-lattice equilibrium.

#### 4.1 The determination of $T_N$

From the calculations for rounding the specific heat curve in a model which assumes a Gaussian distribution of transition points, as given in Ch. I section 3.6.3, it follows that the maximum of a rounded curve may only be identified with the transition point, if the curve near  $T_c$  is symmetric with respect to  $T - T_c$ .

For the bromide this condition is almost fulfilled so that we may identify the transition point,  $T_N$ , with the temperature at which the specific heat curve attains a maximum.

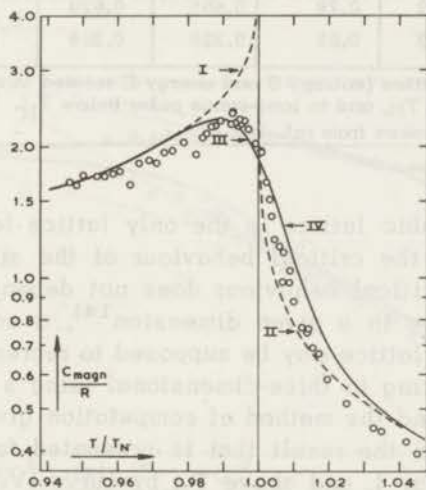


Fig. 4. The logarithm of the specific heat,  $C_{\text{magn}}/R$ , for  $\text{CoCs}_3\text{Cl}_5$  is plotted as a function of  $T/T_N$ .  $T_N = 0.527\text{ K}$  according to the arguments given in the text. Curve I represents the theoretical result for the s.c. Ising  $s = \frac{1}{2}$  lattice (ref. 20) for  $T < T_N$ . Curve II: idem for  $T > T_N$  (ref. 21). Curve III: the theoretical curve for  $T < T_N$  calculated for a Gaussian distribution of transition points, with halfwidth  $F = 0.014 T_N$  (see Ch. I section 3.6.3. Curve IV: idem for  $T > T_N$ .

For the chloride the specific heat curve is strongly asymmetric (fig.4), so that the maximum is shifted towards a lower temperature. The critical temperature may nevertheless be located fairly precisely by the following considerations. As far as the ground doublet is concerned, this salt may be expected to behave according to the Ising model ( $g_{\parallel} \gg g_{\perp}$ ). If in first approximation  $T_N$  is chosen as the temperature at which the specific heat attains a maximum ( $T_{\text{max}} = 0.523\text{ K}$ ), an evaluation of the critical parameters (as defined in table II) indicates that the ordering is three-dimensional. As mentioned in Ch. I section

TABLE II

Thermodynamic quantity	CoCs <sub>3</sub> Cl <sub>5</sub> exp	CoCs <sub>3</sub> Br <sub>5</sub> exp	Ising s.c.	Ising b.c.c.	Ising s.square	Ising triang.
$(S_{\infty} - S_c)/R$	0.106	0.357	0.133	0.107	0.387	0.363
$(S_c - S_o)/R$	0.593	0.321	0.560	0.586	0.306	0.330
$(S_{\infty} - S_c)/R \ln 2$	0.153	0.515	0.192	0.155	0.557	0.526
$-E_c/RT_N$	0.173	0.51	0.218	0.169	0.623	0.549
$(E_c - E_o)/RT_N$	0.459	0.27	0.447	0.460	0.275	0.258
$E_{tot}/RT_N$	0.632	0.78	0.665	0.629	0.881	0.874
$-E_c/E_{tot}$	0.272	0.65	0.328	0.269	0.706	0.666

Thermodynamic quantities (entropy S and energy E related to short-range order above the critical point  $T_N$ , and to long-range order below  $T_N$ ). The theoretical predictions have been taken from ref. 10.

3.6.3, the simple cubic lattice is the only lattice for which explicit formulae describing the critical behaviour of the specific heat are available. As the critical behaviour does not depend sensitively on the specific structure in a given dimension<sup>14</sup>), a calculation of the rounding for the s.c. lattice may be supposed to represent the essential features of the ordering in three-dimensional Ising  $s = \frac{1}{2}$  systems. By using the formulae and the method of computation given in Ch. I section 3.6.3, we obtain the result that is presented for  $T < T_N$  by the drawn curve III in fig. 4, and above  $T_N$  by curve IV. We have used a Gaussian distribution of transition temperatures with a half-width of  $0.014 T_N$ , giving the same maximum as the experimental curve. As one may notice from fig. 4, the overall temperature dependence is fairly well described by the assumed model.

It is clear that the maxima of the curves do not coincide with the critical temperature, but are shifted about 0.7 to 1% towards the low-temperature side. However, the calculated curve is slightly broader than the experimental curve, hence  $T_N$  is not yet fixed accurately. Therefore, in a second approximation we have determined  $T_N$  more precisely (at  $0.527 \pm 0.001$  K), by assuming that the high-temperature side of the experimental curve coincides with the prediction<sup>15</sup>) for the b.c.c. curve for  $T > 1.04 T_N$ . The use of the b.c.c. model is justified since the values of the critical parameters, (given in table II), obtained with  $T_N = 0.527$  K, strongly suggest that the properties of CoCs<sub>3</sub>Cl<sub>5</sub> may be described by a statistical model of 8 effective nearest neighbours in three dimensions.

## 4.2 The critical behaviour

The experimental points may now be represented as a function of  $T/T_N$ . In fig. 4 the logarithm of the magnetic specific heat  $C_{\text{magn}}/R$  is plotted versus  $T/T_N$ . The dashed curves I and II represent the theoretical predictions for the s.c. Ising  $s=1/2$  model mentioned in the preceding section. The drawn curves III and IV represent the rounded theoretical curves for  $T$  below and above  $T_N$ , respectively. In figs. 5 and 6 the temperature is displayed in the form  $1-(T/T_N)^s$ , where  $s=+1$  for  $T < T_N$ , and  $s=-1$  for  $T > T_N$ . In fig. 5 we have plotted the results on a logarithmic scale. The curves I to IV have already been introduced in fig. 4.

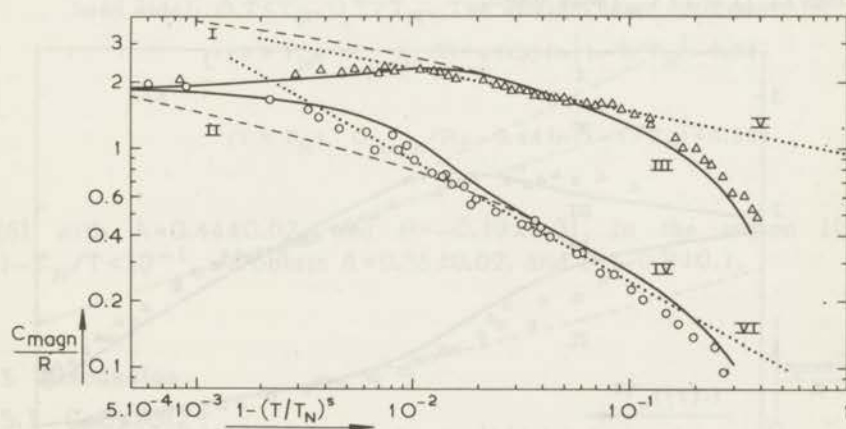


Fig. 5. Heat capacity,  $C_{\text{magn}}/R$ , of  $\text{CoCs}_3\text{Cl}_5$  plotted on a logarithmic scale vs.  $1-(T/T_N)^s$ , with  $s=+1$  for  $T < T_N$ , and  $s=-1$  for  $T > T_N$ . Curves I to IV are defined in the caption of fig. 4. The dotted line V represents the asymptotic behaviour according to formula (5) for  $T < T_N$ , with  $B=0.95 \pm 0.05$  and  $\alpha' = 0.19 \pm 0.04$ . The dotted line VI represents the power-law behaviour for  $T > T_N$  with  $B=0.070 \pm 0.05$  and  $\alpha=0.50 \pm 0.05$ .

We notice that the theoretical curves III and IV agree fairly well with the experimental results over the whole temperature region above and below  $T_N$ . On the low-temperature side, in the limited region  $10^{-2} < 1-T/T_N < 10^{-1}$ , a power law dependence of the form

$$C_{\text{magn}}/R = B \left(1 - \frac{T}{T_N}\right)^{-\alpha}, \quad (5)$$

with  $B=0.95 \pm 0.05$  and  $\alpha'=0.19 \pm 0.04$  describes the experimental results reasonably well. This is shown by the dotted line V in fig. 5.

On the high-temperature side the experimental behaviour in the region  $3 \cdot 10^{-3} < 1 - T_N/T < 10^{-1}$  may be expressed by a power law (5), with the constants  $B = 0.070 \pm 0.05$ , and  $\alpha = 0.50 \pm 0.05$ . This is shown by the dotted line VI in fig. 5.

As to the values of the constants  $B$  and  $\alpha$  for the high-temperature side, we mention that they are different from those published in previous analyses of the data<sup>16,17</sup>):  $B = 0.042$  and  $\alpha = 0.75$ . This difference arises mainly from the choice of  $T_N$  as  $0.527$  K instead of  $T_N = 0.523$  K in refs. 16 and 17 (see section 4.1). A difference of minor importance is formed by the choice of the temperature axis:  $1 - T_N/T$  in conformity with formula (5) given in theoretical publications, whereas in refs. 16 and 17  $|1 - T/T_N|$  was used.

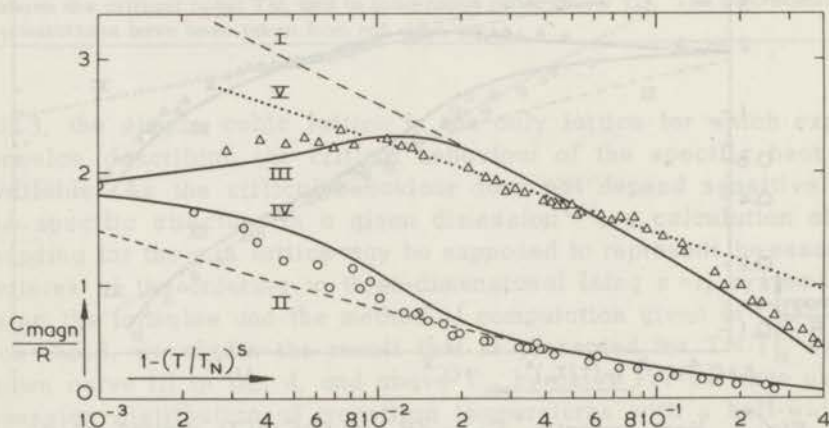


Fig. 6. Heat capacity  $C_{\text{magn}}/R$  of  $\text{CoCs}_3\text{Cl}_5$  plotted on a semi-logarithmic scale vs.  $1 - (T/T_N)^s$ , with  $s = +1$  for  $T < T_N$ , and  $s = -1$  for  $T > T_N$ . Curves I to IV are defined in the caption of fig. 4. Line V represents the asymptotic behaviour for  $T < T_N$  according to formula (6) with  $A = 0.35 \pm 0.03$  and  $B = 0.64 \pm 0.05$ .

In fig. 6 the results are plotted on a semilogarithmic scale. The temperature dependence on the low temperature side, in the region  $10^{-2} < 1 - T/T_N < 10^{-1}$ , is equally well described by a logarithmic function. This is shown by the relation

$$C_{\text{magn}}/R = -A \ln |1 - T/T_N| + B, \quad (6)$$

with  $A = 0.35 \pm 0.03$ , and  $B = 0.64 \pm 0.05$ .

Similarly for the bromide in the region  $10^{-2} < 1 - T/T_N < 10^{-1}$ , ( $T < T_N$ ), we observe a behaviour described by the logarithmic function

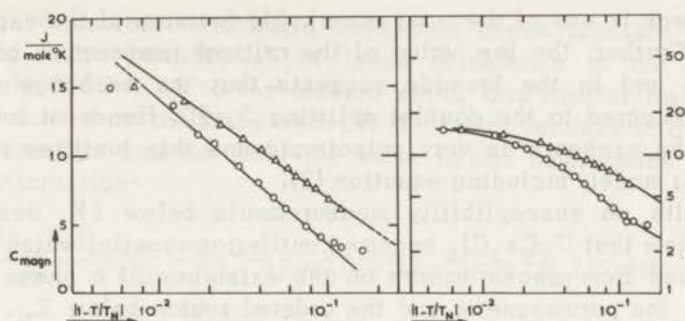


Fig. 7. Heat capacity of  $\text{CoCs}_3\text{Br}_5$  plotted on double logarithmic scales (right-hand side) and on a semilogarithmic scale (left hand side).  $\Delta T < T_N$ ,  $\circ T > T_N$ . The straight lines correspond to

$$(T > T_N) \quad C_{\text{magn}}/R = -0.55 \ln |1 - T/T_N| - 0.83$$

and

$$(T < T_N) \quad C_{\text{magn}}/R = -0.44 \ln |1 - T/T_N| + 0.193$$

(6) with  $A = 0.44 \pm 0.02$ , and  $B = -0.19 \pm 0.01$ . In the region  $10^{-2} < 1 - T_N/T < 10^{-1}$ , we obtain  $A = 0.55 \pm 0.02$ , and  $B = -0.8 \pm 0.1$ .

## 5 Discussion

### 5.1 $\text{CoCs}_3\text{Cl}_5$

#### 5.1.1 Features of the magnetic ordering

From the data (in table II) on entropy and energy it may be seen that the experimental results agree fairly well with the Ising  $s = \frac{1}{2}$  model predictions for a body-centered-cubic structure with coordination number  $z = 8$ . However, in view of the crystal structure which closely resembles a simple cubic lattice ( $z = 6$ ), this result is not likely to have much significance. Therefore, we adopt  $z = 6$  and regard the tendency of the experimental results towards a higher coordination number ( $z = 8$ ) as originating from dipolar interactions and possibly also next-nearest neighbour (n.n.n.) exchange, both of which increase the effective value of  $z$ .

Concerning the Heisenberg model, theoretical values for the thermodynamic quantities of table II are available only to a limited extent<sup>14)</sup>, but the entropy and energy involved in short range ordering are appreciably larger and do not correspond to our experimental results. The sharp descent of the specific heat curve at the high temperature side

of the peak is one of the most remarkable features of the experimental result. Further, the low value of the critical temperature both in the chloride and in the bromide suggests that the exchange energy is small compared to the doublet splitting  $\Delta = 2D$ . Hence at low temperatures the exchange is very anisotropic and this justifies the use of the Ising model, including equation (2).

Results on susceptibility measurements below 1 K, described in ref. 1, show that  $\text{CoCs}_3\text{Cl}_5$  becomes antiferromagnetic, which is further also found from measurements on the existence of a phase boundary between the paramagnetic and the ordered region below  $T_N$ . From  $z=6$  and  $T_N=0.52\text{K}$  a Curie-Weiss constant is to be expected, for instance on basis of a molecular field calculation, of at least a few Kelvin. The experimental result (given in ref. 1) however, is  $\theta = -0.24 \pm 0.02\text{K}$ . Such a low value of  $\theta$  can be explained by assuming that 2 of the 6 nearest neighbours have an exchange coupling of the ferromagnetic sign. In view of the crystal symmetry, these two ions have to be found in the direction of the  $c$  axis. The most simple model in which the above arguments are incorporated, consists of two interpenetrating square sublattices in the  $ab$  plane with antiparallel nearest neighbours and ferromagnetically coupled linear chains along the  $c$  axis.

### 5.1.2 Exchange

The total energy gain in the magnetic ordering process (cf. table II) equals  $0.333 R K$ , from which one derives with the aid of  $E/R = \frac{1}{2}zJ'/k$  and assuming coordination number  $z = 6$  for the number of nearest neighbours in the lattice, that the effective exchange constant  $J'_{\text{eff}}/k = 0.111\text{K}$ . In order to obtain the pure exchange constant, defined in eq. (2) the above result has to be corrected for dipolar coupling. The dipolar interaction in the fully ordered state can easily be calculated since  $g_{\perp} = 0$ . The latter circumstance means that only the  $z$  component of the dipolar field is relevant, which is given by

$$H_{\text{dip}}^z = \sum_{i=2}^{\infty} \frac{g\mu_B S_1^z}{r_i^3} (1 - 3\cos^2 \theta_i) \quad (7)$$

where  $\theta_i$  is the angle subtended by the  $z$  axis and the line connecting ion  $i$  with the origin ( $i=1$ ). A computer calculation for the nearest 1654 neighbours extending to a radius of  $50\text{\AA}$ , resulted in a dipolar field of  $520\text{Oe}$ , assuming 4 antiparallel n.n. in the  $ab$  plane and 2 parallel n.n. along the  $c$  axis. This number fluctuates less than 10% when the number of neighbours is reduced by decreasing the radius of the surrounding sphere down to  $10\text{\AA}$  in steps of  $5\text{\AA}$ . The arrange-

ment of the 6 nearest neighbours mentioned above provides an exceptionally large contribution of these neighbours to the dipolar field, namely 870 Oe. As to the ordered state, this dipolar field does not detract much from the Ising model in our case: because of  $g_{\perp}=0$  the dipolar interaction has not only the same formal hamiltonian as the exchange interaction

$$H = - \sum_{\substack{i,j \\ i > j}} \frac{J'_{\text{dip}}(i,j)}{S^2} S_i^z S_j^z = \sum_{\substack{i,j \\ i > j}} r_{ij}^{-3} q^2 // \mu_B^2 S_i^z S_j^z (1 - 3 \cos^2 \theta_{ij}) (S = \frac{1}{2}), \quad (8)$$

but also is mainly confined to n.n. interaction and does not obtain any significant contributions from distant ions  $r > 10 \text{ \AA}$ ).

The value of  $J'_{\text{eff}}$  corresponds at  $T=0$  to a molecular field of 2780 Oe. Subtracting the dipolar field gives an exchange field of 2260 Oe, which corresponds to an average exchange constant of

$$|J'/k| = 0.0905 \quad \text{or} \quad |J/k| = 0.0201 \text{ K.}$$

Recent results of Van Stapele, Henning, Hardeman and Bongers<sup>18)</sup> on electron-paramagnetic-resonance of exchange coupled  $\text{Co}^{2+}$  pairs in  $\text{Cs}_3\text{ZnCl}_5$  show that the exchange interaction between n.n. in the  $ab$  plane has the antiferromagnetic sign ( $J/k = -0.0204 \text{ K}$ ) and the exchange interaction between n.n. along the  $c$  axis has the ferromagnetic sign ( $J/k = +0.0154 \text{ K}$ ). These exchange constants, averaged over 6 n.n. give  $|J_{\text{av}}/k| = 0.0187 \text{ K}$ , which is only 7% below our value. The difference may be due to next-nearest-neighbour-exchange (n.n.n.), dipolar interactions and, to a small extent, to the difference in lattice constants between the cobalt- and zinc compounds. It seems safe to conclude that n.n. interactions predominate in the chloride and that we may neglect n.n.n. interaction except for (n.n.n.) dipolar interaction. The dipolar field from all but n.n. amounts to  $-350 \text{ Oe}$  at  $T=0$  and decreases in importance at higher temperatures, e.g. it contributes only about 1% to the heat capacity at high  $T$ .

### 5.1.3 Singularity

For the critical behaviour of the specific heat it is important in our case that theoretically the Ising model does not discriminate between antiferromagnetic and ferromagnetic coupling. Further, in  $\text{CoCs}_3\text{Cl}_5$  the magnitude of exchange and dipolar interactions combined happen to be approximately equal for n.n. in the  $ab$  plane and for n.n. along the  $c$  axis: taking E.P.R. data in  $\text{ZnCs}_3\text{Cl}_5$  mentioned in section 5.1.2, one calculates

$$J^c = J_{\text{ex}}^c + J_{\text{dip}}^c = +0.120 \text{ k K}, \quad (9)$$

and

$$J^{\text{ab}} = J_{\text{ex}}^{\text{ab}} + J_{\text{dip}}^{\text{ab}} = -0.122 \text{ k K}. \quad (10)$$

where  $J_{\text{ex}}^c$  is the exchange constant in  $(J'/S^2) S_i S_j$  and  $J_{\text{dip}}^c$  is the coupling constant in eq. (8). Hence  $|J^c| \approx |J^{\text{ab}}|$  and  $\text{CoCs}_3\text{Cl}_5$  may be considered a fair representation of a simple cubic (i.e. coordination number 6) Ising system in the study of the specific heat singularity.

For temperatures below the critical temperature, the prediction of the behaviour of  $C_{\text{magn}}$  as a function of  $T$  is imprecisely known because of the slow convergence of the low-temperature specific-heat series. The power  $\alpha'$  in the divergence of the specific heat (see formula (5)) is estimated<sup>19)</sup> as  $\alpha' = 0.07 \begin{smallmatrix} +0.16 \\ -0.04 \end{smallmatrix}$ . Such a low power law may look deceptively like a logarithm (see formula (6)), especially in the temperature region, where the constant term  $B$  is not negligible with respect to the first right-hand term of (6). This may be illustrated by the comparison of the two different asymptotic relations (curve V in fig. 5, and curve V in fig. 6) which describe the experimental behaviour equally well in the same temperature region. This result justifies the use of the logarithmic temperature dependence<sup>20)</sup> for the calculation of the specific heat near  $T_N$ . Outside the temperature region in which the specific heat curve is rounded ( $T/T_N < 0.98$ ), the theoretical result (curve I in figs. 4, 5 and 6) gives a good description of the experimentally observed temperature dependence of the specific heat.

Above  $T_N$  the theoretical predictions for the cubic Ising  $s = \frac{1}{2}$  lattices<sup>21,15)</sup> are very precise. By using results of the form given in Ch. I section 3.5.1, we have explicitly calculated the  $C_{\text{magn}}/R$  vs.  $T$  predictions for the temperature region studied (curve II in figs. 4, 5 and 6 for the s.c. lattice). It may be noticed that agreement between theory and experiment is very good up to the region in which the rounding occurs ( $1 < T/T_N < 1.02$ ). The tendency towards a coordination number 8 viz. a lower specific heat above  $T_N$  than for  $z = 6$ , is evident from table II and from the figs. 5 and 6.

One may observe from fig. 5 that the Ising model prediction for a s.c. system in which a spread in transition points is assumed (irrespective of the physical origin, see e.g. Ch. I section 3.6) may be described by a power law with  $\alpha$  as large as 0.50 for a large temperature region ( $0.006 < 1 - T_N/T < 0.02$ ). Secondly we may remark that the critical exponent,  $\alpha = \frac{1}{8}$ , involved in the singular part of the formula describing the temperature dependence of the cubic Ising models, will only be observed in a plot on a logarithmic scale if  $1 - T_N/T$  is of the

order of  $10^{-8}$ . Clearly, however, this region lies outside the experimentally accessible range.

We conclude that it is experimentally found that a three dimensional Ising system has an extremely sharp peak in the specific heat for  $T > T_N$  and that at the low temperature side probably a logarithmic dependence predominates. It may be of interest to study further critical properties in this salt, notably the sublattice magnetization.

#### 5.1.4 Specific heat below $T_N$

Baker<sup>20)</sup> has calculated the specific heat curve for temperatures near  $T_N$  and also appreciably lower than  $T_N$  in case of a simple cubic Ising spin system. From his curve we calculate, taking  $J'/k = 0.12$  K from the previous section, a theoretical curve, which is shown in fig.8.

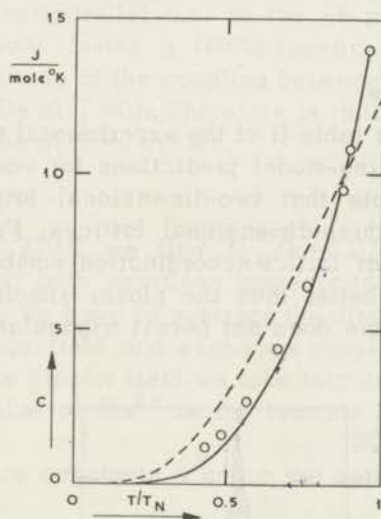


Fig. 8. Heat capacity of  $\text{CoCs}_3\text{Cl}_5$  below  $T_N$  plotted versus  $T/T_N$ . The circles denote experimental results. The dotted curve represents molecular field theory, the drawn curve gives the result of Baker's calculation on a simple cubic Ising model.

When the experimental data are plotted on a reduced temperature scale,  $T/T_N$ , there is reasonable agreement, at least when contrasted to molecular field theory. (The use of molecular field theory for extrapolating to  $T=0$  in section 4 remains a good approximation, since there the dotted curve was fitted to the experimental points at relatively high  $T$  by choosing an appropriate value of the molecular field at  $T=0$ ). The experimental result indicates that the heat capacity in this

three-dimensional Ising system goes to zero even more rapidly than according to molecular field theory.

The choice of the exchange constant  $J'/k = 0.12\text{K}$  implies the position of  $T_N$  in the Ising model; in a simple cubic lattice  $kT_N/zJ' = 0.752$  is predicted, which may be compared to the experimental ratio  $0.527/0.720 = 0.731$ . In this comparison only n.n. dipolar interaction is accounted for, in virtue of the discussion of section 5.1.3. Going to the other extreme of including all dipolar coupling by taking  $J'_{\text{eff}} = 0.111\text{kK}$ , one would obtain  $kT_N/zJ'_{\text{eff}} = 0.795$ . Since dipolar interactions of distant neighbours become relatively unimportant at high  $T$ , it is not unreasonable that an exchange constant intermediate between  $J'/k = 0.12\text{K}$  and  $J'_{\text{eff}}/k = 0.111\text{K}$  has to be taken in order to arrive at the experimental  $T_N = 0.527\text{K}$  with the aid of the theoretical s.c. Ising model ratio  $kT_N/zJ' = 0.752$ .

## 5.2 $\text{CoCs}_3\text{Br}_5$

### 5.2.1 Magnetic structure

From a comparison in table II of the experimental results on energy and entropy with the Ising-model predictions for various geometrical structures, one may note that two-dimensional lattices give much better agreement than three-dimensional lattices. Further it is seen that the planar triangular lattice (coordination number 6) predictions fit the data somewhat better than the planar simple square lattice. Since the crystal structure does not permit triangular spin arrays, the

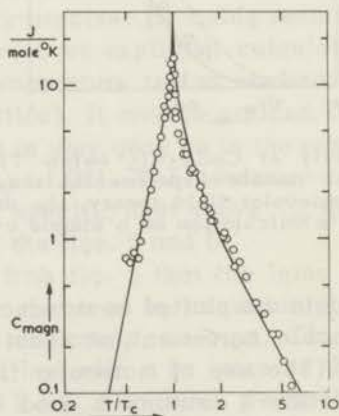


Fig. 9. Heat capacity of  $\text{CoCs}_3\text{Br}_5$  (circles are experimental points) compared to the theoretical curve of Onsager for a two-dimensional simple square Ising (anti) ferromagnet.

outcome of the above comparison is suggestive of mainly two-dimensional ordering in a simple square structure, however, with an additional tendency of the Co-spins to have a somewhat higher coordination number than  $z = 4$ .

From phase boundary and susceptibility measurements, described in ref. 1, one finds that  $\text{CoCs}_3\text{Br}_5$  becomes antiferromagnetic and that the Curie-Weiss constant is even much smaller than in the chloride; further,  $\text{CoCs}_3\text{Br}_5$  is found<sup>1)</sup> to show properties, which agree with theoretical predictions for a two-dimensional Ising model. Therefore we plotted our heat capacity results on a reduced temperature scale  $T/T_N$ , and compared them with the exactly calculated curve of Onsager<sup>22)</sup> for a simple square (anti-)ferromagnetic Ising model, as shown in fig.9. Although there is some disagreement at  $T > T_N$ , one may note a striking similarity between the experimental results and Onsager's curve.

Assuming 4 antiparallel n.n. in the  $ab$  plane, one finds that the dipolar interactions favour a ferromagnetic coupling between the  $ab$  planes (the magnitude of the coupling between adjacent planes amounting to about 90 Oe at  $T = 0$ ). Therefore is quite possible that the same magnetic structure at  $T = 0$  occurs.

### 5.2.2 Exchange

From  $E/R = 0.220 \text{ K}$  we find  $J'_{\text{eff}}/k = 0.073^3 \text{ K}$  if  $z = 6$ , or  $J'_{\text{eff}}/k = 0.110 \text{ K}$  if  $z = 4$ ; both solutions correspond to a molecular field of 1820 Oe at  $T = 0$ . We have to subtract the dipolar field in order to find the pure exchange field and exchange coupling constant  $J'$ . For the calculation of the dipolar field we take into account:

1. that the  $g$ -value of  $\text{Co}^{2+}$  in the bromide is 1% larger than in the chloride
2. that the lattice constants  $a$  and  $c$  are both 4.2% larger than in the chloride
3. that at  $T = 0$  there are 4 antiparallel n.n. in the  $ab$  plane and two parallel n.n. along the  $c$  axis.

This yields  $H_{\text{dip}} = 460 \text{ Oe}$ , so that after subtraction of  $H_{\text{dip}}$  the residual exchange field is 1360 Oe, corresponding to an exchange constant

$$J'/k = -0.082 \text{ K} \quad (J/k = -0.018 \text{ K}),$$

if the coordination number is assumed to be four. Consequently, the bromide is, in view of the smallness of the ratio  $J'/D$ , perfectly anisotropic in conformity with the requirement of the Ising model. Neglecting for a while dipolar interactions and taking the parameter  $\frac{1}{2}zJ'_{\text{eff}}/k = E/R$

as representing the total exchange interaction for a comparison with  $T_N$ , we find

$$kT_N/zJ'_{\text{eff}} = 0.640.$$

This ratio is higher than predicted by the simple quadratic or triangular Ising lattices (0.567 and 0.607 respectively), but much lower than the predicted ratios for three-dimensional cubic lattices. In conjunction with the broad high temperature curve in  $C_{\text{magn}}$  and the values of  $S_{\infty} - S_c$  and  $E_{\infty} - E_c = -E_c$ , it may be concluded that it is relatively difficult to establish long-range order in this three-dimensional (almost cubic) spin arrangement. On the other hand, assuming mainly two-dimensional ordering to start with, the relatively strong dipolar interactions tend to promote long range order, giving higher  $T_N$  than would otherwise have been obtained for coordination number 4 or even 6 in a planar spin arrangement.

By means of electron-paramagnetic-resonance experiments on exchange-coupled pairs of Co ions in a  $\text{Co}^{2+}$ -doped  $\text{ZnCs}_3\text{Br}_5$  crystal<sup>12)</sup>, a relatively large ferromagnetic exchange coupling was deduced between a pair of n.n. ions along the *c*-axis, viz.  $J_{//}/k = 0.0106 \text{ K}$  which is equivalent to  $J'_{//}/k = 0.048 \text{ K}$ , whereas a smaller exchange coupling was found between a n.n. pair of ions in the *ab* plane, viz.  $J/k = -0.0049 \text{ K}$  or  $J'/k = 0.022 \text{ K}$ . The Curie-Weiss constant,  $\theta$ , derived from these exchange constants has the value  $+0.007 \text{ K}$ , which compares favourably with the experimental value  $\theta = -0.01 \pm 0.02 \text{ K}^{1)}$ . However, the agreement may be fortuitous as our value of  $J'_{\text{ex}}/k$  is much larger, which suggests the presence of next-nearest-neighbour exchange. Such an explanation would signify that the available interaction energy,  $E$  is shared among more than  $z = 4$  neighbours and this in turn will reduce the heat capacity at relatively high temperature. On the other hand, taking  $z = 4$  and consequently  $J'$  as high as possible in view of  $E/R$ , we find at high  $T$  and  $S = \frac{1}{2}$ ,

$$C/R \propto b/T^2 = \frac{1}{2}z(J'/kT)^2 = 0.024/T^2,$$

or  $b = 0.20 \text{ JK/mole}$ , to be compared to  $b = 0.33 \text{ JK/mole}$  in fig.3. Due to deviation from a  $1/T^2$  dependence at  $T \approx 2T_c$  in the Onsager curve, the theoretical value should be increased to  $b = 0.25$  for a proper comparison with the experimental result.

As to the caloric and magnetic<sup>1)</sup> results, the observed behaviour closely resembles that predicted for an isotropic two-dimensional antiferromagnetic Ising net. This result is suggestive of a fairly strong

coupling in  $ab$  planes and a smaller coupling between the successive planes. In order to comply with the experimentally found<sup>1)</sup> small value of  $\theta$ , one has to adopt some n.n.n. interaction.

Another interpretation of the results may be found by introducing a model that has a fairly strong coupling of a pair of ions along the  $c$  axis and a smaller coupling of a pair of ions in the  $ab$  plane ( $|J_{//}| > |J_{\perp}|$ ). This model incorporates the E.P.R. results of Henning et al.<sup>12)</sup>. It lies intermediate between a three dimensional Ising system ( $|J_{\perp}| = |J_{//}|$ ) and a linear Ising chain ( $|J_{\perp}|/|J_{//}| = 0$ ). If the ratio of the two interaction constants is such that the short-range ordering equals that found for a square Ising model, it might be supposed that these two systems will also resemble each other as to other thermodynamic properties, such as the singularity of the specific heat curve and the boundary between the antiferromagnetic and paramagnetic phases<sup>1)</sup>.

### 5.2.3 Singularity

The predominantly two-dimensional kind of the magnetic ordering suggested by various pieces of experimental evidence may also have a decisive influence on the character of the heat capacity singularity. We will compare the experimental results, which in fig.7 are seen to fit a logarithmic dependence of  $C_{\text{magn}}$  on  $|T - T_N|$  appreciably better than a  $|T - T_N|^{-\alpha}$  relation, to the exact theoretical calculation of Onsager<sup>22)</sup> near  $T_N$ . Onsager gives (eq.8.1 loc.cit.) an explicit  $\ln |T - T_N|$  dependence of the heat capacity at  $T \approx T_N$  in the form of an asymptotic formula:

$$C/R \propto f_1(T) \ln |T - T_N| + f_2(T), \quad (11)$$

where  $f_1$  and  $f_2$  are slowly varying compared to  $T - T_N$  (but not when compared to  $\ln |T - T_N|$ ). When evaluated numerically, eq.(11) is found to deviate by more than 35% at  $|1 - T/T_N| = 0.1$  from pure logarithmic behaviour, both for  $T < T_N$  and  $T > T_N$ , as may also be seen in fig.10.

The exact Onsager solution, on the other hand, agrees numerically at  $|1 - T/T_N| = 0.1$  to within 4% (fig.10) with

$$C/R = -0.49 \ln |1 - T/T_N| - 0.29. \quad (12)$$

We notice that it may be more effective to put theoretical results in the form of numerical computations versus  $T/T_N$  than to rely too heavily on asymptotic expressions when experimental data are to be compared to theory.

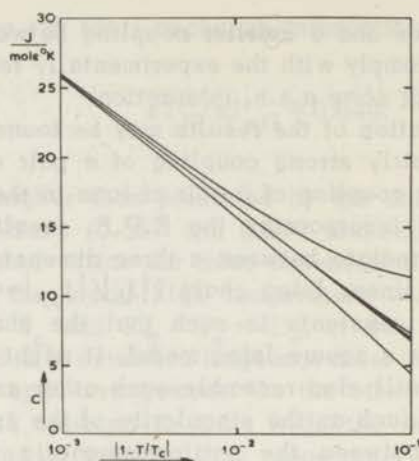


Fig. 10. Onsager's theoretical calculations on the heat capacity of a two-dimensional simple square Ising (anti)-ferromagnet plotted versus the logarithm of  $|1 - T/T_c|$ ,  $T_c$  being the critical temperature. The upper ( $T < T_c$ ) and lower ( $T > T_c$ ) curve refer to an asymptotic approximation containing an explicit  $\ln |1 - T/T_c|$  term; the curves in the middle are Onsager's exact calculations for  $T < T_c$  (lower middle) and  $T > T_c$  (upper middle) compared to a straight line (central)

$$C/R = -0.49 \ln \left| 1 - \frac{T}{T_c} \right| - 0.29.$$

As to our results on  $\text{CoCs}_3\text{Br}_5$  one may note that the two coefficients  $A$  in the regions  $T < T_N$  and  $T > T_N$  are  $-0.44$  and  $-0.55$  respectively, so that the theoretical coefficient lies between the two experimental coefficients. Similarly for  $\Delta$ , we obtain the values  $+0.2$  for  $T < T_N$  and  $-0.8$  for  $T > T_N$ , compared to  $-0.29$  of Onsager's solution.

Like in the energy and entropy consideration (5.2.2) one may ascribe the difference between the experimental coefficients and Onsager's theoretical one to deviations from two-dimensionality and coordination number four, probably due to long range dipolar forces.

Apart from these shortcomings it may be concluded that  $\text{CoCs}_3\text{Br}_5$  behaves, *grosso modo*, as a two-dimensional Ising antiferromagnet.

## References

1. MESS, K.W., LAGENDIJK, E., CURTIS, D.A. and HUISKAMP, W.J., Commun. Kamerlingh Onnes Lab., Leiden No. 354d; Physica 34(1967)126.
2. POWELL, H.M. and WELLS, A.F., J.chem.Phys. Soc. (1935)359.
3. FIGGIS, B.N., GERLOCH, M. and MASON, R. Acta Cryst. 17(1964)506.
4. BOWERS, K.D. and OWEN, J., Rep.Progr.Phys. 18(1955)304.
5. BELJERS, H.G., BONGERS, P.F., VAN STAPELE, R.P. and ZIJLSTRA, H., Phys. Letters 12(1964)81.
6. VAN STAPELE, R.P., BELJERS, H.G., BONGERS, P.F. and ZIJLSTRA, H., J. chem. Phys. 44(1966)3719.
7. VAN STAPELE, R.P., private communication.
8. MIEDEMA, A.R., WIELINGA, R.F. and HUISKAMP, W.J., Phys. Letters 17(1965)87.
9. DOMB, C., Magnetism Vol. IIA ed. G.T.RADO and SUHL, (Acad.Press, N.Y. 1965), p.1.
10. DOMB, C. and MIEDEMA, A.R., Progr. low Temp.Phys.IV, ed. C.J. Gorter, (North Holland Publ. Comp. Amsterdam 1964), p. 296.
11. GRIFFITH, J.S., The theory of transition metal ions, (University Press, Cambridge, 1961).
12. HENNING, J.C.M., VAN STAPELE, R.P., HARDEMAN, G.E.G. and BONGERS, P.F., Proc. of the XIVth Colloque Ampère, Ljubljana, 1966, session 26, nr. 1, (p. 1204).
13. BOERSTOEL, B.M. has kindly provided us with these results.
14. FISHER, M.E., Rep. on Progr. in Physics, vol. XXX pt. II (1967)615.
15. SYKES, M.F. has kindly provided us with this result.
16. MIEDEMA, A.R., WIELINGA, R.F. and HUISKAMP, W.J., Phys.Letters 17(1965)87.
17. WIELINGA, R.F., BLÖTE, H.W.J., ROEST, J.A. and HUISKAMP, W.J., Physica 34(1967)223; Commun. No. 345c from the Kamerlingh Onnes Laboratorium, Leiden, Nederland.
18. VAN STAPELE, R.P., HENNING, J.C.M., HARDEMAN, G.E.G. and BONGERS, P.F., Phys.Rev. 150(1966)310.
19. BAKER, G.A.Jr. and GAUNT, D.S., Phys.Rev. 155(1967)545.
20. BAKER, G.A.Jr., Phys.Rev. 129(1963)99.
21. SYKES, M.F., MARTIN, J.L. and HUNTER, D.L., Proc.Phys.Soc. 91(1967)671.
22. ONSAGER, L., Phys.Rev. 65(1944)117.

## Chapter IV

EXPERIMENTAL STUDY OF THE BODY-CENTERED-CUBIC  
HEISENBERG FERROMAGNET

## 1 Introduction

Several years ago measurements on heat capacity and magnetic properties of  $\text{CuK}_2\text{Cl}_4 \cdot 2\text{H}_2\text{O}$  and  $\text{Cu}(\text{NH}_4)_2 \cdot 2\text{H}_2\text{O}$  have been performed by Miedema et al.<sup>1)</sup> The zero-field susceptibility in the *c* axis was reported to reach the values  $N^{-1}$  ( $N$ =demagnetizing factor) per  $\text{cm}^3$ , from which it was concluded that the crystals are ferromagnetic below the critical temperature.

The heat capacity curves of the two salts were shown to be very similar and values were reported for  $S_\infty - S_c$ , the part of the entropy removed above  $T_c$ , and for  $(E_\infty - E_c)/RT_c$ , where  $E$  is the magnetic energy. Using  $\text{CuRb}_2\text{Cl}_4 \cdot 2\text{H}_2\text{O}$  and  $\text{Cu}(\text{NH}_4)_2\text{Br}_4 \cdot 2\text{H}_2\text{O}$  the investigations on this group of ferromagnetic salts were continued for several reasons. If more heat capacity curves are available which can be brought to coincidence using a reduced temperature scale, the values of  $S_\infty - S_c$  and  $E_\infty - E_c$  will have more weight as representing the properties of the body-centered-cubic (b.c.c.) Heisenberg ferromagnet. All kinds of deviations from the ideal model such as a small anisotropy, the difference between the tetragonal crystal structure and the b.c.c. structure and the presence of next nearest magnetic neighbours interactions may be expected to be different for different salts. Hence, if the specific heat curves would coincide, one might conclude that these deviations are not of practical importance.

Also some information can be obtained as to the dependence of the magnetic super-exchange on the copper-copper distance and the type of intervening atoms.

Special attention will be paid to the temperature dependence in the immediate neighbourhood of  $T_c$ . The data in ref.1 were not sufficiently detailed to perform an analysis and therefore new experiments were started with a different apparatus.

A detailed comparison as to the prediction of the spin wave theory will be made for  $\text{Cu}(\text{NH}_4)_2\text{Br}_4 \cdot 2\text{H}_2\text{O}$ , chosen partly because of its relatively high transition temperature and also because the hyperfine structure contribution to the heat capacity is smaller than in the other salts.

## 2 Crystal structure

The salts of the general formula  $\text{Cu}(\text{M}^+)_2\text{X}_4 \cdot 2\text{H}_2\text{O}$ , where  $\text{M}^+$  stands for  $\text{K}^+$ ,  $\text{NH}_4^+$  or  $\text{Rb}^+$  and  $\text{X}$  is  $\text{Cl}^-$  or  $\text{Br}^-$ , crystallize in the tetragonal system<sup>2)</sup>. There are two molecules in the unit cell with the copper

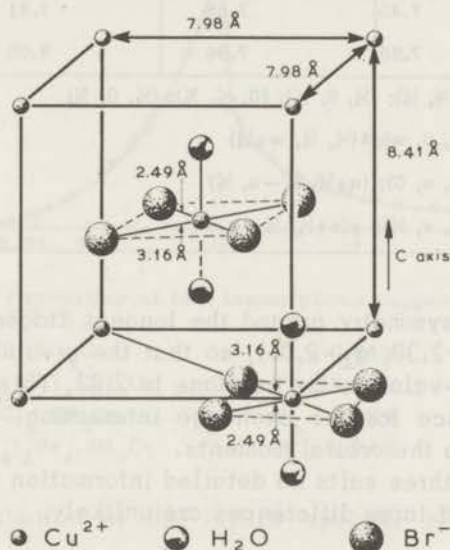


Fig. 1. The unit-cell of  $\text{Cu}(\text{NH}_4)_2\text{Br}_4 \cdot 2\text{H}_2\text{O}$ . The  $c$  axis is about 5% longer than the  $a$  axis.

ions at the equivalent positions  $(0, 0, 0)$  and  $(\frac{1}{2}, \frac{1}{2}, \frac{1}{2})$ . Each copper ion is surrounded by an approximate octahedron of four chlorine ions and two water molecules (see figure 1 and table I for the  $\text{M}^+$  and  $\text{H}_2\text{O}$  positions). The line connecting the water molecules is parallel to the crystallographic  $c$  axis; the chlorine ions lie in the  $aa$  plane in a rhombohedron, the longest diagonal of which points to the  $[110]$  direction for one of the copper ions and to the  $[\bar{1}\bar{1}0]$  direction for the other.

The cell dimensions are somewhat different for the four salts, as may be seen in table I. One may notice that the structure is only slightly different from body-centered-cubic. Each copper ion has 8 nearest neighbours and 6 next-nearest-neighbours which are about 15 percent further away. For nearest magnetic ions the super-exchange interaction may be transferred by means of a chlorine ion and a water molecule.

For  $\text{CuK}_2\text{Cl}_4 \cdot 2\text{H}_2\text{O}$  it has been found that the  $g$ -values of the copper

TABLE I

The unit cell of four copper salts, with the general formula $\text{CuM}_2\text{X}_4 \cdot 2\text{H}_2\text{O}$ . The parameters $u$ , $v$ and $w$ are approximately equal to 0.22, 0.22 and 0.25, respectively				
salt	$\text{CuK}_2\text{Cl}_4 \cdot 2\text{H}_2\text{O}$	$\text{Cu}(\text{NH}_4)_2\text{Cl}_4 \cdot 2\text{H}_2\text{O}$	$\text{CuRb}_2\text{Cl}_4 \cdot 2\text{H}_2\text{O}$	$\text{Cu}(\text{NH}_4)_2\text{Br}_4 \cdot 2\text{H}_2\text{O}$
$a_0$ (Å)	7.45	7.58	7.81	7.98
$c_0$ (Å)	7.88	7.96	8.00	8.41
positions $\text{M}^+$	$(0, \frac{1}{2}, \frac{1}{4}); (\frac{1}{2}, 0, \frac{1}{4}); (0, \frac{1}{2}, \frac{3}{4}); (\frac{1}{2}, 0, \frac{3}{4})$			
positions $\text{H}_2\text{O}$	$\pm(0, 0, w); \pm(\frac{1}{2}, \frac{1}{2}, w + \frac{1}{2})$			
positions $\text{X}_\text{I}$	$\pm(u, u, 0); (u + \frac{1}{2}, \frac{1}{2} - u, \frac{1}{2})$			
positions $\text{X}_\text{II}$	$\pm(v, v, \frac{1}{2}); \pm(v + \frac{1}{2}, \frac{1}{2} - v, 0)$			

ions have axial symmetry around the longest diagonal in the chlorine rhombhedron ( $g_{\parallel} = 2.38$ ,  $g_{\perp} = 2.06$ ), so that the  $g$ -value along the  $c$  axis is 2.06 and the  $g$ -value in the  $aa$  plane is 2.22. This anisotropy has no direct consequence for the exchange interaction, since it is nearly completely due to the orbital moments.

For the other three salts no detailed information is available on the magnetic axes but large differences are unlikely.

### 3 Experimental method

For details concerning the apparatus and methods used we refer to chapter II. The specific heat singularity of  $\text{CuK}_2\text{Cl}_4 \cdot 2\text{H}_2\text{O}$  was studied by means of a cobalt-cesium-tutton-salt thermometer. For the other measurements cerium-magnesium-nitrate has been used as magnetic thermometer.

### 4 Heat capacity results

The heat capacity of the 4 salts is shown in figure 2, the temperatures being plotted in units  $T_c$ . The data on  $\text{Cu}(\text{NH}_4)_2\text{Cl}_4 \cdot 2\text{H}_2\text{O}$  and  $\text{CuK}_2\text{Cl}_4 \cdot 2\text{H}_2\text{O}$ , already reported in ref.1, were obtained for single crystals of about 0.5 gram, the data on  $\text{CuRb}_2\text{Cl}_4 \cdot 2\text{H}_2\text{O}$  and  $\text{Cu}(\text{NH}_4)_2\text{Br}_4 \cdot 2\text{H}_2\text{O}$  were obtained on powdered samples (grain size  $\approx 0.1$  mm). We also investigated the heat capacity of a powdered sample of  $\text{Cu}(\text{NH}_4)_2\text{Cl}_4 \cdot 2\text{D}_2\text{O}$ . There was no difference with the hydrated salt, i.e. the transition temperature was the same within the measuring accuracy of a few millidegrees.

On the low temperature side a small h.f.s. term ( $\propto T^{-2}$ ) has been subtracted, which becomes only important near  $T = 0.1 T_c$ ; even at

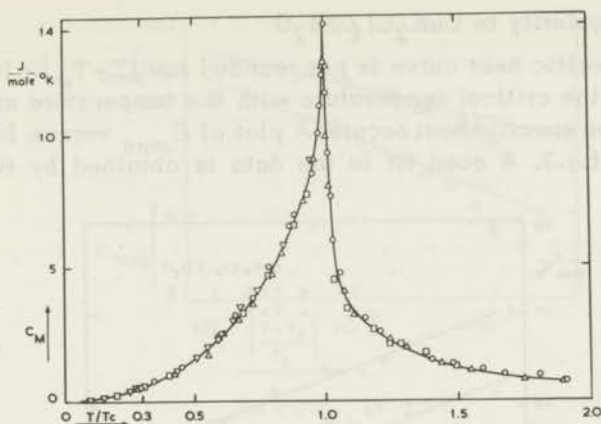


Fig. 2. Heat capacities of four isomorphous copper salts plotted as functions of  $T/T_c$ .

○ $\text{CuK}_2\text{Cl}_4 \cdot 2\text{H}_2\text{O}$	$T_c = 0.88 \text{ K}$
△ $\text{Cu}(\text{NH}_4)_2\text{Cl}_4 \cdot 2\text{H}_2\text{O}$	$T_c = 0.70 \text{ K}$
□ $\text{CuRb}_2\text{Cl}_4 \cdot 2\text{H}_2\text{O}$	$T_c = 1.02 \text{ K}$
▽ $\text{Cu}(\text{NH}_4)_2\text{Br}_4 \cdot 2\text{H}_2\text{O}$	$T_c = 1.74 \text{ K}$

$T \approx 2T_c$  the contribution of the lattice specific heat is negligibly small.

It may be seen that one single curve may represent the results for the 4 salts; the values tabulated (table II) are read from this curve. The entropy corresponding to the curve of figure 2 equals exactly  $R \ln 2$ , the energy is  $0.725 RT_c$  per mole ( $E/T_c = 6.03 \text{ J/mole K}$ ).

TABLE II

Specific heat of four ferromagnetic copper salts. At temperatures above $1.5T_c$ the specific heat is described by $C_{\text{mag}}(T/T_c)^2 = 0.34R$					
$T/T_c$	$C_{\text{mag}}$ (J/mole)	$T/T_c$	$C_{\text{mag}}$ (J/mole)	$T/T_c$	$C_{\text{mag}}$ (J/mole)
0.05	0.024	0.93	8.00	1.02	6.10
0.10	0.071	0.95	8.56	1.03	5.40
0.15	0.141	0.97	9.52	1.05	4.60
0.20	0.240	0.98	10.15	1.07	4.10
0.30	0.54	0.985	10.75	1.10	3.40
0.40	1.00	0.990	11.50	1.15	2.92
0.50	1.62	0.995	12.50	1.20	2.50
0.60	2.51	0.998	14.15	1.30	2.00
0.70	3.72	1.002	10.00	1.50	1.35
0.80	5.20	1.005	8.40	1.90	0.77
0.85	6.08	1.010	7.20		
0.90	7.40	1.015	6.55		

#### 4.1 The singularity in $\text{CuK}_2\text{Cl}_4 \cdot 2\text{H}_2\text{O}$

As the specific heat curve is not rounded for  $|T - T_c| > 10^{-3}T_c$ , we may identify the critical temperature with the temperature at which the maximum in the specific heat occurs. A plot of  $C_{\text{mag}}$  versus  $\log |1 - T/T_c|$  is shown in fig.3. A good fit to the data is obtained by two parallel

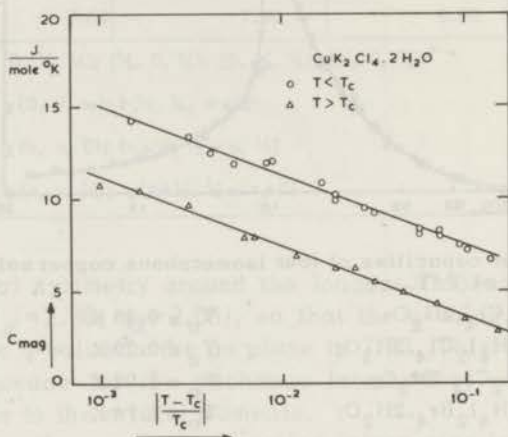


Fig. 3. Heat capacity of  $\text{CuK}_2\text{Cl}_4 \cdot 2\text{H}_2\text{O}$  between  $0.9T_c$  and  $1.1T_c$ , plotted on a semilogarithmic scale. The lines are represented by the formula  $C_{\text{mag}}/R = -A \ln |1 - T/T_c| + B$ .

lines, which are represented by

$$C_{\text{mag}}/R = -A \ln |1 - T/T_c| + B, \quad (1)$$

with  $A = 0.203$  and  $B = 0.43$  for  $T < T_c$  and with  $A = 0.203$  and  $B = -0.05$  for  $T > T_c$ . The formula describes our data for  $10^{-3} < |(T - T_c)/T_c| < 10^{-1}$ .

In order to see whether the logarithmic formula (1) gives a better fit to the experimental data than a formula of the form

$$C_{\text{mag}} = B |1 - T/T_c|^{-\alpha}, \quad (2)$$

we plotted both  $C_{\text{mag}}$  and  $|1 - T/T_c|$  on a logarithmic scale in figure 4. The data can be described by formula (2) in a small region viz.  $10^{-3} < |1 - T/T_c| < 10^{-2}$ , whereas formula (1) represents the data over two decades. The lines in fig.4 correspond to  $\alpha = 0.2$  for  $T > T_c$  and to  $\alpha = 0.1$  for  $T < T_c$ .

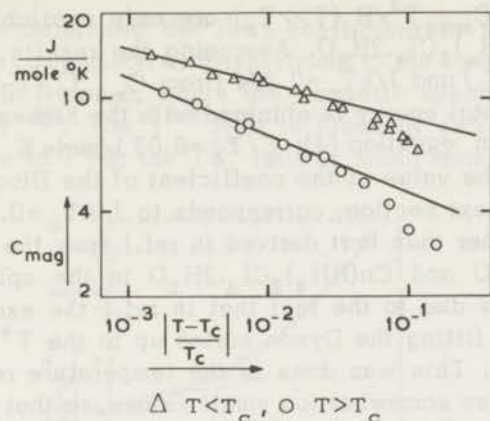


Fig. 4. Heat capacity of  $\text{CuK}_2\text{Cl}_4 \cdot 2\text{H}_2\text{O}$  between  $0.9T_c$  and  $1.1T_c$ . Both  $|T - T_c|/T_c$  and  $C_{\text{mag}}$  are plotted on a logarithmic scale. The straight lines correspond to a formula of the form  $C_{\text{mag}} = B |1 - T/T_c|^{-a}$ .

#### 4.2 The exchange constant

One of the results, which can be obtained from the data, is the magnitude of the exchange constant  $J$  compared to the critical temperature  $T_c$ . Assuming that the magnetic interaction occurs only among nearest magnetic neighbours the  $J/kT_c$  ratio can be obtained from 4 different experimental quantities:

- $\theta$ , the Curie-Weiss constant, which is found at relatively high temperatures,
- the constant  $C_{\text{mag}} T^2$ , which describes the specific heat at high temperatures.
- the energy gained by the magnetic ordering,
- the experimental value of  $C_{\text{mag}} T^{-3/2}$  which describes  $C_{\text{mag}}$  versus  $T$  in the very low temperature region (spin waves, Bloch-term).

The following formulae are used:

$$\theta = 2zS(S+1)J/3k \quad (3)$$

$$E/R = zS^2 |J/k| \quad (4)$$

$$C_{\text{mag}} T^2/R = 2zS^2(S+1)^2 J^2/3k^2 \quad (5)$$

$$B_0 = C_{\text{mag}} (T/T_c)^{-3/2} = 5.68 \times 10^{-2} (J/kT_c)^{-3/2} \quad (6)$$

Data on  $\theta$  and  $C_{\text{mag}} T^2/R$  ( $T \gg T_c$ ) are only available for  $\text{CuK}_2\text{Cl}_4 \cdot 2\text{H}_2\text{O}$  and  $\text{Cu}(\text{NH}_4)_2\text{Cl}_4 \cdot 2\text{H}_2\text{O}$ . Averaging the results we get  $J/kT_c = 0.340$  (from  $\theta/T_c$ ) and  $J/kT_c = 0.334$  (from  $C_{\text{mag}}(T/T_c)^2$ ). Of the four quantities, the total energy is obtained with the highest accuracy. The result quoted in equation (4):  $E/T_c = 6.03 \text{ J/mole K}$  corresponds to  $J/kT_c = 0.364$ . The value of the coefficient of the Bloch  $T^{3/2}$  term, as obtained in the next section, corresponds to  $J/kT_c = 0.368$ . This value is somewhat higher than that derived in ref.1 from the heat capacities of  $\text{CuK}_2\text{Cl}_4 \cdot 2\text{H}_2\text{O}$  and  $\text{Cu}(\text{NH}_4)_2\text{Cl}_4 \cdot 2\text{H}_2\text{O}$  in the spin wave region. The difference is due to the fact that in ref.1 the exchange constant was obtained by fitting the Dyson series up to the  $T^4$  term to the experimental curve. This was done in the temperature region where the Dyson series gives somewhat too small values, so that a too low value for  $J$  was obtained. One may say that the value of  $J/kT_c$ , derived from four experimental quantities agree rather well to  $J/kT_c = 0.35 \pm 0.015$ .

Recently, by analysis of the high-temperature series for the Heisenberg  $s=1/2$  model, Baker et al.<sup>3)</sup> have derived the critical parameter  $J/kT_c$  for the cubic lattices. The results are 0.5962, 0.3973, and 0.2492 for the s.c., b.c.c., and f.c.c. lattices respectively. As one may notice, our value is close to the theoretical value for the b.c.c. lattice.

#### 4.3 Comparison with spinwave theory

The data obtained on  $\text{Cu}(\text{NH}_4)_2\text{Br}_4 \cdot 2\text{H}_2\text{O}$  are especially useful for comparison with spin wave theory, due to the high value of  $T_c$  and the rather low h.f.s. specific heat. The magnetic and nuclear contributions to the specific heat are approximately equal at  $T = 0.03 T_c$ .

For an ideal ferromagnet (identical spins, isotropic Heisenberg exchange interactions among nearest neighbours only) Dyson<sup>4)</sup> calculated that the heat capacity in the spin wave temperature region can be described by:

$$C_{\text{mag}}/R = b_0(kT/J)^{3/2} + b_1(kT/J)^{5/2} + b_2(kT/J)^{7/2} + b_3(kT/J)^4 + \dots(7)$$

The  $T^{3/2}$  term is the original Bloch result and the terms proportional to  $T^{5/2}$  and  $T^{7/2}$  are due to the discreteness of the lattice. The first term arising from interactions is proportional to  $T^4$ .

For the b.c.c. lattice with spin  $1/2$  the Dyson prediction is:

$$b_0 = 5.68 \times 10^{-2}$$

$$b_2 = 6.45 \times 10^{-3}$$

$$b_1 = 1.56 \times 10^{-2}$$

$$b_3 = 1.85 \times 10^{-3}$$

One may try to determine the first coefficient in the Dyson series by confining the comparison with experiment to the lowest temperatures. This is shown in figure 5, where the magnetic specific heat is multiplied by  $(T/T_c)^{-3/2}$ . The  $T^{3/2}$  term is found by extrapolating the experimental curve to  $T=0$ ; the  $T^{5/2}$  term is found from the derivative at  $T=0$ .

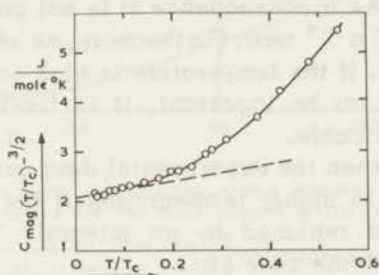


Fig. 5. The specific heat of  $\text{Cu}(\text{NH}_4)_2\text{Br}_4 \cdot 2\text{H}_2\text{O}$  in the spin wave temperature region. The specific heat is plotted as  $C_{\text{mag}}(T/T_c)^{-3/2}$  so that the value at  $T/T_c=0$  gives the coefficient of the first term of the Dyson series; the tangent at  $T=0$  gives the coefficient of the second,  $T^{5/2}$  term. The hyperfine structure contribution ( $\propto T^{-2}$ ) has been subtracted.

The results are  $B_0^* = 0.250$ ,  $B_1^* = 0.21$ , defining  $B_0$  and  $B_1$  by:

$$C_{\text{mag}}/R = B_0(T/T_c)^{3/2} + B_1(T/T_c)^{5/2}, \quad (8)$$

while the asterisk denotes the experimental values. The relation between  $B_0, B_1$  and  $b_0, b_1$  are  $b_0/B_0 = (J/kT_c)^{3/2}$  and  $b_1/B_1 = (J/kT_c)^{5/2}$ . Using  $J/kT_c = 0.35$  we obtain  $b_0^* = 0.052$  and  $b_1^* = 0.015$ , which may be compared with Dyson's (Bloch) values given above.

An alternative method of determining the first two coefficients in the Dyson series consists of fitting the polynomial (8) to the experimental points in the temperature region below  $T/T_c = 0.2$ , using a least squares method. This gives

$$C_{\text{mag}}/R = (0.242 \pm 0.005)(T/T_c)^{3/2} + (0.32 \pm 0.02)(T/T_c)^{5/2}.$$

If the least squares fit is restricted to the more limited temperature region  $T/T_c < 0.1$  (i.e. 11 experimental points) one finds for  $\text{Cu}(\text{NH}_4)_2\text{Br}_4 \cdot 2\text{H}_2\text{O}$ :

$$C_{\text{mag}}/R = 0.247(T/T_c)^{3/2} + 0.30(T/T_c)^{5/2}.$$

Comparing the results of the two procedures (graphical and least squares fitting) one may see that the accuracy of  $b_1^*$  is not better than 25 percent.

For the evaluation of the higher order terms in the Dyson series, only data obtained at  $T > 0.2 T_c$  can be used since the  $T^{3/2}$  and  $T^{5/2}$  terms together account for more than 90 percent of the heat capacity at lower temperatures. As a consequence it is not possible to distinguish between a  $T^{7/2}$  and a  $T^4$  term. Furthermore, as stated by McCollum and Callaway<sup>5)</sup> for EuS, if the temperature is high enough for the  $T^{7/2}$  and higher order terms to be important, it is likely that the Dyson series is no longer applicable.

The comparison between the experimental data and linear spin wave theory may be pursued to higher temperatures if the series expansion in odd-half powers is replaced by an integral. This requires the summation over the Brillouin zone of:

$$C_{\text{mag}}/R = \sum (W_{\mathbf{k}}/kT)^2 e^{W_{\mathbf{k}}/kT} (e^{W_{\mathbf{k}}/kT} - 1)^{-2}, \quad (9)$$

where

$$W_{\mathbf{k}} = 4JS \left[ \{1 - \cos \frac{1}{2}a(k_x + k_y + k_z)\} + \{1 - \cos \frac{1}{2}a(k_x - k_y + k_z)\} + \{1 - \cos \frac{1}{2}a(k_x + k_y - k_z)\} + \{1 - \cos \frac{1}{2}a(-k_x + k_y + k_z)\} \right], \quad (10)$$

and  $a$  is the lattice constant.

The influence of spin wave interactions may be taken into account by a procedure described by Bloch<sup>6)</sup> and applied successfully to  $\text{MnF}_2$  and EuS, and which is called renormalization of the spin wave spectrum. The renormalization consists of multiplying  $W_{\mathbf{k}}$  with a temperature dependent factor:

$$W_{\mathbf{k}}(T) = \{1 - \Delta(T)\} W_{\mathbf{k}}(T=0), \quad (11)$$

where

$$\Delta(T) = 1 - \frac{1}{2zJNS^2} \sum W_{\mathbf{k}} (e^{W_{\mathbf{k}}/kT} - 1)^{-1}. \quad (12)$$

This correction amounts to 2% at  $T/T_c = 0.35$ , whereas it would have been 1.5% according to the  $T^4$  term in the Dyson series; at  $T/T_c = 0.6$  the correction in  $C_{\text{mag}}$  is about 13%.

The results are shown in figure 6. The series expansion deviates from the integral for  $T/T_c > 0.25$ , the difference being about 20 percent at  $T/T_c = 0.5$ . It may be seen that the agreement between integral and

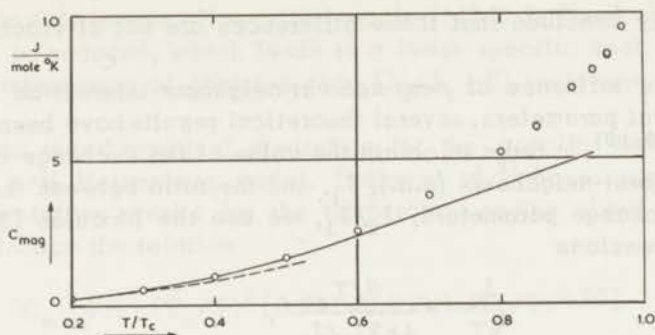


Fig. 6. Comparison with spin wave theory. The experimental points are averages for the four copper salts (table I).

Dyson series, formula 7 } calculated with  $J/kT_c = 0.35$   
 Integral, formulae 9-12 }

experiment is very good for temperatures up to  $T/T_c = 0.5$  but one must keep in mind that the choice of  $J/kT_c$  is rather important. We used the average value  $J/kT_c = 0.35$ , as obtained in the foregoing section. At higher temperatures the experimental curve rises much faster than the calculated one; this is not surprising in view of the fact that the interaction between the spin waves becomes increasingly more important near the critical temperature.

It is concluded that

- 1) spin wave theory describes the experimental data quite well up to  $T = 0.5 T_c$ ,
- 2) the integral approaches the experimental data more closely than does the series expansion.

## 5 Discussion

We conclude that the 4 copper salts, which were investigated are to a good approximation representative for the b.c.c. Heisenberg ferromagnet with mainly nearest neighbour interactions from the following:

- (1) the thermal properties of the four salts are identical, apart from a constant factor in the temperature;
- (2) the susceptibility in the ordered region shows only slight anisotropy.
- (3) the values of  $J$ , derived from different experimental results and using formulae which contain  $J$  and  $z$  in a different way, agree;
- (4) the low temperature heat capacity agrees with spin wave theory.

It may be expected that the anisotropy energy and slight deviations from the b.c.c. structure will not be equal for the four salts investigated. From the coincidence of the specific heat curves for these

salts we may conclude that these differences are not of practical importance.

As to the influence of *next-nearest-neighbour interaction* (n.n.n.) on the critical parameters, several theoretical results have been derived recently<sup>7,8,9,10</sup>). In order to obtain the value of the exchange coupling between nearest-neighbours (n.n.),  $J_1$ , and the ratio between the n.n.n. and n.n. exchange parameters,  $J_2/J_1$ , we use the formulas (3) to (5) and the expressions

$$\frac{J_1}{kT_c} = \frac{\theta/T_c}{4+3J_2/J_1} \quad (13)$$

$$\frac{J_1}{kT_c} = \frac{0.241 E}{4+3J_2/J_1} \quad (14)$$

$$\left(\frac{J_1}{kT_c}\right)^2 = \frac{0.1605 C_{\text{mag}}(T/T_c)^2}{4+3(J_2/J_1)^2} \quad (15)$$

taken from ref.9. These formulae are derived for the b.c.c. structure. The quantities  $E$  and  $C_{\text{mag}}(T/T_c)^2$  are given in Joules per mole. By substituting the experimental values,  $\theta/T_c=1.36$ ,  $E=6.03$  J/mole and  $C_{\text{mag}}(T/T_c)^2=2.83$  J/mole K into the formulae, we obtain  $J_2/J_1=0.25\pm 0.1$ , and  $J_1/kT_c=0.31\pm 0.02$ . The result  $J_2/J_1=0.25\pm 0.1$  is supported by comparing the observed and predicted values of the magnetic energy yield,  $(E_\infty-E_c)/RT_c$ , and entropy change,  $(S_\infty-S_c)/R$ , in the short-range ordering process (see table III).

From these results it may be concluded that ferromagnetic next-nearest-neighbour interactions are present. Their influence on the specific heat as predicted by spin-wave theory is not large as has

TABLE III

Experimental and theoretical values for the critical parameters $(E_\infty-E_c)/RT_c$ and $(S_\infty-S_c)/R$ , for the b.c.c. lattice. $J_2/J_1$ denotes the ratio of the n.n.n. to n.n. exchange coupling.					
	This experiment	Theory <sup>9)</sup>			
$J_2/J_1$		0	0.2	0.3	0.4
$(E_\infty-E_c)/RT_c$	0.392	0.460	0.419	0.404	0.393
$(S_\infty-S_c)/R$	0.218	0.235	0.229	0.225	0.223

been shown by Wood and Dalton<sup>9)</sup>. This would not be surprising for the following reason. If e.g. in formula (14)  $E$  is fixed and  $J_2/J_1 > 0$ ,  $J_1$  will be reduced, which leads to a lower specific heat, whereas the n.n.n. interaction of positive sign ( $J_2/J_1 > 0$ ) increases the specific heat.

As to the theoretical prediction for the specific heat singularity of the  $s=1/2$  Heisenberg model, Baker et al.<sup>3)</sup> have recently derived some tentative results for the temperature region above  $T_c$ . For the b.c.c. lattice the relation

$$C_{\text{mag}}/R = (T_c/T)^2 [0.971 - 0.668(1 - T_c/T)^{0.20}] \quad (16)$$

was deduced in the range  $0.75 < T_c/T < 0.95$ . If the range of validity of this relation may be extended up to  $T_c$ , viz.  $0.95 < T_c/T < 1$ , the singularity has the form of a cusp with a top value of 0.97, and an infinite slope near  $T_c$ . This result, however, might be modified when further computations near  $T_c$  become available.

The highest observed value for  $C_{\text{mag}}/R$  is 1.5, which is obtained at  $1 - T/T_c = 10^{-3}$ , whereas the theoretical value at  $T = 1.001 T_c$  is only 0.83. At  $T = 1.01 T_c$  the experimental value is 0.88, while the theoretical one is 0.71. At  $T = 1.04 T_c$  the values are equal, but at still higher temperatures the experimental values lie about 10% lower than the theoretical ones. The latter result is not surprising, since the theoretical value for the entropy yield above  $T_c$ ,  $(S_\infty - S_c)/R$ , also lies about 10% higher than the observed value. However, formula (16) does not give a proper description of the observed behaviour in the temperature range  $0.95 < T_c/T < 1$ .

By comparing the values of  $T_c$  of the four copper salts, some information can be obtained on the mechanism of *superexchange*. There seems to be no simple relation to atomic distance, since  $\text{CuRb}_2\text{Cl}_4 \cdot 2\text{H}_2\text{O}$  has a higher Curie temperature than  $\text{CuK}_2\text{Cl}_4 \cdot 2\text{H}_2\text{O}$ , while the axes are 5 percent longer. Replacing  $\text{Cl}^-$  by  $\text{Br}^-$  increases the exchange interaction, again in spite of a larger copper-copper distance.

Looking to the crystal structure, both a chlorine ion and a water molecule seem to be essential for transferring the exchange interaction. The importance of the  $\text{H}_2\text{O}$  molecule can be derived from the fact that replacement of  $\text{H}_2\text{O}$  by  $\text{NH}_3$  in  $\text{Cu}(\text{NH}_4)_2\text{Cl}_4 \cdot 2\text{NH}_3$  reduces the ordering temperature by approximately a factor 10, while the copper-copper distance hardly changes. Only the oxygen of the  $\text{H}_2\text{O}$  is found to be important, because the deuterated copper ammonium chloride has the same transition temperature as the normal salt.

## References

1. MIEDEMA, A.R., VAN KEMPEN, H. and HUISKAMP, W.J., Commun. Kamerlingh Onnes Lab., Leiden No. 336a; Physica 29(1963)1266.
2. WYCKOFF, R.W.G., Crystal structures Vol. III, Interscience Publishers, 1948 New York.
3. BAKER, G.A. Jr., GILBERT, H.E., EVE, J. and RUSHBROOKE, G.S., Phys. Rev. 164(1967)800.
4. DYSON, F.J., Phys. Rev. 102(1956) 1217 and 1230.
5. McCOLLUM, D.C. and CALLAWAY, I., Phys. Rev. Letters 9(1962)376; Phys. Rev. 130(1963)1741.
6. BLOCH, M., Phys. Rev. Letters 9(1962)286; J. appl. Phys. 34(1963)1151.
7. DALTON, N.W. and WOOD, D.W., Phys. Rev. 138A(1965)779.
8. PIRNIE, K., WOOD, D.W. and EVE, J., Mol. Phys. 11(1966)551.
9. WOOD, D.W. and DALTON, N.W., Proc. Phys. Soc. (London), 87(1966)755.
10. LOLY, P.D., J. appl. Phys. 39(1968)1109.

## Chapter V

THE SPONTANEOUS MAGNETIZATION OF THE B.C.C.  
HEISENBERG FERROMAGNET  $\text{Cu}(\text{NH}_4)_2\text{Br}_4 \cdot 2\text{H}_2\text{O}$ .

## 1 Introduction

The discovery of a number of ferromagnetic insulators in recent years viz.  $\text{CrBr}_3$  ( $s=5/2$ , Tsubokawara<sup>1)</sup>),  $\text{EuO}$  ( $s=7/2$ , Matthias et al.<sup>2)</sup>),  $\text{EuS}$  (Moruzzi and Teaney<sup>3)</sup>),  $\text{EuBr}_3$  (Gossard et al.<sup>4)</sup>),  $\text{GdCl}_3$  ( $s=7/2$ , Wolf et al.<sup>5)</sup>),  $\text{CuK}_2\text{Cl}_4 \cdot 2\text{H}_2\text{O}$  and  $\text{Cu}(\text{NH}_4)_2\text{Br}_4 \cdot 2\text{H}_2\text{O}$  ( $s=1/2$ , see ch.IV and refs. 6 and 7), has provided an opportunity for comparing experimental results with statistical theories assuming an interaction between localized spins, such as the Heisenberg model.

Confining the discussion to temperatures below the critical point, the majority of the experimental results has been interpreted on the basis of the spin-wave theory, which applies in general to the lower values of  $T/T_c$ . This has been done for example by Mc Collum and Callaway<sup>8)</sup>, Gossard et al.<sup>4)</sup>, Low<sup>9)</sup>, Miedema et al.<sup>6,7)</sup>, Wood and Dalton<sup>10)</sup> and Loly<sup>11)</sup>. With the aid of a cluster theory (Kasteleijn and Van Kranendonk<sup>12)</sup> and Green's functions techniques (Callen and Callen<sup>13)</sup>, Cooke and Gersch<sup>14)</sup>, Liu and Siano<sup>15)</sup>) theoretical results up to  $T=T_c$  have been obtained and compared with experimental evidence (Callen and Callen<sup>16)</sup>, Heller and Benedek<sup>17)</sup>, Eibschütz et al.<sup>18)</sup>).

Statistical theories can best be tested for spin  $1/2$ , since the difference in theoretical predictions is most pronounced for the lowest value. Therefore, the above mentioned copper salts are favourable for comparing theories with the experiment. Previous experiments on these salts<sup>6,7)</sup> have shown that a) the interactions between the ions are nearly isotropic, b) the deviation from the actual b.c.c. structure is small and of practically no importance for the magnetic properties, and c) the second-neighbour interaction is small and positive for the specially investigated<sup>10)</sup> potassium and ammonium chlorides. Similarly, in section 6, a small second-neighbour interaction of positive sign is deduced for the salt  $\text{Cu}(\text{NH}_4)_2\text{Br}_4 \cdot 2\text{H}_2\text{O}$ , which influences the theoretical result obtained for nearest-neighbour interaction to a small degree only. As  $T_c$  for this salt is 1.74K, a temperature stability of  $10^{-5}\text{K}$  can easily be achieved, if an ordinary  $^4\text{He}$  bath is used. For these reasons we have preferred to perform the magnetization measurements on this salt.

It will be shown that the experimental result agrees with the Green's functions calculation in second order, as given by Cooke and Gersch<sup>14)</sup> over the whole temperature region ( $0.05 < T/T_c < 0.99$ ) studied.

## 2 Experimental method

The measurement of the magnetization consists of measuring the flux change in a coil system, when varying an external field. The magnetization can be measured accurately, as has been shown by Argyle and Pugh<sup>19)</sup>. The difference between their method and ours is, that in the former the temperature is changed at constant field, while in our method the field is varied at constant temperature. The accuracy of the measurement is mainly determined by the stability of the electronic integrator. Since no detailed investigation near zero temperature was aimed at, we contented ourselves with an accuracy of a few tenths of a percent.

Fig. 1a shows the apparatus used for temperatures between 0.101 and 1.05K, to be called series *a*. The measurements are performed in high vacuum, in a slightly modified apparatus for adiabatic demagnetization experiments, as described by Mess et al<sup>20)</sup>. The sample consisted of two crystals, forming an approximate ellipsoid with axes of 11.2, 7.9 and 7.9 mm length. The longest axis of each crystal lies in the *aa* plane, this being the plane of highest *g*-value. The pick-up coil is made up of two sections wound in opposite directions, each coil having 5160 turns of 0.07 mm Cu wire. The field is generated by a Nb coil, which is placed in the <sup>4</sup>He bath. The field is homogeneous within 0.5% over a length of 3 cm along the axis of the coil. The temperature is measured by a Speer resistor of 220 Ohms, ½ Watt (see ref. 21), which has been calibrated versus the susceptibility reading of a cerium-magnesium-nitrate crystal. The resistor is in good thermal contact with the rod. The resistance is measured by a bridge, which is operated at 220 Hz. The off-balance voltage of the lock-in amplifier was recorded. This voltage, which is proportional to the difference between the temperature of the bath and that corresponding to the setting of the bridge, is converted to a current through the heater resistance. This variable heat input serves to stabilize the temperature. The heater in case *a* consists of a manganin wire of about 1800 Ohms. The heat sink is formed by a Cr-alum cooling salt (see e.g. ref. 21). A superconducting coil operates a lead heat-switch into a thermally conducting state at temperatures below about 0.3K and into a superconducting state at higher temperatures.

In fig. 2b the construction, used for measurements in the temperature region above 0.95 to 3.40 K is shown. The sample, coil system, and field coil are the same as those used below 1 K. The temperature is measured by calibrating an enamelled Allen and Bradley resistor of 0.1 Watt, nominally 32 Ohms, versus the vapour pressure of the <sup>4</sup>He bath. At *T*=1.75 K a change in resistance of 0.01 Ohm could be detected

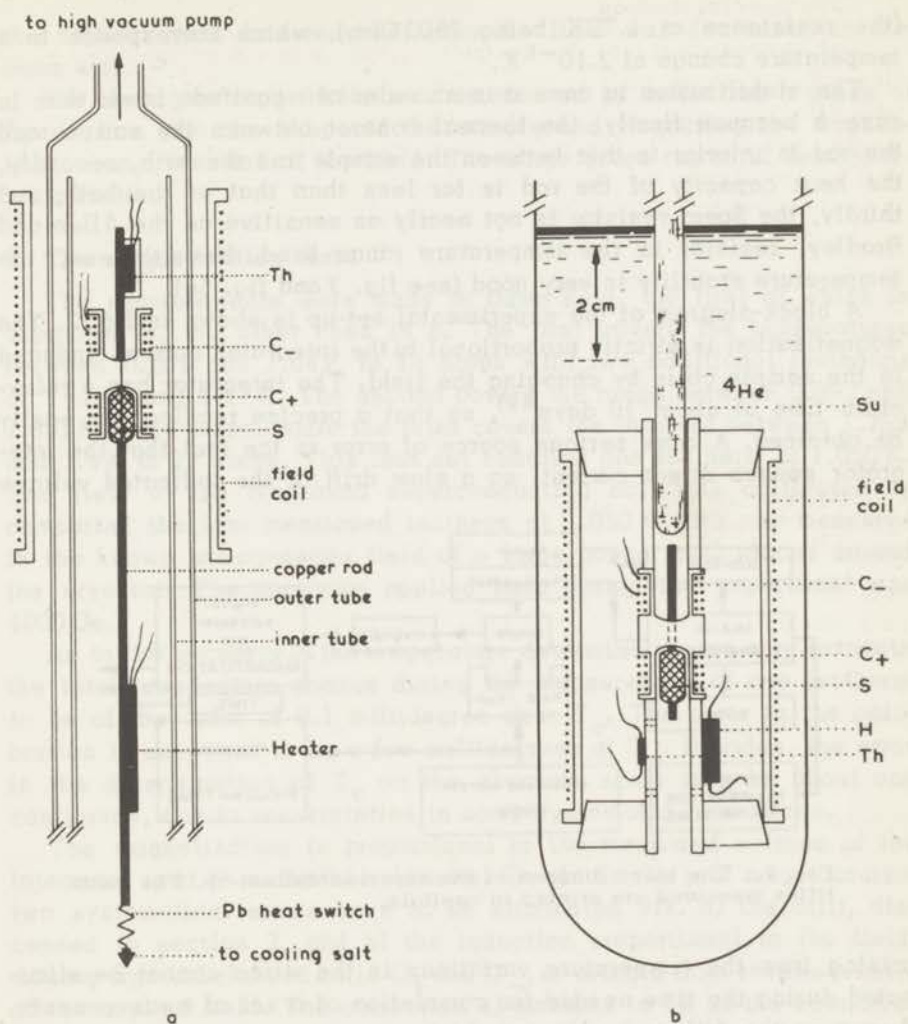


Fig. 1. *a* Apparatus for the measurement of magnetization, used for temperatures between 0.10 and 1.05 K.

*b* Apparatus in use for temperatures above 0.95 K.

S : sample.

Th : thermometer.

H : heater resistor for stabilization of the temperature.

Su : glass tube support.

C<sub>+</sub> : search coil.

C<sub>-</sub> : compensating coil, consisting of a number of turns equal to that of C<sub>+</sub>, but wound in the reverse direction.

The dimensions are on scale.

(the resistance at 1.75 K being 2600 Ohm), which corresponds to a temperature change of  $2 \cdot 10^{-6}$  K.

The stabilization in case *a* is an order of magnitude lower than in case *b* because firstly, the thermal contact between the sample and the rod is inferior to that between the sample and the bath, secondly, the heat capacity of the rod is far less than that of the bath, and thirdly, the Speer resistor is not nearly as sensitive as the Allen and Bradley, resistor in the temperature range used. Nevertheless, the temperature stability is very good (see fig. 3 and fig. 5a).

A block-diagram of the experimental set-up is shown in fig. 2. The magnetization is strictly proportional to the integrated current induced in the sample coils by changing the field. The integrator has a relaxation time of about 10 days<sup>22)</sup>, so that a precise reading can easily be obtained. A more serious source of error is the fact that the integrator senses direct current, so a slow drift of the indicated voltage

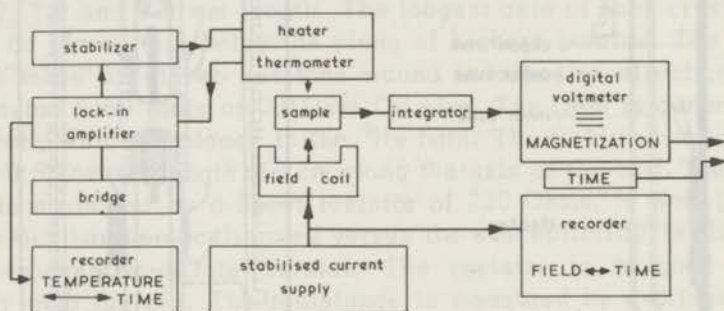


Fig. 2. The block diagram of the experimental set-up. The quantities measured are printed in capitals.

arising from the temperature variations in the wires cannot be eliminated during the time needed for completion of a set of measurements. Assuming the drift to be linear, which was correct in most cases, one can eliminate this effect, if the field respectively magnetization versus time relation is recorded. This is easily achieved, if one uses a solenoid and records the current.

The measuring procedure is as follows: the temperature is chosen and stabilized in a few minutes; the drift of the integrator is minimized; the field is quickly turned on to the maximum values and to zero again a few times to check for remanence effects (within 0.2% of the total magnetization no remanence could be detected at any temperature); starting from zero field a small field was turned on, subsequently the voltage of the integrator was read; and so forth until in about 20 steps

the highest field was reached; then the field was decreased in the same way.

The demagnetizing factor was determined by modelling a piece of Armco iron into the shape of the sample and measuring the magnetization as a function of the field. The slope gives the total demagnetizing factor.

### 3 The magnetization data

The measurements were made in three sets, the first of which in apparatus *a*, the other ones in *b*. The first covers the temperatures between 0.101 and 1.04 K in 14 steps with two additional isotherms at  $T=1.22$  and 1.27 K. The second covers the range between 0.992 and 1.802 K in 34 steps, while the third covers the interval between 1.759 and 3.4 K in 27 steps. This last set contains one isotherm at 1.050 K. The field of the Nb-wound superconducting coil was calibrated by comparing the last mentioned isotherm at 1.050 K with one measured in the known homogeneous field of a large copper coil placed around the cryostat. The maximum applied field during the experiment was 1000 Oe.

As to the accuracy of the temperature determination we may estimate the total temperature change during the measurement of one isotherm to be of the order of 0.1 millidegree near  $T_c$ . The error in the calibration is supposed to be a few millidegrees at  $T_c$ . Besides, the error in the determination of  $T_c$  on the absolute scale may be about one centigrade, due to uncertainties in some systematic corrections.

The magnetization is proportional to the measured voltage of the integrator read on a digital voltmeter. To obtain the real magnetization two systematic errors have to be eliminated viz. a) the drift, discussed in section 2, and b) the induction proportional to the field, arising from unbalanced coils  $C_+$  and  $C_-$ , or arising from inhomogeneity of the applied field. The correction a) amounts to 1% of the saturation magnetization at zero temperature, while the correction b) was less than 5% of  $M(0)$  at 1000 Oe. A more serious consequence of the small inhomogeneity of the field consists of rounding the sharply curved part of the  $M$  vs.  $H$  curves. This effect is largest at the lowest temperature because the applied field is largest (300 Oe), and the curvature is most pronounced. The inhomogeneity of the field at the position of the sample, amounting to at most 1% will round the  $M$  vs.  $H$  curves over an interval of about 3 Oe.

The field  $H$  for a homogeneously magnetized sample can be calculated according to the relation  $H = H_{ext} - NM$ , where  $H_{ext}$  denotes the applied field,  $N$  the demagnetizing factor, and  $4\pi M$  the measured in-

duction. In an imperfectly shaped sample,  $NM$  is not constant. This causes a spread in  $H$  as a function of position. The rounding of the  $M$  vs.  $H$  curves arising from this cause, will amount to a few Oe at the lowest temperatures.

A few of the isotherms are given in fig. 3. Section *a* shows two isotherms chosen at both ends of the interval  $(0,1)$  for  $T/T_c$ . For the open symbols, the horizontal axis represents the applied field, for the half closed symbols, the horizontal axis represents the field after correction for the demagnetizing effect. One may observe in the first place that the initial slopes of the curves drawn through the half closed symbols are not infinite. This result is definitely outside the experimental error. In order to check this result the measurements were repeated for two other samples, one being an ellipsoid with axes of about 14, 8, 8 mm, and oriented in such a way that the angle between the longest axis and the  $c$  axis was  $55^\circ$ , the other being an approximate ellipsoid with axes of 25, 4, 4 mm, while the angle between the

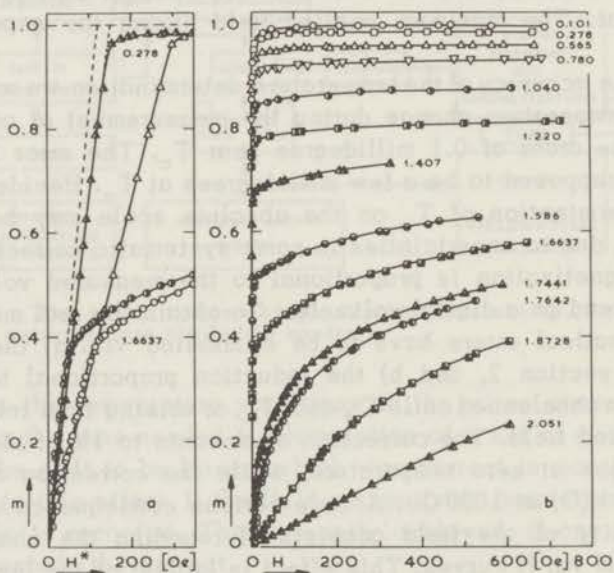


Fig. 3. Section *a* shows the magnitude of the correction of the external field due to the demagnetizing field for two temperatures, which are far apart. For the open circles and triangles,  $H^*$  denotes the external field. For the half filled symbols,  $H^*$  denotes the external field corrected for the demagnetizing field. Section *b* shows part of the total number of measured isotherms. The relative magnetization  $m=M(T)/M(0)$  is plotted versus  $H$ , which denotes the external field corrected for the demagnetizing field and the (slightly temperature dependent) anisotropy field.

longest axis and the  $c$ -direction was  $70^\circ$ . The two sets of measurements show the same behaviour. The fields required to obtain complete saturation at  $T/T_c = 0.05$  were about 80 and 50 Oe respectively, and will henceforth be called anisotropy field. In the second place one may note that the anisotropy field is a function of the temperature, which varies slightly, but does not vanish at  $T_c$ . In section 4 an attempt is made to interpret these data in terms of anisotropy energy. In view of this interpretation and in order to be able to compare the resulting spontaneous magnetization with various theories, the magnetization data are plotted as a function of the field,  $H$ , that denotes the applied field, corrected for the demagnetizing field and for the temperature dependent anisotropy field. This procedure, however, does not alter the values of the spontaneous magnetization, derived when using the isotherms given by the half closed symbols of fig. 3, section  $a$ , by more than 2%. Therefore this method has no practical consequence for the discussion in section 6.

Inspection of the isotherms (fig. 3b) shows that saturation at the lowest temperature is readily attained. The saturation value diminishes only slightly for temperatures up to 0.6 K. Above this temperature the saturation value at the available field of 700 Oe decreases rapidly. The forms of the curves near  $T_c$  change markedly until at about 2.05 K the magnetization at the lower field is almost linearly dependent on the field.

#### 4 The anisotropy energy

The initial slopes of the  $M$  vs.  $H$  curves at various temperatures (two of which are shown in fig. 3 section  $b$ ) and for three different directions with respect to the  $c$  axis, were always smaller than  $1/N$ , where  $1/N$  denotes the demagnetizing factor. We suggest that anisotropy energy may account for the discrepancy between the initial susceptibility and the expected maximum value per cc viz.  $1/N$ .

From recent electron-spin-resonance measurements Suzuki and Watanabe<sup>23</sup>) deduced an (extrapolated) anisotropy field of 200 Oe for a direction in the  $aa$  plane with respect to the easy axis ( $c$  axis). These authors calculated the anisotropy of the dipolar interaction at zero temperature and obtained a value of about 1 Oe. As their experimental results may be described by assuming a small anisotropy term in the exchange interaction within the formalism of the molecular field theory, Suzuki and Watanabe attributed the anisotropy field to anisotropy of the exchange coupling.

The effect of the anisotropy energy on the static susceptibility in a direction perpendicular to the easy axis of magnetization and along

a principal axis of the demagnetizing tensor (being an axis of the ellipsoid in our case) is given by the expression.

$$\chi = \frac{1}{N + 2K/M^2} \quad (1)$$

In this formula  $N$  is the demagnetizing factor in the direction of  $\vec{H}$ , and  $K$  is the anisotropy energy. This formula is derived by minimizing the free energy with respect to  $\theta$ , the angle between the domain magnetization,  $\vec{M}$ , and the easy axis. The magnitude of  $\vec{M}$  is assumed to remain constant and therefore we have omitted exchange energy terms from the derivation. The change in free energy arising from a slight rotation of  $\vec{M}$  is given by

$$dF = -(H - NM_{\perp})dM_{\perp} + d(K \sin^2 \theta). \quad (2)$$

Substituting  $M_{\perp} = M \cos \theta$ , we obtain

$$F(\theta) - F(0) = -HM \sin \theta + \frac{1}{2}NM^2 \sin^2 \theta + K \sin^2 \theta \quad (3)$$

after integration. The extreme value of  $F$  determined by

$$\frac{\partial F}{\partial \theta} = -HM \cos \theta + NM^2 \sin \theta \cos \theta + 2K \sin \theta \cos \theta = 0 \quad (4)$$

is a minimum, since the second derivative of  $F$  with respect to  $\theta$  is positive at this point. Inserting  $\sin \theta$  from eq. (4) in the expression

$$\chi = \frac{M \sin \theta}{H} \quad (5)$$

eq. (1) is derived. Introducing the internal field by  $H_1 = H - NM$  and the anisotropy field by  $H_A = 2K/M$  we obtain

$$\frac{M_{\perp}}{M} = \frac{H_1}{H_A} \quad (6)$$

from eq. (1), so that the rotation of the spontaneous magnetization of a domain is determined by the ratio of the internal field along  $\vec{H}$  and the anisotropy field along the easy axis. For the more general case that the angle which  $\vec{H}$  makes with the easy axis lies between 0 ( $\chi=1/N$ ) and  $\pi/2$  ( $\chi=1/(N+2K/M^2)$ ),  $\chi$  assumes an intermediate value.

Relation (1), however, cannot account for the experimental result. On increasing the temperature from  $T/T_c=0.1$  to 1, the experiment shows that the anisotropy field is reduced to only 80%, whereas  $K$  is

predicted<sup>24)</sup> to vary as the third power of  $M$ . Therefore,  $1/\chi$  is expected to approach the value  $N$  in this model, if  $T$  tends to  $T_c$ .

Three plausible mechanisms causing an anisotropy field will be discussed. The first mechanism is *anisotropy of the dipolar interaction*. At zero temperature we have calculated the dipolar fields in the directions of the  $c$  axis and an  $a$  axis. The evaluation has been performed for an ion at the centre of a sphere with a radius of  $150 \text{ \AA}$ , containing 52830 ions. In both cases the field is less than 1 Oe. Therefore, the anisotropy field originating from this mechanism may be neglected entirely.

The second mechanism is the *anisotropic hyperfine-structure-coupling* (h.f.s.). For the copper salt investigated, no h.f.s. coupling constants are known. However, one may take the largest value known for several copper salts. If the anisotropic part of the h.f.s. coupling is expressed in the form of an anisotropy field at saturation magnetization, it is smaller than  $0.8/T$  (Oersted/Kelvin). This field will be negligible at temperatures above 0.3 K.

A third source of anisotropy energy might be formed by *anisotropic exchange interaction*, for instance the pseudo-dipolar anisotropy according to Van Vleck<sup>25)</sup>. This anisotropy energy is given by  $(\lambda/\Delta E)^2 J_f$ , where  $\lambda$  is the spin-orbit coupling parameter,  $\Delta E$  the energy splitting of the lowest lying orbital levels and  $f$  a constant, depending on the orbitals participating in the interaction. The values of  $f$  differ considerably for various types of bonds, but they are roughly of the order unity<sup>26)</sup>. For the Cu-ion  $\lambda/\Delta E = 0.05$ . If we take  $J/kT_c = 0.35$ <sup>7)</sup> and  $f = 2$ , the above-cited formula yields an anisotropy field,  $H_A$ , of about 45 Oe, which is of the right order of magnitude.

As mentioned above, if one accounts for the effects of anisotropic exchange by means of the expression (1) and the molecular field concept, one encounters the problem, that the anisotropy energy tends rapidly to zero, if  $T$  approaches  $T_c$ . However, in the molecular field approximation, at  $T = T_c$  not only the anisotropy energy, but also the exchange energy vanishes. A clue may be found in the observation that short-range ordering energy and spin-spin correlations are present, even for temperatures well above  $T_c$ . It follows from the experimental result obtained from several isomorphous salts (see ch. IV) that 55% of the total energy involved in the phase transition is removed above the critical temperature. Theoretically, for the Heisenberg  $s = 1/2$  model and b.c.c. lattice, the critical parameter  $(E_\infty - E_c)/RT_c$  denoting the energy removal on a reduced scale, is predicted<sup>27)</sup> to take the value 0.41, while the next-nearest-neighbour coupling constant  $J_2$  has the value  $0.25 J_1$  (see section 6). Experimentally<sup>7)</sup> this parameter was

found to be 0.392.

A qualitative interpretation of the experimental data may be found, if for  $T=T_c$  we consider the crystal as consisting of coupled pairs of neighbouring Cu-ions. The coupling will be ferromagnetic ( $s=1$  lowest) for the majority of pairs, due to short-range spin-spin correlation, and will furthermore be anisotropic. A Hamiltonian for anisotropic exchange between a pair of Cu-spins may be given by:

$$H = -2 [J_{//} s_i^z s_j^z + J_{\perp} (s_i^x s_j^x + s_i^y s_j^y)], \quad (7)$$

where  $J_{//}$  and  $J_{\perp}$  denote exchange constants, and  $i$  and  $j$  denote a pair of nearest-neighbour ions. The  $z$  axis is not necessarily identical to a crystalline axis, but may coincide e.g. with the line joining the ions  $i$  and  $j$ . The ground state for a pair of ions with  $s=1/2$  is threefold degenerate, in the case  $J_{//}=J_{\perp}>0$ . For slightly anisotropic exchange ( $J_{//}>J_{\perp}$ ) the degeneracy is removed, and a splitting ( $J_{//}-J_{\perp}$ ) results between the  $s^z=\pm 1$  ground state and a  $s^z=0$  singlet, in analogy with a crystalline field splitting  $D(s^z)^2$  for ions having  $s^z=1$ .

For the purpose of discussion, we introduce two assumptions. a) The influence of the surrounding ions is approximated by a molecular field proportional to the mean magnetization. This procedure is comparable to the constant-coupling approximation of Kasteleijn and Van Kranendonk<sup>28)</sup>, which at  $T=T_c$  gives a value of 0.60 for the correlation between a pair of neighbouring spins. b) The crystal consists of domains, in each of which all pairs have identical  $z$  axes, i.e. identical axes of preferred alignment, and hence coincide with the direction of the domain magnetization.

On the basis of assumption a), one may deal with the anisotropy energy,  $(J_{//}-J_{\perp})(s^z)^2$  for pairs (with  $s^z=1$ ), classically, using eq.(3). Let  $N_f(T)$  denote the number of pairs per cc. in the  $s=1$  state. Using the assumption b), the anisotropy energy  $K$  for a domain magnetized in the  $z$  direction has been calculated<sup>29)</sup> as:

$$K = N_f(T)Ds(s-1/2). \quad (8)$$

Eq.(8) may also be written as:

$$K = 1/2 N_f(T) (J_{//} - J_{\perp}). \quad (9)$$

Eq.(1) now becomes:

$$\frac{1}{\chi} = N + 1/2 N_f(T)D \sin^2 \theta. \quad (10)$$

If  $N_f$  is known, an estimate of the anisotropy energy per pair of ions,  $K/\frac{1}{2}N$ , can be derived from (9) by using  $J/k=0.35 T_c^{7)}$  and assuming an anisotropy of the exchange interaction of 2 per cent. In the constant-coupling (c.c.) approximation<sup>28)</sup> the spin-spin-correlation at  $T_c$  is found to be 0.60.

A preciser evaluation of the spin-pair correlation at  $T_c$  may be obtained from the series development method above  $T_c$  in the Heisenberg model. It may be inferred from a comparison of the fractions of the total energy involved in the phase transition,  $(E_\infty - E_c)/(E_\infty - E_0)$ , removed above  $T_c$  (this fraction is related to the spin-pair correlation) for the c.c. approximation<sup>28)</sup> and the series-development<sup>27)</sup> calculation. The former yields 43%, the latter 61%. From this consideration we estimate the spin-pair correlation to be about 0.7, which also represents the fraction of pairs in the  $s=1$  state,  $N_f/\frac{1}{2}N$ . If we express the anisotropy energy by an anisotropy field at saturation magnetization;  $H_A = -2K/M$ , we obtain an anisotropy field of 120 Oe. This is roughly the value required for explaining the initial susceptibility in fig. 3a. More significantly, the temperature dependence of the anisotropy-field on the basis of this interpretation agrees with that observed experimentally.

However, the  $z$  axes for various domains and pairs will very probably be different, since e.g. there are two kinds of Cu-ions, differing in the directions of their respective axes of large  $g$ -value. Consequently, when evaluating the macroscopic  $\chi$ , a directional averaging procedure has to be applied. Therefore, the direction of maximal  $\chi$  will not necessarily be related to the crystalline axes. In other words, deviations from  $\chi=1/N$  may be found for all directions in the crystal, and these deviations may persist at  $T=T_c$ .

## 5 The determination of the spontaneous magnetization and critical temperature

The reduced spontaneous magnetization  $M(T)/M(0)$  for  $T < T_c$  is theoretically well defined in zero field. The macroscopic reduced magnetization, however, has a notably lower value because of domain structure. To overcome this effect a field must be applied and the spontaneous magnetization has to be deduced from the measurements of the magnetization versus field.

The molecular field theory gives a simple relation from which  $M(T)/M(0)$  can be deduced for  $0 < T/T_c < 1$  viz.:

$$T/T_c = \frac{M(T)/M(0) + H/W M(0)}{\tanh^{-1}(M(T)/M(0))} \quad (11)$$

where  $H$  is the internal field and  $WM(0)$  the Weiss field at zero temperature. To obtain the spontaneous magnetization as a function of  $T$  one chooses a fixed value of  $M(T)$  between 0 and  $M(0)$  and uses (11) in the form  $T = a + bH$ . If the experimental points show this linear relation between  $H$  and  $T$  at constant  $M$ , the linear portion may be extrapolated to  $H=0$ , so that one obtains the temperature intercept  $T$ , belonging to the magnetization chosen, which by definition equals the spontaneous magnetization. Fig. 4 shows that the relation (11) is approximately satisfied for  $T$  lower than 1.72 K. For  $H < 20 \text{ Oe} (\equiv H^*)$ , eq. (11) is not satisfied. This is not surprising since the turning of the domains in

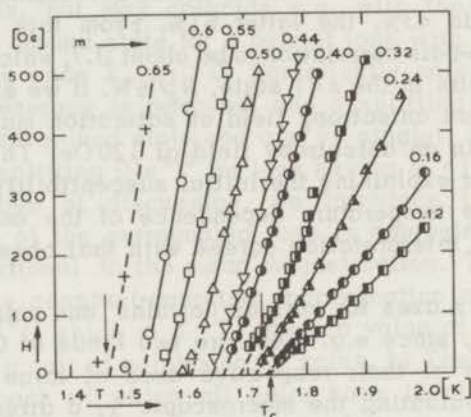


Fig. 4. The internal field as defined in fig. 3 section b is plotted versus the temperature for several values of the relative magnetization,  $m$ . The arrows indicate the temperature region, in which the extrapolation procedure as described by eq. (11) may be used to obtain the spontaneous magnetization as a function of the temperature.

the presence of anisotropy energy has not been taken into account in the derivation of eq. (11). The experimental points of  $\text{Ni}(T_c = 627.2 \text{ K})$  deviate from relation (11) for  $H^* < 8 \text{ KOe}^{30)}$ . The value of  $H^*/T_c$  for both substances are of the same order of magnitude.

For temperatures above 1.72 K,  $T$  and  $H$  are not related linearly, so that the value of the spontaneous magnetization cannot be deduced with this extrapolation procedure. Below 1.47 K the isotherms flatten markedly, so that only a few isotherms may be used to construct each of the curves  $(H, T)_M$ , which quickly introduces an error into the extrapolation.

Following a suggestion of Weiss and Forrer, a second method of extrapolation was used. Particularly below 1 K where the curves are

rather flat, the spontaneous magnetization  $M_S(T)$  may be found from the isothermal relation<sup>31)</sup>:

$$M(T) = M_S(T) (1 - a/H - b/H^2 \dots) + p(H), \quad (12)$$

where  $M(T)$  is the measured magnetization on applying the field  $H$ ,  $a$  and  $b$  are constants determining the approach to saturation, the term  $a/H$  accounting for the displacements of the domain walls and the term  $b/H^2$  accounting for turning the domains, while the term  $p(H)$  relates the polarization of the individual moments to the applied field strength. In a good approximation  $p(H) = \chi_o H$ , where  $\chi_o = \text{constant}$ . For  $H > 100$  Oe the terms  $a/H$  and  $b/H^2$  are very small compared to unity, so that a simple linear extrapolation to  $H=0$  of the isotherms provides us with the value of  $M_S(T)$ .

On decreasing the temperature, the results obtained by the two methods approach each other asymptotically<sup>30)</sup>. Therefore we have taken the average of both results for the temperature region between 1.0 and 1.45 K. The saturation value at  $T=0$  K has been obtained from the data by extrapolation according to the Bloch formula:

$$M(T) = M(0) [1 - \alpha_o (\frac{kT}{J})^{3/2}], \quad (13)$$

which is valid for small spin deviations in a Heisenberg ferromagnet.

Since the molecular field theory neglects correlation, it is not correct near  $T_c$ , so that we are left with the problem how to locate  $T_c$  precisely. The Heisenberg model, which has been shown (see ch.IV) applicable to this salt, takes account of the interactions between nearest-neighbours. The susceptibility  $\chi$  in this model is predicted<sup>32)</sup> to behave asymptotically as

$$\chi_o^{-1} \sim (T - T_c)^\gamma, \quad (14)$$

with  $\gamma = 1.43$ . The experimental value of  $\gamma$  is 1.40 for this salt<sup>33)</sup>. The deviation of  $\chi_o^{-1}$  from relation (14) in the temperature range  $T - T_c < 0.05 T_c$  is less than 5% (see ch. 1 section 3.5.2). In order to deduce  $T_c$  let us define the function  $T^*$  according to

$$T^*(T) \equiv 1/(d/dT) \ln (\chi_o^{-1}) = (T - T_c)/\gamma. \quad (15)$$

Experimentally  $T^*$  can be found from a plot of  $\chi_o^{-1}$  vs.  $T$  according to the identity

$$1/(d/dT) \ln(\chi_o^{-1}) = \chi_o^{-1}/(d(\chi_o^{-1})/dT). \quad (16)$$

Linear extrapolation of the plot of  $T^*$  vs.  $T$  to  $T^* = 0$  yields  $T_c$ .

The susceptibility,  $\chi_o = (\partial M / \partial H)_{H=0}$  cannot be accurately determined from a plot of  $M$  vs.  $H$ , since such a graph is strongly curved for temperatures near the Curie temperature (see fig. 3b). The graphs of the data are far less curved, if they are plotted as  $m^2$  vs.  $H/m$ , where  $m$  stands for the relative magnetization (fig. 5a). This technique has been proposed by several authors<sup>34,35</sup> and it has been applied to several experiments<sup>36,37</sup>. Extrapolation of the linear part of the graphs to  $m^2 = 0$  provides us with the values of  $A\chi_o^{-1}$ . The numerical constant  $A$ , however, cancels from the expression for  $T^*$ , as may be seen from eq. (16).

A theoretical basis for the  $m^2$  vs.  $H/m$  technique is furnished by considering a system of independent spins that interact with a mean field. Assume that the magnetization produces a mean field  $H_{mf}$

$$H_{mf} = H_o m, \quad (17)$$

where  $m$  denotes the relative magnetization and  $H_o$  an experimental constant having the dimension of a field. The field  $H_{eff}$  acting on an ion, is now given by

$$H_{eff} = H + m H_o. \quad (18)$$

Using Boltzmann statistics one obtains

$$m = \tanh(\alpha) \quad (19)$$

for a system of independent spins ( $s = 1/2$ ). In eq.(19)  $\alpha = \mu H_{eff} / kT$  and  $\mu = g \mu_B s$ . If  $\alpha \ll 1$ , the right-hand side of eq.(19) may be expanded in powers of  $\alpha$ . Retaining terms up to the third order in  $\alpha$ ,

$$m = \alpha - 1/3 \alpha^3. \quad (20)$$

Substituting  $\alpha$  into eq.(20) one may obtain

$$\frac{H}{m} = \left( \frac{kT}{\mu} - H_o \right) + 1/3 \left( \frac{\mu}{kT} \right)^2 m^2 H_o^3 \left( 1 + \frac{H}{m H_o} \right)^3 \quad (21)$$

after some manipulation. If  $T \rightarrow T_c$  and  $H \rightarrow 0$ ,  $m \rightarrow 0$  and the inverse susceptibility  $1/\chi = H/mM(0)$  tends to zero, so that

$$\frac{kT_c}{\mu} = H_o \quad (22)$$

On substitution of  $H_o$  for  $kT_c/\mu$  in eq.(21) we obtain

$$\frac{H}{m} = \frac{H_o}{T_c} (T - T_c) + 1/3 H_o \left(\frac{T_c}{T}\right)^2 \left(1 + \frac{H}{mH_o}\right)^3 m^2. \quad (23)$$

Assuming a)  $H/mH_o \ll 1$  so that

$$\left(1 + \frac{H}{mH_o}\right)^3 \simeq \left(1 + 3 \frac{H}{mH_o}\right),$$

eq.(23) takes the form

$$\frac{H}{m} = \frac{\frac{H_o}{T_c} (T - T_c) + 1/3 H_o \left(\frac{T_c}{T}\right)^2 m^2}{1 - \left(\frac{T_c}{T}\right)^2 m^2}. \quad (24)$$

If b)  $m^2 \left(\frac{T_c}{T}\right)^2 < 0.1$ , one may simplify eq.(24) to

$$\frac{H}{m} = \frac{H_o}{T_c} (T - T_c) + 1/3 H_o \left(\frac{T_c}{T}\right)^2 m^2, \quad (25)$$

which for experimental purpose may be written as

$$\frac{H}{m} = A(T) + B(T) m^2. \quad (26)$$

$A(T)$  may be determined from a graph of  $m^2$  vs.  $H/m$ . Clearly  $(H/m)_{m \rightarrow 0} = A(T)$ . The assumption a) is consistent with eq.(25) because  $H/mH_o \ll 1$  according to eq.(25), if assumption b) is fulfilled and  $(T - T_c)/T_c \ll 1$ .

Fig. 5a shows us the plot of the quantity  $m^2$  vs.  $H/m$  for a set of isotherms with  $T$  near  $T_c$ . The isotherms for  $T \geq 1.7441$  K furnish us with an unambiguous value of the quantity  $(H/m)_{m \rightarrow 0}$  (being proportional to  $\chi_o^{-1}$ ). This quantity has been plotted as a function of  $T$  in fig. 5b. Using eq.(16),  $T^*$  defined by relation (15) can now be calculated from this plot. The result is also shown in fig. 5b. As one may see,  $T^*$  is linear in  $T$ , so that the intercept of the graph extrapolated to  $T^* = 0$  that gives the critical temperature, is found to be  $T_c = 1.735 (\pm 0.002)$  K.

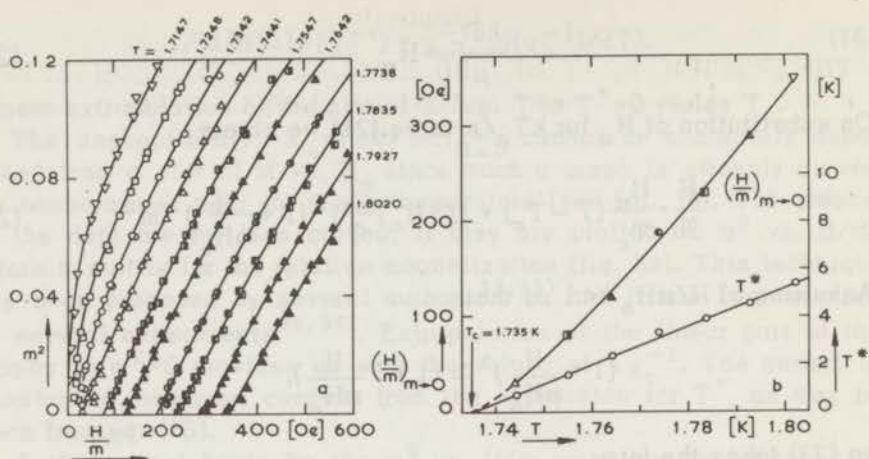


Fig. 5. Section a shows the isotherms at temperatures between 1.7147 and 1.8020 K, plotted as  $m^2$  vs.  $H/m$ . The intercepts of these curves with the axis  $m^2=0$ ,  $(H/m)_{m \rightarrow 0}$  (being proportional to  $\chi_0^{-1}$ ), are plotted in section b as a function of  $T$ .  $T^* = \chi_0^{-1} / (d(\chi_0^{-1})/dT)$  (see the text) plotted vs.  $T$  in section b yields  $T_c = 1.735 \pm 0.002$  K.

The slope of the line given by  $T^* = (T - T_c)/\gamma$  is  $1/\gamma$ . From our data we find  $\gamma = 1.25 (\pm 0.1)$ , which is somewhat lower than the value found by means of a.c. susceptibility measurements,  $\gamma = 1.40^{33}$ . This difference may be related with the temperature-dependent contribution (arising from the anisotropy energy) to the susceptibility (eq. (1)). This contribution depends on the direction of measurement with respect to the crystalline axes.

A plot of  $H/M$  vs.  $M^2$  of the measurements on the ferromagnetic substances EuO and GdN, with  $s=7/2$ , performed by Junod and Lévy<sup>37</sup>, yields straight lines also. As the solution (19) to (18) for general  $s$  is given by the Brillouin function, which is spin-dependent, the values of  $A$  and  $B$  for  $s \neq 1/2$  are different from those given in eq. (26).

The data of the relative spontaneous magnetization,  $m$ , vs. the relative temperature,  $t$ , have been collected in table I.

## 6 Discussion of the results

In fig. 6 the experimental values of the reduced magnetization vs. the reduced temperature, collected in table I have been plotted. For comparison we have also plotted the recently published results on the calculation of the spontaneous magnetization of the Heisenberg

TABLE I

The reduced spontaneous magnetization,  $m=M(T)/M(0)$ , is presented as a function of the reduced temperature  $t=T/T_C$ ,  $T_C=1.735(\pm 0.002)K$  according to figure 5b. The symbols a and b denote measurements in different apparatus as described in section 2.

a				b			
t	m	t	m	t	m	t	m
0.058	0.998	0.324	0.954	0.664	0.822	0.899	0.55
0.0608	0.992	0.368	0.943	0.701	0.795	0.926	0.5
0.136	0.984	0.417	0.933	0.732	0.775	0.944	0.44
0.160	0.986	0.448	0.920	0.777	0.731	0.957	0.40
0.200	0.982	0.493	0.904	0.806	0.700	0.972	0.32
0.231	0.974	0.546	0.887	0.845	0.65	0.989	0.24
0.274	0.970	0.597	0.859	0.879	0.60	0.997	0.16

$s=1/2$  ferromagnet (s.c. and f.c.c. structures) by Cooke and Gersch<sup>14</sup>, Liu and Siano<sup>15</sup>, and Loly<sup>11</sup>). Cooke and Gersch obtained their results by means of Green's functions technique in second order. This theory covers the whole temperature region, whereas the spin-wave theory may only be applied in a limited temperature region. The dashed curve represents the calculations for the f.c.c. structure, the dash-dotted curve those for the s.c. structure. Taking account of the fact that the theoretical values for the b.c.c. lattice will lie between those for the s.c. and f.c.c. lattices, we find a striking agreement between this theoretical result and the experimental curve.

In the low temperature region a more sensitive criterion for testing the theory is furnished by comparing the specific heat results with the theory. As on the low temperature side the Green's functions method yields exactly the same result as the spin wave theory, this comparison has essentially been made in chapter IV.

Liu and Siano have also used a Green's functions technique, but only in first order. The decoupling scheme used by these authors has been introduced by Tyablikov<sup>38</sup>), and is different from the method used by Cooke and Gersch. Some results for the f.c.c. lattice, denoted by a + symbol have been plotted in fig. 6. The calculated curve for the s.c. lattice has not been plotted, as this curve would also lie appreciably below the curve obtained by Cooke and Gersch for the same crystal structure. One may notice that even the f.c.c. curve calculated by Liu and Siano lies appreciably lower than the experimental curve. This disagreement may be due to the incorrectness of the decoupling scheme used, or to the fact that the calculations are made to first order only.

Recently Loly<sup>11</sup>) has applied the technique of the self-consistently

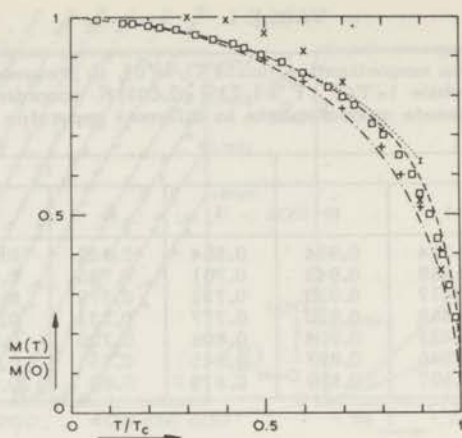


Fig. 6. The reduced spontaneous magnetization  $m$  is shown versus  $T/T_c$  for the present measurement and several statistical theories.  $\square$  The present measurement.

- f.c.c. } Heis. model  $s=1/2$ , calculated by Cooke and Gersch<sup>14)</sup>
- · - s.c. } with Green's functions technique in second order.
- +++ f.c.c. Liu and Siano<sup>15)</sup>, Heis.  $s=1/2$ , Green's functions calculation with Tyablikov's decoupling procedure.
- ... b.c.c. Loly's result<sup>11)</sup> on the Heisenberg  $s=1/2$  ferromagnet, calculated with (renormalized) spin-wave theory. The second neighbour exchange coupling  $J_2=0.15 J_1$ . The results at  $T/T_c=0.9$  for  $J_2=0$  and  $J_2=0.3 J_1$  are given by the end points of the bar attached to the result at  $T/T_c=0.9$  for  $J_2=0.15 J_1$ .

xxx Molecular field model for  $s=1/2$ .

renormalized spin wave approximation in a somewhat modified version, combined with a non-zero second neighbour exchange constant to the calculation of the relative magnetization of the b.c.c. Heisenberg  $s=1/2$  ferromagnet, up to  $T/T_c=0.9$ . Various theoretical predictions have recently been derived on the influence of n.n.n. exchange on the value of critical parameters such as energy and entropy removed above  $T_c$  by the short-range ordering process<sup>27,39,40</sup>). By applying these results to the experimentally obtained values<sup>6,7)</sup>, Dalton and Wood<sup>40)</sup> deduced  $J_2/J_1=0.25\pm 0.1$  for the ratio between nearest and next-nearest-neighbours exchange coupling (for more details see ch.IV). Loly has calculated the spontaneous magnetization for the b.c.c.  $s=1/2$  Heisenberg model with  $J_2/J_1=0.15$  and  $J_2/J_1=0.25$ . The results are represented by the dotted curve. The difference between curves for  $\alpha=0.15$  and  $\alpha=0.25$  (and consequently for  $\alpha=0$ ) is hardly noticeable in fig. 6. The largest difference, which is found at the highest temperature, is shown in the figure as a small bar at  $T/T_c=0.9$ .

It may be noted that the recent calculations of Loly agree quite well with the results of Cooke and Gersch up to  $T/T_c = 0.55$ , but at higher temperatures they are systematically higher than both the latter theory and this experiment. Furthermore, one may note the striking difference between the Heisenberg  $s = \frac{1}{2}$  curve and the molecular field results for  $T < 0.7 T_c$ . This difference is expected to decrease for increasing spin values, which has actually been calculated by Callen and Callen for the spin =  $7/2$  ferromagnet of f.c.c. structure. In the temperature region between  $0.75 T_c$  and  $0.90 T_c$  the molecular field theory for  $s = \frac{1}{2}$  seems to be a good approximation, which is confirmed by the applicability of the extrapolation procedure for finding  $M_S(T)$  based on this theory.

In fig. 7 the reduced spontaneous magnetization has been plotted as a function of  $\epsilon = 1 - T/T_c$ . The value of  $T_c$  viz.  $1.735 (\pm 0.002) K$  has been derived from fig. 5b. The length of the bars attached to

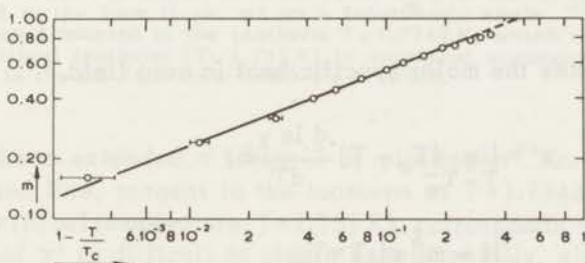


Fig. 7. The relative spontaneous magnetization,  $m$ , is plotted vs.  $(1 - T/T_c)$  on a logarithmic scale.  $T_c = 1.735 \pm 0.002 K$  (see fig. 5b). The bars indicate the ambiguity in position, due to the uncertainty in  $T_c$ . The straight line represents the fit:  $m = B(1 - T/T_c)^\beta$ , with  $\beta = 0.38 \pm 0.04$ , and  $B = 1.33 \pm 0.15$ .

several points indicate the uncertainty in  $\epsilon$ . This uncertainty in  $\epsilon$  is caused firstly by the inaccuracy in the determination of  $T_c$  (see fig. 5b), and secondly the uncertainty in the determination of  $T$ , which is obtained by means of the extrapolated curve  $m(H, T)_{H \rightarrow 0} = \text{constant}$  (fig. 4). For  $10^{-2} < \epsilon < 0.2$  the best fit to the experimental values is found to be a straight line, corresponding to the relation

$$m = B(1 - T/T_c)^\beta, \quad (27)$$

with  $\beta = 0.38 (\pm 0.04)$ , and  $B = 1.33 (\pm 0.15)$ . The uncertainties indicated include errors in  $1 - T/T_c$  and in  $m$ .

The values for  $\beta$  and  $B$  in this salt are higher than the values found

in most experiments, as one may notice from a recent review on the subject by Heller<sup>41)</sup>. The values for two ferromagnetic substances are close to ours. For  $\text{CrBr}_3$  Senturia and Benedek<sup>42)</sup> have found  $B=1.32 (\pm 0.07)$  and  $\beta=0.365 (\pm 0.015)$  while  $7.10^{-3} < 1 - T/T_c < 5.10^{-2}$ . For Ni, Howard et al.<sup>43)</sup> fit their measurements with  $B=1.5 (\pm 0.1)$  and  $\beta=0.37 (\pm 0.03)$  in the temperature region:  $10^{-3} < \epsilon < 10^{-1}$ . Up to now for the Heisenberg model no firm theoretical results have been derived for  $\epsilon < 10^{-1}$ , not even for  $s=1/2$ .

However, using certain statistical assumptions, several relations between critical exponents have been derived. (For recent reviews see refs. 44 and 45). The exponents we will consider, i.e.  $\alpha'$ ,  $\gamma'$ ,  $\delta$  and  $\beta$  are defined by the relations

$$\alpha' = \lim_{T \rightarrow T_c^-} (T_c - T) \frac{d \ln c_H}{dT}, \quad (28)$$

where  $c_H$  denotes the molar specific heat in zero field,

$$\gamma' = \lim_{T \rightarrow T_c^-} (T_c - T) \frac{d \ln \chi_0}{dT}, \quad (29)$$

$$H \propto m^\delta \text{ at } T = T_c, \quad (30)$$

$\beta$  is defined by relation (27).  $T - T_c^-$  denotes the approach of  $T_c$  from the low-temperature side. In general the primed quantities refer to the temperature region below  $T_c$ .

The following two relations will be considered, viz.

$$\alpha' + \beta(\delta + 1) \geq 2 \text{ (see ref. 46),} \quad (31)$$

and

$$\alpha' + 2\beta + \gamma' \geq 2 \text{ (see ref. 47).} \quad (32)$$

Experimentally  $\alpha'$  is found to be  $0.00 \pm 0.03^7)$  and  $\beta=0.38 \pm 0.04$ . The value of  $\delta$  can be derived from a plot of the critical isotherm on a logarithmic scale. The critical isotherm might be obtained from a straightforward interpolation of the graphs of the isotherms on both sides of  $T_c$  as plotted in fig. 5a. However, we have preferred to plot the three isotherms nearest to  $T_c$ , so that the small differences in the slope may be estimated (fig. 8). For a better display the horizontal

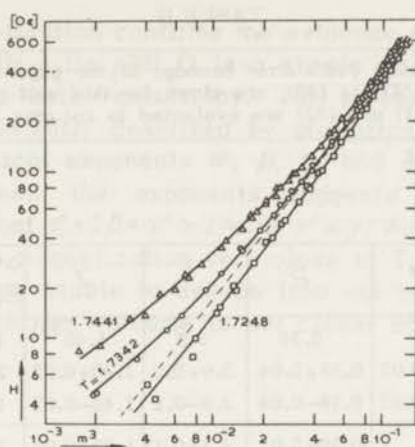


Fig. 8. The isotherms at  $T=1.7441$ ,  $1.7342$  and  $1.7248$  K are plotted in the form  $H$  vs.  $m^3$  on a logarithmic scale. The dashed line being tangent to the isotherm  $T=1.7342$  K, which represents the critical isotherm ( $T=1.735$  K) to graphical accuracy, corresponds to the relation  $H \propto m^\delta$  with  $\delta = 3.9 \pm 0.2$ .

scale has been extended a factor 3 by plotting  $m^3$  vs.  $H$ . The slope of the dashed line, tangent to the isotherm at  $T=1.7342$  K (being very close to the critical temperature,  $T=1.735$  K), corresponds to  $\delta = 3.9 (\pm 0.2)$ . The value of  $\gamma'$  is difficult to obtain experimentally, since the initial susceptibility of a ferromagnet is infinite for  $T < T_c$ . For the Heisenberg model  $\gamma'$  is not known. For the simple quadratic and triangular lattices in the Ising model  $\gamma' = \gamma (= 1.75)^{48)}$ , while numerical evidence for the three-dimensional cubic lattices  $^{49)}$  suggests  $\gamma' \neq \gamma$  ( $\gamma' = 1.31_{-0.05}^{+0.04}$ ,  $\gamma = 1.25 \pm 0.01$ ).

In the first four columns of table II we list the experimental values of the four exponents known for this salt and for Ni. The fifth column contains the values of  $\alpha' + \beta(1 + \delta)$ . Assuming  $\gamma' = \gamma$ , the value of  $\alpha' + 2\beta + \gamma'$  is found (column 6). Assuming the equality signs in eqs. (31) and (32) to obtain,  $\alpha'$  can be eliminated between (31) and (32), so that  $\gamma'$  may be calculated (column 7).

If we assume  $\alpha' = 0$  for both salts, a set of values  $(\beta, \delta)$  may be found that satisfies the equality contained in eq. (31), and lies within the error bounds given in table II. This set of values  $(\beta, \delta)$  is listed in table III. The value of  $\gamma'$  for each pair  $(\beta, \delta)$  may be calculated, if it is assumed that the equality sign in eq. (32) holds too (third row of table III). The fourth row lists the values of  $\gamma - \gamma'$  for each  $(\beta, \delta)$ . We notice that  $\gamma' \neq \gamma$ , which indicates that full symmetry between the ex-

TABLE II

The experimental values (with error bounds) of the exponents $\alpha'$ , $\beta$ , $\delta$ and $\gamma$ , defined by the eqs. (27) to (30), are given for this salt and Ni. The left-hand sides of relations (31) and (32) are evaluated in columns 5 and 6 respectively.							
	$\alpha'$	$\beta$	$\delta$	$\gamma$	$\alpha' + \beta(1+\delta)$	$\alpha' + 2\beta + \gamma'$	If (31) and (32) hold as equalities:
							$\gamma' = \beta(\delta - 1)$
$\text{Cu}(\text{NH}_4)_2\text{Br}_4 \cdot 2\text{H}_2\text{O}$	0.00 <sup>7)</sup>	0.38	3.9	1.40 <sup>33)</sup>	1.86	2.16	1.10
	0.00+0.03	0.38+0.04	3.9+0.2	1.40+0.02	2.17	2.29	1.30
	0.00-0.03	0.38-0.04	3.9-0.2	1.40-0.02	1.57	2.03	0.85
Ni	0.00	0.38±0.01	4.3±0.1	1.33±0.02	2.01	2.09	1.25
	Ref.	50)	43,51,52)	36,52)	36,52)		

TABLE III

The sets of extreme values of ( $\beta$ , $\delta$ ) satisfying the equalities in relations (31) and (32). The third and fourth rows list $\gamma'$ and ( $\gamma - \gamma'$ ) respectively.					
exponent	$\text{Cu}(\text{NH}_4)_2\text{Br}_4 \cdot 2\text{H}_2\text{O}$ :		Ni(refs. are given in table II):		
	condition				
	$\beta_{\text{max}}$	$\delta_{\text{max}}$	central values	$\delta_{\text{min}}$	$\delta_{\text{max}}$
$\beta$	0.42	0.39	0.38	0.39	0.37
$\delta$	3.8	4.1	4.3	4.2	4.4
$\gamma' = \beta(\delta - 1)$	1.16	1.21	1.25	1.25	1.26
$\gamma - \gamma'$	0.24	0.19	0.08	0.08	0.07

ponents below and above the critical temperature does not obtain. In the case of the three-dimensional lattices in the Ising model  $\gamma' \neq \gamma$ , while for the two substances cited  $\gamma' < \gamma$ .

Another way of interpreting the experimental results starts with the assumption  $\gamma' = \gamma$ . In this case the inequality sign in relation (32) obtains for any experimentally allowed set of values ( $\beta$ ,  $\delta$ ) while the equality sign of relation (31) holds for an ample set of values ( $\beta$ ,  $\delta$ ), although not for all.

Summing up the results we may state that the measurement of the

spontaneous magnetization confirms the evidence of ref. 7 and ch. IV that the salt  $\text{Cu}(\text{NH}_4)_2\text{Br}_4 \cdot 2\text{H}_2\text{O}$  is a simple  $s = \frac{1}{2}$  b.c.c. Heisenberg ferromagnet having little anisotropy. The properties measured are shown to be consistently described by statistical theories. A comparison of the critical exponents  $\alpha'$ ,  $\beta$ ,  $\gamma$ , and  $\delta$  with two rigorous inequalities between the exponents suggests that either  $\gamma' < \gamma$  ( $\gamma - \gamma' \approx 0.20$ ), or that  $\alpha' + 2\beta + \gamma' > 2$  with  $\gamma' \equiv \gamma$ . Accurate determination of the spontaneous magnetization very close to  $T_c$  ( $T_c - T < 0.01 T_c$ ), which we have been unable to deduce from our measurements in an external field, would be welcome to set closer bounds on the value of the exponent  $\beta$ .

### References

1. TSUBOKAWARA, I., *J. Phys. Soc. Japan* 15(1960)1664.
2. MATTHIAS, B.T., BOZORTH, R.M. and VAN VLECK, J.H., *Phys. Rev. Letters* 7(1961)160.
3. MORUZZI, V.L. and TEANEY, D.T., *Solid State Commun.* 1(1963)127.
4. GOSSARD, A.C., JACCARINO, V. and REMEIK, J.P., *Phys. Rev. Letters* 7(1961)122.
5. WOLF, W.P., LEASK, M.J.M., MANGUM, B. and WYATT, A.F.G., *J. Phys. Soc. Japan (Suppl.)* 17(1962)487.
6. MIEDEMA, A.R., VAN KEMPEN, H. and HUISKAMP, W.J., *Physica* 29(1963)1266; *Commun. Kamerlingh Onnes Lab., Leiden No. 336a*.
7. MIEDEMA, A.R., WIELINGA, R.F. and HUISKAMP, W.J., *Physica* 31(1965)1585; *Commun. Leiden No. 345a*.
8. McCOLLUM, D.C. and CALLAWAY, I., *Phys. Rev.* 130(1963)1741.
9. LOW, G.G., *Proc. Phys. Soc. (G.B.)*, 82(1963)992.
10. WOOD, D.W. and DALTON, N.W., *Proc. Phys. Soc. (G.B.)* 87(1966)755.
11. LOLY, P.D., *J. appl. Phys.* 39, pt. II (1968), 1109.
12. KASTELEIJN, P.W. and VAN KRANENDONK, J., *Physica* 22(1956)317.
13. CALLEN, H.B. and CALLEN, E., *Phys. Rev.* 136(1964)A1675.
14. COOKE, J.F. and GERSCH, H.A., *Phys. Rev.* 153(1967)A641.
15. LIU, S.H. and SIANO, D.B., *Phys. Rev.* 164(1967)A697.
16. CALLEN, E. and CALLEN, H.B., *J. appl. Phys.* 36(1965)1140.
17. HELLER, P. and BENEDEK, G.B., *Phys. Rev. Letters* 14(1965)71.
18. EIBSCHUTZ, M., SHTRIKMAN, D. and TREVES, D., *Phys. Rev.* 156(1967)A562.
19. ARGYLE, B.E. and PUGH, E.W., *J. appl. Phys.* 32 (Suppl) (1961)334.
20. MESS, K.W., LAGENDIJK, E., CURTIS, D.A. and HUISKAMP, W.J., *Physica* 34(1967)126; *Commun. Leiden No. 354d*.
21. EDELSTEIN, A.S. and MESS, K.W. *Physica* 31(1965)1707; *Commun. Leiden No. 344c*.
22. GOEDEMOED, S.H., thesis, Leiden, p. 29.
23. SUZUKI, H. and WATANABE, T., *Phys. Lett.* 26A(1967)103.
24. VAN VLECK, J.H., *J. Phys. Radium* 20(1959)124; *Colloq. int. de Magnétisme, Grenoble, 1958, p. 60 (1959)*.
25. VAN VLECK, J.H., *Phys. Rev.* 52(1937)1178.
26. KANAMORI, J., "Anisotropy and Magnetostriction", Ch. IV of "Magnetism" I, eds. Rado, G.T. and Suhl, H., (Academic Press, New York, London), p. 165.
27. DALTON, N.W. and WOOD, D.W., *Phys. Rev.* 138A(1965)779.

28. KASTELEYN, P.W. and VAN KRANENDONK, J., *Physica* 22(1956)317.
29. Ref. 26, p. 149.
30. WEISS, P. and FORRER, R., *Ann. de Phys.*, 10<sup>me</sup>s., tome 5(1967)153.
31. KNELLER, E., "Ferromagnetismus", p.152, Springer Verlag, ed. 1962.
32. BAKER, G.A.Jr., GILBERT, H.E., EVE, J. and RUSHBROOKE, G.S., *Phys. Rev.* 164(1967)800.
33. DE JONGE, L.J., MIEDEMA, A.R. and WIELINGA, R.F., to be published.
34. BELOV, K.P. and GORYAGA, A.N., *Fiz.Met.Metallov.* 2, No. 1(1956)3; Part is translated in English in: Belov, K.P.: 'Magnetic transitions', Consultants bureau N.Y. (1961).
35. KOUVEL, J.S., General Electric Res. Lab. Rept. No. 57-RL-1799 (1957), unpublished.
36. KOUVEL, J.S. and FISHER, M.E., *Phys.Rev.* 136(1964)A1626.
37. JUNOD, P. and LEVY, F., *Phys.Lett.* 23(1966)624.
38. BOGOLYUBOV, N.N. and TYABLIKOV, S.V., *Soviet Physics Doklady* 4(1959)604.
39. PIRNIE, K., WOOD, D.W. and EVE, J., *Mol.Phys.* 11(1966)551.
40. WOOD, D.W. and DALTON, N.W., *Proc.Phys.Soc. (London)*, 87(1966)755.
41. HELLER, P., "Experimental investigations of critical phenomena", *Rep. on Progr. in Phys.* vol. 30(1967)731.
42. SENTURIA, S.D. and BENEDEK, G.B., *Phys.Rev.Letters* 17(1966)475.
43. HOWARD, D.G., DUNLAP, B.D. and DASH, J.G., *Phys.Rev.Letters* 15(1965) 628.
44. KADANOFF, L.P., GÖTZE, W., HAMBLÉN, D., HECHT, R., LEWIS, E.A.S., PALCIAUSKAS, V.V., RAYL, M., SWIFT, J., ASPNES, D., KANE, J., 'Static phenomena near critical points: theory and experiment', *Revs.of Mod.Phys.* 39(1967)395.
45. FISHER, M.E., *Rep. on Progr. in Physics*, 30 pt II(1967)615.
46. GRIFFITHS, R.B., *Phys.Rev.Letters* 14(1965)623.
47. RUSHBROOKE, G.S., *J.chem.Phys.* 39(1963)842.
48. ESSAM, J.W. and FISHER, M.E., *J.chem.Phys.* 38(1963)802.
49. BAKER, G.A.Jr., GAUNT, D.S., *Phys.Rev.* 155(1967)545.
50. KRAFTMAKHER, Ya.A., *Fiz. Tverdogo Tela (USSR)*, 8(1966)1306; Engl. transl. in *Sov. Phys. Sol. St. (USA)* 8(1966)1048.
51. An analysis of the data of ref. 30 made by us.
52. NOAKES, J.E. and ARROTT, A., *J.appl.Phys.* 38 pt II(1968)1235.

## Chapter VI

THE SPECIFIC HEAT OF TWO DIPOLAR ANTIFERROMAGNETS  
AND ONE FERROMAGNET BELOW 1 KELVIN

## 1 Introduction

Heat capacity measurements are of interest for the study of magnetic interactions in ionic compounds, since the interaction strength may often be derived from the position of the heat capacity singularity and from the corresponding energy yield.

In Gd compounds considerable contributions to the heat capacity arise from crystalline field interaction. Early adiabatic demagnetization experiments<sup>1,2,3,4</sup> on  $\text{Gd}_2(\text{SO}_4)_3 \cdot 8\text{H}_2\text{O}$  were analyzed in terms of cubic Stark splittings and showed the absence of strong magnetic interactions. The Stark levels have recently been determined<sup>5</sup> by electron paramagnetic resonance (E.P.R.) measurements and it was found that the crystalline electric field is predominantly axial, although some deviation from axial symmetry is found in the sulphate. In terms of the spin-hamiltonian:

$$H = g\beta H \cdot s + b_2^0 \left\{ s_z^2 - \frac{1}{3}s(s+1) \right\} + \frac{b_2^2}{3} (s_x^2 - s_y^2) + \\ + b_4^0 \left[ \frac{7}{12}s_z^4 - \left\{ \frac{1}{2}s(s+1) - \frac{5}{12} \right\} s_z^2 - \frac{1}{10}s(s+1) + \frac{1}{20}s^2(s+1)^2 \right]$$

(where  $s = \frac{7}{2}$ ,  $g = 2$ , while higher terms are omitted) it is found that  $b_4^0/b_2^0 < 0.1$  and  $b_2^2 < b_2^0$  in most Gd salts so far investigated. For  $\text{Gd}_2(\text{SO}_4)_3 \cdot 8\text{H}_2\text{O}$  one has approximately  $b_4^0/b_2^0 = -0.02$  and  $\frac{1}{3}b_2^2 \approx \frac{1}{5}b_2^0$  at low temperatures.

The Stark levels for Gd sulphate as determined by interpolation of E.P.R. results on  $\text{Gd}^{3+}$  in Nd, Sm and Y-sulphate are  $E/k = 0\text{K}, 0.320\text{K}, 0.710\text{K}$  and  $1.257\text{K}$ , assuming  $s_z = \pm \frac{1}{2}$  levels lowest, i.e.  $b_2^0$  positive. An analysis of Bogle and Toutenhoofd<sup>6</sup> of heat capacity data of Van Dijk e.a.<sup>3,4</sup> has shown that  $b_2^0$  cannot be negative in the sulphate.

It has been shown by Iveranova e.a.<sup>7</sup> that the crystal structure of the sulphate octohydrate is equivalent to that of the other isomorphous rare earth compounds from Pr to Y, in which series monotonic increasing lattice constants have been measured. The structure is monoclinic<sup>8</sup> (space group  $C_{2h}^6$ ) with a tetramolecular unit cell having dimensions  $a_0 = 18.303 \text{ \AA}$ ,  $b_0 = 6.74 \text{ \AA}$  and  $c_0 = 13.539 \text{ \AA}$ , and  $\beta = 102^\circ$ . This leads to a unit cell volume of  $1633 \pm 9 \text{ \AA}^3$  and a density of  $2.99 \text{ g/cm}^3$ , corresponding to  $4.87 \times 10^{21}$  ions per  $\text{cm}^3$ . The positions ( $a, b, c$ ) of the metal

ions vary probably appreciably over the rare earth series as can be seen from the differences between the  $(a, b, c)$  values in the Nd and Sm salt. Following Zachariassen<sup>8)</sup> and taking the Sm compound as a model for the Gd salt, one has  $a=0.106a_0$ ,  $b=0.025b_0$  and  $c=-0.231c_0$ . This leads to Gd-Gd distances among the positions  $\pm(a, b, c)$ ,  $\pm(\frac{1}{2}-a, b, \frac{1}{2}-c)$ ,  $\pm(a+\frac{1}{2}, \frac{1}{2}-b, c)$  and  $\pm(a, b+\frac{1}{2}, c+\frac{1}{2})$  of 5.08 Å, 5.51 Å, 6.13 Å, 6.48 Å, 2 times 6.74 Å etc. The E.P.R. results of Bogle *e.a.*<sup>5)</sup> on Gd ions in the isomorphous rare earth sulphates are referred to an  $(x, y, z)$  coordinate system, in which the  $z$  axis makes an angle of  $55^\circ$  with the twofold  $b$  axis. They find two distinct kinds of ions, differing in a rotation of the  $z$  axis about the twofold  $b$  axis. It should be noticed that, whereas Bogle takes  $\beta=118^\circ$ , the results of Iveranova show that  $\beta=102^\circ$ .

The crystal structure of  $\text{GdCl}_3 \cdot 6\text{H}_2\text{O}$  has been investigated more precisely than that of the sulphate, while on the other hand no precise E.P.R. data are available. Marezio *e.a.*<sup>9)</sup> have shown the crystal structure to be monoclinic (space group  $C_{2h}^4$ ) with a bimolecular unit cell of dimensions  $a_0=9.651\text{Å}$ ,  $b_0=6.525\text{Å}$ ,  $c_0=7.923\text{Å}$  and  $\beta=93.65^\circ$  (see also fig.8).

The unit cell volume is  $498.4\text{Å}^3$  and the calculated density is  $2.478\text{g/cm}^3$ , the number of ions per  $\text{cm}^3$  is  $4.02 \times 10^{21}$ . The Gd ions have positions  $\pm(a, b, c)$ ,  $\pm(a+\frac{1}{2}, -b, c+\frac{1}{2})$ . The Gd ions form a primitive translational lattice and nearest neighbours are found in pairs at 6.52 Å, 6.55 Å and 6.56 Å. The two members of a pair are not diametrically opposed except for the nearest pair along the  $c$  axis; although the unit cell is nearly orthorhombic, there are no nearly right angles between the lines connecting a Gd ion with its nearest neighbours. For a description of the magnetic ions, it may be useful to consider the Gd ions arranged in linear chains along the  $b$  axis, intersecting the  $ac$  plane in a nearly simple square lattice of 6.1 Å spacing. The Gd ions of adjacent chains are shifted by 1.98 Å along the  $b$  axis, so that planes through the Gd ions parallel to the  $ac$  plane are spaced alternately by 1.98 Å and 4.54 Å. The Gd ions are surrounded by 6 water molecules and two chlorine ions, forming two complexes  $[\text{Cl}_2\text{Gd}(\text{OH}_2)_6]$  per unit cell and leaving one Cl ion per mole isolated. Each complex has an axis of twofold symmetry and since the predominant part of the crystalline field is due to the anions of the complex, it may be assumed for practical purpose that one axis of the crystalline field coincides with the twofold  $b$  axis.

The ground state of dysprosium ethylsulphate is formed by a doublet having highly anisotropic  $g$ -values ( $g_{\parallel} \simeq 10.8$ ,  $g_{\perp} \simeq 0$ )<sup>10)</sup>. The next doublet is found to lie at  $\Delta E/k=22.5\text{K}$ <sup>11)</sup>, which can therefore be neglected at temperatures near 1 K.

Susceptibility<sup>12,10)</sup> and relaxation measurements performed in the temperature region between 20 and 1 K have been successfully interpreted in terms of dipolar interactions. The experimental value of  $\theta$  measured in the direction of the highest g-value ( $\parallel$  c axis) was found to be  $\theta_{\parallel} = +0.12$  K, which agrees closely with the value  $\theta_{\parallel} = +0.126$  K, calculated from the formulae given by Daniels<sup>13)</sup>. Demagnetization- and susceptibility measurements by Cooke et al.<sup>14)</sup> also show that dysprosium ethylsulphate becomes ferromagnetic near 0.13 K ( $T_c = +0.127 \pm 0.005$ ). The adiabatic magnetization curves at temperatures above and below the transition point were interpreted by a model using Ising interactions between ions lying in chains parallel to the c axis<sup>14)</sup>.

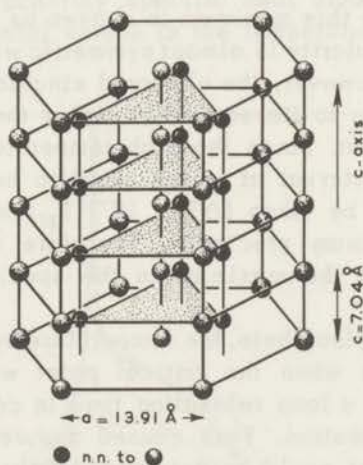


Fig. 1. The relative positions are shown of nearest-neighbour (n.n.) and next-nearest-neighbour (n.n.n.) chains of Dy ions with respect to a central chain of Dy ions.

The crystal structure has been determined by Ketelaar<sup>15)</sup>. The elementary cell having the space group symmetry  $C_{6h}^2$  contains two equivalent dysprosium ions of trigonal-dipyramidal symmetry ( $C_{3h}$ ). Fig. 1 shows the relative positions of nearest- and next-nearest neighbour chains to a central chain of dysprosium ions. The length of the  $a$  axis of the elementary cell is  $13.906 \text{ \AA}$ , while that of the  $c$  axis is only  $7.04 \text{ \AA}$ . Each Dy ion has 2 nearest neighbours at  $7.04 \text{ \AA}$  along the  $c$  axis, 6 neighbours at  $8.75 \text{ \AA}$ , arranged in two triangles lying above and below this central ion respectively, and 6 neighbours at  $13.91 \text{ \AA}$  arranged hexagonally around this ion in a plane perpendicular to the  $c$  axis.

## 2 Experimental method and determination of the critical temperature

The experimental arrangement has already been described in ch.II. As to the consistence of the samples, measurements on the gadolinium sulphate were performed on powdered crystals, while those on gadolinium trichloride hexahydrate and dysprosium ethylsulphate were performed on single crystals. In view of the arguments given in ch.I, section 3.6.1, the difference in consistence is unimportant as far as the specific heat is concerned that is measured with temperature differences larger than  $10^{-3}T_N$ .

The transition temperatures were derived from the measurements of the specific heat. In a first approximation they are identified with the temperature at which the specific heat attains its maximum. For the hydrated sulphate this maximum is chosen as  $T_N$  (see ch.I, section 3.6.3), since the singularity is almost symmetric with respect to  $|T - T_N|$ .

In the chloride, however, the observed singularity is asymmetrical, so that we expect  $T_N$  to lie somewhat higher than the temperature of maximum specific heat. Since the high temperature side of the curve drops steeply, the interval at which specific heat points of reasonable accuracy could be taken ( $\Delta T \simeq 10^{-3}T_N$ ) was still too small to determine this maximum precisely. Therefore we may identify the temperature at which the maximum in the specific heat is observed with  $T_N$ .

In dysprosium ethylsulphate, the temperature versus time recordings were rather irregular when the critical point was approached. This effect may be due to a long relaxation time in conjunction with ferromagnetic domain formation. This caused a spread in the results so that the critical point could be determined only to about 1 part in a hundred ( $T_c = 0.115$  K).

The lattice does not make a noticeable contribution to the specific heat in either salt in the temperature region studied. Throughout this chapter the specific heat originating from the magnetic dipole coupling between the  $Gd^{3+}$ -ions and the coupling with the crystalline field will be called magnetic specific heat and will be denoted as  $c_m$ , referring to one gram ion Gd or Dy.

## 3 Specific heat

### 3.1 Gadolinium sulphate octohydrate, $Gd_2(SO_4)_3 \cdot 8H_2O$

The heat capacity of gadolinium sulphate octohydrate is plotted in fig. 2 on a logarithmic scale. From the data a critical temperature of  $T_N = 0.182 \pm 0.001$  K can be derived (see sections 2 and 3.4).

The entropy,  $S_\infty - S_c$ , involved in short range ordering amounts to

1.49 R/gram ion, which may be compared to a total measured entropy  $S_\infty = 2.08 R \approx R \ln(2s + 1)$ . Since  $S_\infty - S_c = 2.13 R \ln 2 \approx R \ln 4$ , one sees that at the critical point practically only the lowest Stark doublet remains populated. Correspondingly, the energy yield between high  $T$  and the critical temperature  $T_N$  is found to be 6.66 J/gram ion, which amounts to about 90% of the total gain of 7.37 J/gram ion. From the energy levels, due to Stark splitting, one derives a crystalline field energy yield of 4.75 J/gram ion if  $s_z = \pm \frac{1}{2}$  is lowest or 5.72 J/gram ion if  $s_z = \pm \frac{7}{2}$  is lowest.

In fig. 2 also the Schottky heat capacity based on the energy level scheme mentioned in section 1 ( $s_z = \pm \frac{1}{2}$  lowest) is indicated for comparison with the experimental data. If the level scheme were reversed ( $s_z = \pm \frac{7}{2}$  lowest) the Schottky specific heat alone would considerably exceed the experimental values in the temperature region between 0.3

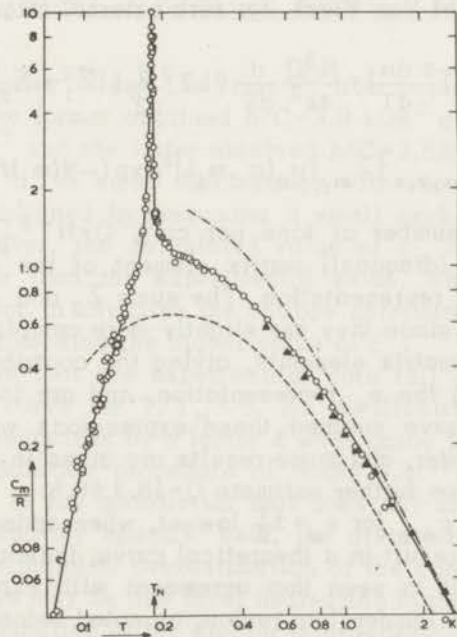


Fig. 2. Heat capacity  $c_m/R$  of  $Gd_2(SO_4)_3 \cdot 8H_2O$  as a function of temperature on a logarithmic scale. The singularity occurs at  $T_N = 0.182 \pm 0.001$  K. The dashed line represents the Schottky specific heat for  $s_z = \pm \frac{1}{2}$  lowest, and the dot-dashed line gives the sum of Schottky and dipolar heat capacities. The triangles are points taken from refs. 3 and 4.

and 2 K. Hence we agree with the conclusion of Bogle and Toutenhoofd<sup>6)</sup> that the ground state is  $s_z = \pm \frac{1}{2}$ . Bogle and Symmons<sup>5)</sup> have noted that the crystalline field energy levels  $E/k = -0.572$  K,  $-0.252$  K,  $+0.138$  K and  $+0.685$  K can reasonably well be represented by:

$$b_2^0 \left\{ s_z^2 - \frac{1}{3} s(s+1) \right\} + \frac{1}{3} b_2^2 (s_x^2 - s_y^2),$$

with  $b_2^0/k = 0.1$  K and  $\frac{1}{3} b_2^2/k = 0.02$  K. One sees that the crystalline field is predominantly axial, not cubic as was formerly supposed. Hence the four twofold degenerate levels may be denoted as  $s_z = \pm \frac{1}{2}$ ,  $\pm \frac{3}{2}$ ,  $\pm \frac{5}{2}$  and  $\pm \frac{7}{2}$  levels respectively, to a good approximation. We shall apply this approximation for calculating the dipolar interaction, modified by the above crystalline fields. Such calculations are based on the formulae of Van Vleck<sup>16)</sup> and have been carried out earlier for cubic fields by Hebb and Purcell<sup>2)</sup>.

In the notation of Van Vleck, for zero external magnetic field,

$$c_{\text{dipolar}} = \frac{d}{dT} (kT^2 \frac{d\alpha}{dT}) = \frac{N^3 Q}{4k^2} \frac{d}{dT} \left\{ kT^2 \frac{d}{dT} \left( (\Sigma_1 + \Sigma_2 + \Sigma_3)/T^2 \right) \right\}$$

$$\Sigma_1 = \sum_{q=x,y,z} \left\{ \sum_{m_i} |\mu_q(m_i, m_i)|^2 \exp(-W(m_i)/kT) \right\}^2,$$

where  $N$  is the number of ions per  $\text{cm}^3$ ,  $Q = N^{-2} \sum_i 2r_{ij}^{-6}$ , and where  $\mu_q(m_i, m_i)$  is the (diagonal) matrix element of the magnetic moment operator in the  $s_z$  representation. The sums  $\Sigma_2$  and  $\Sigma_3$  have not been explicitly written since they are slightly more complicated. They contain nondiagonal matrix elements, giving the contributions of  $\mu_x$  and  $\mu_y$  when adopting the  $s_z$  representation, and are incorporated in the calculation. We have summed these expressions with the aid of a 360/50 IBM-computer, and some results are given in table I. From the crystal structure we further estimate  $Q = 18.3 \pm 0.5$ .

The values of  $c_{\text{dip}}$  for  $s_z = \pm \frac{1}{2}$  lowest, when added to the Schottky specific heat  $c_s$ , result in a theoretical curve, indicated in fig. 2 by a dashdotted line. It is seen that agreement with experiment is satisfactory in the high temperature region, as noted before by Bogle e.a.<sup>6)</sup> and by Van Dijk e.a.<sup>3,4)</sup>. Neither our caloric data, nor those of Van Dijk<sup>3)</sup>, extend to sufficiently high  $T$  in order to make an accurate derivation of the asymptotic value of  $c_m T^2/R$  possible. This may be connected to deviations from  $c_m \propto T^{-2}$  which are apparent in the Schottky specific heat between for instance 1 and 3 K (cf.  $c_s$  in table I). For the entropy determination we have therefore adopted the calculated value  $c_m T^2/R = 0.33 \text{ K}^2$ . Higher values of  $c_m T^2/R$  were reported e.g.

TABLE I

The results of calculations of the Schottky term and dipolar term in the specific heat are presented. The summed contributions are plotted in figs. 2 and 3 respectively as a dash-dotted curve						
T [K]	$\text{Gd}_2(\text{SO}_4)_3 \cdot 8\text{H}_2\text{O}$			$\text{GdCl}_3 \cdot 6\text{H}_2\text{O}$		
	$\frac{c_s}{R}$	$\frac{c_{\text{dip}}}{R}$	$\frac{c_s + c_{\text{dip}}}{R}$	$\frac{c_s}{R}$	$\frac{c_{\text{dip}}}{R}$	$\frac{c_s + c_{\text{dip}}}{R}$
0.4	0.522	0.632	1.154	0.505	0.781	1.286
0.6	0.349	0.326	0.675	0.317	0.286	0.603
0.8	0.238	0.186	0.424	0.208	0.130	0.347
1.0	0.167	0.117	0.284	0.144	0.0808	0.225
1.4	0.095	0.0573	0.152	0.0800	0.0369	0.117
2.0	0.049	0.0271	0.076	0.0413	0.0167	0.0580
3.0	0.0225	0.0118	0.0343	0.0190	0.00713	0.0261
4.0	0.0131	0.0066	0.0197	0.0109	0.00393	0.0148
10.0	0.00219	0.00109	0.00328	0.00178	0.00061	0.02329
T	$0.2196/T^2$	$0.109/T^2$	$0.328/T^2$	$0.179/T^2$	$0.0608/T^2$	$0.240/T^2$

by Broer and Gorter<sup>17)</sup> and De Vries<sup>18)</sup> from paramagnetic relaxation experiments. The former obtained  $b/C=3.9 \text{ kOe}^2$  at 77 K, which gives  $c_m T^2/R=0.36 \text{ K}^2$  and the latter obtained  $b/C=3.8 \text{ kOe}^2$  at 20 K, giving  $c_m T^2/R=0.35 \text{ K}^2$ . The small discrepancy with our calculated value of  $c_m$  might be explained by assuming a small exchange interaction. In this case, however, the calculated value of  $c_m$  above 2K would be about 8% higher than the experimental value, which is outside the experimental error. In any case the entropy determination is practically not affected by choosing the higher value of  $c_m$ .

One may note that the experimental data fall considerably below the theoretical curve for  $T/T_N < 5$ . As an illustration, the value of  $(c_m - c_s)T^2/R$  decreases by a factor 4 when going from 2.5K to 0.25K. Since the interpolation procedure of Bogle e.a.<sup>5)</sup> for estimating the Stark splittings in the gadolinium salt does not allow much variation (<1%) in the Schottky specific heat, the discrepancy has to a large extent to be attributed to overestimation of the contribution of dipolar interactions. This may be due to: a) neglecting higher terms ( $T^{-3}, T^{-4}$ ) in the partition function of the dipolar interactions, and b) to the circumstance that averaging over the angular variable in  $(1 - 3\cos^2\theta_{ij})^2$  in the dipolar sum, while allowed in the  $T^{-2}$  approximation for isotropic ions ( $g_{\parallel}=g_{\perp}$ ), is inadmissible when crystalline field levels are partially depopulated. In this case the statistical weighting factors for the highest levels decrease. For these levels the effective g-value has the property  $g_{\perp}^{\text{eff}}=0$  and then the averaging procedure for  $(1 - 3\cos^2\theta_{ij})^2$  is no longer correct. Taking the angular variables for neighbouring ions

into account, however, would require an elaborate computational procedure, i.e. essentially a combination of the techniques of Van Vleck<sup>16)</sup> and of Daniels<sup>13)</sup>.

We suggest that the series expansion of  $c_m$  in powers of  $1/T$  has at least one significant term with the negative sign which is to be contrasted to the series expansions of  $c_m$  in case of exchange interactions<sup>19)</sup>. As a consequence the transition point is comparatively low and deviations from  $c \propto 1/T^2$  behaviour occur at a relatively high  $T/T_N$ . Van Vleck calculated negative coefficients of  $T^{-3}$  and  $T^{-4}$  terms in  $c_{dip}$  for cubic lattices, but their magnitude remained uncertain.

We conclude that exchange interactions are negligible and that Stark splittings and dipolar interactions explain the data at high  $T$ , but that the high temperature approximation  $c_{dip}/R = \frac{1}{6} Q \tau^2 / T^2$ , where

$$\tau = N g^2 \beta^2 s(s+1) / k = 0.191 \text{ K},$$

is only valid for  $\tau/T < \frac{1}{5}$ .

Considerable deviation of the heat capacity from theoretical estimates at relatively high  $T$  was also reported by several authors<sup>32)</sup> in cerium magnesium nitrate. In this salt one also has  $g_{\perp} \gg g_{\parallel}$  and predominance of dipolar coupling.

### 3.2 Gadolinium trichloride hexahydrate, $GdCl_3 \cdot 6H_2O$

In fig. 3 the heat capacity of gadolinium chloride hexahydrate is given as a function of temperature. The singularity at  $T_N = 0.185 \pm 0.001 \text{ K}$  is due to a magnetic ordering transition, while the broad anomaly underneath is almost certainly due the Stark splitting of the  $^8S_{7/2}$  ground state. Experimental data on many ionic Gd compounds have shown that the crystalline field splittings have the order of magnitude of  $1 \text{ cm}^{-1}$  and this agrees roughly with the position of the temperature scale of the Schottky anomaly under the sharp singularity of the magnetic interactions.

The change in entropy when cooling the crystal to  $T_N$  amounts to  $1.480R$  which is slightly more than  $R \ln 4$ . At  $T = 0.10 \text{ K}$  the entropy change is  $2.009R$  which is 3% less than the expected total entropy  $R \ln(2s+1)$  at  $T = 0 \text{ K}$ . The unusually high entropy above  $T_N$  corroborates the assumption that the crystalline field splittings contribute to the heat capacity. The energy yield above  $T_N$  is  $E_{\infty} - E_c = 6.25 \text{ J/mole}$ , while below  $T_N$  the energy change amounts to  $0.534 \text{ J/mole}$ , hence  $E_{tot} = 6.78 \text{ J/mole}$  and  $-E_c/E_{tot} = 0.92$ .

The heat capacity for  $T > 1 \text{ K}$  is over a rather limited temperature region represented approximately by  $c_m T^2 / R = 0.240 \text{ K}$ . Hellwege e.a.<sup>20)</sup>

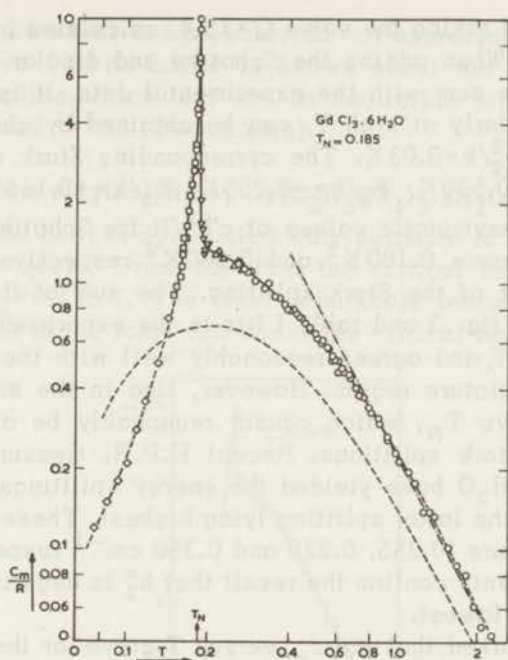


Fig. 3. Heat capacity  $c_m/R$  of  $GdCl_3 \cdot 6H_2O$  as a function of temperature  $T$  on a logarithmic scale. A singularity is found at  $T_N = 0.185 \pm 0.001$  K. The dashed line indicates the estimated Schottky specific heat. The dash-dotted line corresponds to the sum of Schottky specific heat and dipolar specific heat.

have measured the heat capacity in the region  $1.1 < T < 260$  K. Their values for  $c_m$  at  $T > 1.5$  K are slightly higher than ours, but our data agree with theirs within the accuracy of the measurements between 1.1 and 1.5 K. According to the high temperature expansion:

$$c/R \sim Tr H^2/k^2 T^2 = \frac{1}{45} s(s+1)(2s+3)(2s-1) \{ (b_2^0)^2 + \frac{1}{3} (b_2^2)^2 \} / k^2 T^2$$

Levy<sup>21)</sup> derived  $b_2^0/k = -0.085$  K and  $\frac{1}{3} b_2^2/k = 0.03$  K from our preliminary susceptibility data<sup>22)</sup> and Hellwege's heat capacity data. From the eigenvalue equation in the parameters  $b_2^0$  and  $b_2^2$  one finds the crystalline field energy levels  $W_1/k = -0.619$  K,  $W_2/k = -0.169$  K,  $W_3/k = +0.156$  K and  $W_4/k = +0.632$  K. A crystalline field energy of  $0.619R = 5.15$  J/mole would therefore contribute 76% to the total energy gain  $E_{tot} = 6.78$  J/mole.

The dipolar specific heat may be calculated following the methods

of section 3.1 and taking the value  $Q=15.4$ , calculated by Levy<sup>21)</sup> for the dipolar sum. When adding the Schottky and dipolar specific heat and comparing the sum with the experimental data, it is found that a better fit, particularly at high  $T$ , can be obtained by choosing  $b_2^0/k = -0.07\text{K}$  and  $\frac{1}{3}b_2^2/k = 0.03\text{K}$ . The corresponding Stark energy levels are then  $W_1/k = -0.530\text{K}$ ,  $W_2/k = -0.205\text{K}$ ,  $W_3/k = +0.115\text{K}$  and  $W_4/k = +0.620\text{K}$ . The asymptotic values of  $cT^2/R$  for Schottky and dipolar specific heat become  $0.180\text{K}^2$  and  $0.060\text{K}^2$  respectively, the latter being independent of the Stark splitting. The sum of the two contributions shown in fig. 3 and table I fits to the experimental result for  $c_m T^2/R$  at high  $T$ , and agrees reasonably well with the data over an appreciable temperature region. However, like in the sulphate, deviations occur above  $T_N$ , which cannot reasonably be attributed to a poor choice of Stark splittings. Recent E.P.R. measurements<sup>23)</sup> on Gd-doped  $\text{YCl}_3 \cdot 6\text{H}_2\text{O}$  have yielded the energy splittings  $0.257$ ,  $0.236$  and  $0.372\text{ cm}^{-1}$ , the latter splitting lying highest. These results agree fairly well with ours ( $0.255$ ,  $0.220$  and  $0.350\text{ cm}^{-1}$  respectively). The E.P.R. measurements confirm the result that  $b_2^0$  is negative so that the  $s_z = \pm \frac{7}{2}$  level lies lowest.

It may be remarked that the  $c_m$  versus  $T$  curve for the sulphate is strikingly similar to that of the chloride. We emphasize a peculiar aspect of these curves namely a relatively flat region above  $T_N$ , preceded by a steep descent very close to the critical point. This may be characteristic of dipolar interactions, which apparently lead to a comparatively low critical point, reflected in a high value of  $(E_{\text{tot}} - E_{\text{Stark}})/RT_N = E_{\text{dip}}/RT_N$  compared to what is found for exchange interactions.

As in the sulphate octohydrate there is no indication that exchange interactions play a significant role in the chloride. It may be mentioned that in the anhydrous chloride two  $\text{Gd}^{3+}$  ions are separated by only one chlorine ion at a distance of  $2.86\text{ \AA}$  and  $3.05\text{ \AA}$  for the two Gd ions respectively. In  $\text{GdCl}_3 \cdot 6\text{H}_2\text{O}$  the linkage between, for instance, two Gd ions in the  $ac$  plane will be formed by one water molecule at  $2.42\text{ \AA}$  and one chlorine ion (at  $2.77\text{ \AA}$ ). These belong to two different  $[\text{GdCl}_2(\text{OH}_2)_6]$  complexes, the chlorine and water molecule being at a distance of  $3\text{ \AA}$  with respect to each other. In  $\text{GdCl}_3$  the value of the exchange constant for nearest neighbour exchange<sup>24)</sup>  $-2J\mathbf{s}_1 \cdot \mathbf{s}_2$  amounts to  $J/k = -0.08\text{ K}$ , while in our case the exchange constant is at least 10 times smaller.

At  $T \approx 0.05\text{ K}$  a few points in the heat capacity data (not shown in fig.3) having an upward trend with decreasing  $T$ , may indicate the presence of hyperfine contributions to the heat capacity. E.P.R. data<sup>25)</sup> show that magnetic h.f.s. contributions in most salts e.g.  $\text{Gd}^{3+}$  in

$\text{LaCl}_3 \cdot 7\text{H}_2\text{O}$  are small and probably do not appreciably affect the heat capacity above 0.05 K. Little is known about the electric hyperfine structure coupling which may not be negligible for the odd-odd isotopes  $^{155}\text{Gd}$  and  $^{157}\text{Gd}$  ( $Q \approx 1.4$  barn).

### 3.3 Dysprosium ethylsulphate, $\text{Dy}(\text{C}_2\text{H}_5\text{SO}_4)_3 \cdot 9\text{H}_2\text{O}$

The specific heat of dysprosium ethylsulphate is shown in fig. 4 on a logarithmic scale. From the data the critical temperature may be located at  $T_c = 0.115$  K. The most remarkable feature of the specific heat curve lies in the large tail above the critical temperature.

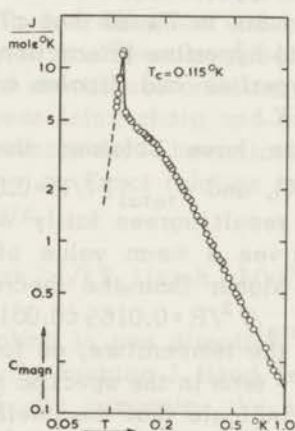


Fig. 4. The heat capacity of dysprosium ethylsulphate as a function of  $T$  plotted on a logarithmic scale.  $T_c = 0.115$  K.

Before analysing the energy and entropy involved in the phase transition, the specific heat originating from hyperfine interactions of the  $^{161}\text{Dy}$  and  $^{163}\text{Dy}$  isotopes must be subtracted from the data. From paramagnetic resonance results obtained by Park<sup>26)</sup>, a hyperfine contribution to the specific heat,  $c_{\text{hfs}} T^2/R = 0.00095$  was calculated by Cooke et al.<sup>12,10)</sup> Applying this correction to the data we obtain  $\Delta E/RT_c = 0.92$  for the energy released above  $T_c$ , and  $\Delta S/R = 0.47$  for the entropy change above  $T_c$ . These values are still higher than, for instance, those calculated for a two-dimensional (quadratic) Ising lattice with isotropic  $J$  values:  $\Delta E/RT_c = 0.623$ , and  $\Delta S/R = 0.387$ .

Because of poor heat contact between the single crystal and the specimenholder, it was difficult to obtain precise results below about 0.09 K. Therefore, these results have not been plotted in fig. 4. For this reason the evaluation of the entropy and energy change below  $T_c$

remains somewhat imprecise. Using the dashed line in fig. 4 as an extrapolation, we obtain  $(E_c - E_o)/RT_c = 0.18$  and  $(S_c - S_o)/R = 0.22 \pm 0.03$  for the energy and entropy change below  $T_c$ , respectively. The total entropy involved in the phase transition equals  $0.69R$  per gramion which agrees with the expected value of  $R \ln 2 = 0.693R$ .

The high temperature magnetic specific heat ( $0.3K < T < 1K$ ) is accurately described by the relation  $c_{\text{magn}} T^2/R = 0.0155 \pm 0.0004K$ . An upper bound to the error may be obtained from the consideration that the total entropy involved in the phase transition is given by  $R \ln 2$ . The error involved in the determination of the entropy change below  $T_c$  is estimated as  $0.03R$ . An upper bound to the error in  $cT^2/R$  arising from this inaccuracy amounts to 7% so that  $cT^2/R = 0.0155 \pm 0.0011K$ . By using the  $g$ -values and hyperfine interaction constants, as referred to in section 1, the hyperfine and dipolar contributions amount to  $(c_{\text{hfs}} + c_{\text{dip}})T^2/R = 0.0131K$ .

Other experimentalists have obtained the values  $c_{\text{total}} T^2/R = 0.0134K^{11)}$  (for  $T > 1K$ ), and  $c_{\text{total}} T^2/R = 0.0136 + 20/T^{10)}$  for  $1K < T < 1.6K$ . The former result agrees fairly well with the theoretical one, while the latter gives a mean value of  $c_{\text{total}} T^2/R = 0.0150K$ , which lies appreciably higher than the theoretical one but is still lower than our value  $c_{\text{total}} T^2/R = 0.0165 \pm 0.0011K$ . The slight upward curvature on decreasing the temperature, as found by Cooke et al.<sup>10)</sup> and expressed by the  $T^{-3}$  term in the specific heat, disagrees strongly with our results, which indicate that the coefficient of the  $T^{-3}$  term is much smaller and of negative sign ( $-0.0001/T^3$ ). For this reason the experimental value of the coefficient of the  $T^{-2}$  term must be chosen much higher viz.  $0.0148$ .

From the experimental results we may conclude that the interactions in dysprosium ethylsulphate are predominantly of the dipolar kind. The small discrepancy between the observed and calculated values of  $cT^2/R$  may be due either to an erroneously small value of  $g$  or to the presence of a small exchange interaction.

The fractions of the total energy and entropy removed above  $T_c$  are found to be as high as 84% and 69% respectively. For the quadratic Ising net these values are 70.6% and 55.7%. In the ordering of a linear chain these values are 100%, as the transition point lies at zero temperature. The experimental result may therefore be interpreted by a model in which the predominant interaction occurs between ions in a one-dimensional arrangement. The ordering between the chains will occur at a fairly low temperature determined by the interaction between the chains as compared to the interaction in a chain.

A glance at the crystal structure (fig. 1) shows that the dipolar

interactions strongly favour alignment of the spins parallel to the  $c$  axis since  $c/a=0.506$ . At zero temperature, the relative strength of the dipolar fields originating from the ions in a chain parallel to the  $c$  axis ( $H_{\text{dip}}$ ), compared to that originating from the three nearest-neighbour chains ( $H'_{\text{dip}}$ ), can be calculated easily. By considering 7 ions upward and downward along the  $c$  axis in each chain, we obtain  $H'_{\text{dip}}/H_{\text{dip}}=1.06/6.84=0.155$ . It can be estimated that the dipolar field originating from the n.n.n. chains is smaller than  $H'_{\text{dip}}$  and in a first approximation these interactions may be neglected.

Since  $g_{\parallel} \gg g_{\perp}$ , dysprosium ethylsulphate behaves like an Ising  $s=\frac{1}{2}$  system (albeit with long range interactions) characterized by strong interactions in one direction and by weaker interactions in a plane perpendicular to it. Phenomenologically the total interaction leads to an amount of short range ordering which is found for a system lying between a linear Ising chain and an isotropic quadratic Ising system (with n.n. interactions). Theoretically, for the quadratic lattice, Onsager<sup>27)</sup> has given an exact relation between the critical temperature  $kT_c$ ,  $J$  and  $J'$  viz.

$$(\sinh 2J/kT_c)(\sinh 2J'/kT_c) = 1, \quad (1)$$

where  $J$  is the coupling in one direction, and  $J'$  that in a direction perpendicular to it. By keeping  $J$  fixed,  $kT_c$  may be evaluated as a function of  $J'/J \leq 1$ . By comparing the specific heat curve of dysprosium ethylsulphate with the specific heat curve for  $J'/J=0.01$ , plotted in fig. 7 of Onsager's article as a function of  $2/(J/kT+J'/kT)$ , the transition temperature of the salt may be located at

$$2 kT_c/(J+J') = 1.75. \quad (2)$$

From eqs. (1) and (2) we obtain  $J'/J=0.14$ . This result agrees well with the value  $H'_{\text{dip}}/H_{\text{dip}}=0.16$  derived from the relative strength of the inter- and intra-chain coupling. The small value of  $J'/J$  indicates that dysprosium ethylsulphate may in first approximation be described by a linear chain model.

As a conclusion we may state that the magnetic interactions are predominantly of the dipolar kind, and the crystal structure strongly favours coupling in chains. The coupling between the chains may be estimated as about one seventh of that deduced for the coupling within the chains. The resulting effective coupling is found to resemble closely a linear chain interaction.

## 3.4 Singularities of the two gadolinium salts

The results of the specific heat measurements of the two gadolinium salts are presented in tables II and III. In fig. 5 the logarithm of the

TABLE II

Specific heat,  $c_m$ , of  $Gd_2(SO_4)_3 \cdot 8H_2O$  as a function of  $(T-T_N)/T_N$  near the transition temperature;  $T_N=0.1822$  K is used as a reference point (see section 2). The two runs are made on the same day

$(T-T_N)/T_N$ x 100	$c_m/R$						
run 1		1.237	2.905	-13.6	0.946	0.610	7.28
-35.85	0.305	1.78	2.26	-10.78	1.164	0.871	5.56
-31.03	0.385	2.33	1.60	-8.41	1.381	1.24	4.96
-26.10	0.494	3.12	1.618	-6.43	1.68	1.66	2.50
-21.77	0.658	4.38	1.513	-5.08	1.89	2.16	1.57
-17.88	0.828	6.49	1.358	-3.79	2.40	2.77	1.56
-14.33	0.917	9.44	1.302	-2.70	2.99	3.29	1.61
-11.39	1.01	13.86	1.249	-2.05	3.24	3.92	1.49
-8.50	1.36	22.0	1.043	-1.60	3.92	4.70	1.50
-5.74	1.84	29.5	1.104	-1.26	4.49	6.06	1.337
-3.27	2.63	38.7	1.077	-0.959	5.08	8.32	1.323
-1.52	4.06	50.1	1.022	-0.689	6.20	11.63	1.233
-0.433	6.77	run 2		-0.447	7.28	15.87	1.185
+0.084	8.00	-27.45	0.463	-0.233	8.03	20.84	1.134
0.340	7.82	-24.23	0.523	-0.012	10.13	25.9	1.112
0.581	6.97	-20.98	0.647	+0.17	8.74	32.2	1.098
0.885	4.77	-17.02	0.801	0.36	8.78	39.9	1.056

TABLE III

The specific heat  $c_m/R$  of  $GdCl_3 \cdot 6H_2O$  as a function of  $T$  near the transition point  $T_N=0.185$  K is tabulated. The results of several days and runs are presented.

T K	$c_m/R$						
4-4-'66		0.19547	1.43	6-4-'66		0.17635	2.64
0.17957	3.20	0.19657	1.43	run 1		0.17793	2.85
0.18204	4.53	1-4-'66		0.16106	1.29	run 2	
0.18332	4.33	0.1816	3.45	0.16194	1.36	0.14961	0.90
0.18357	4.52	0.1821	4.03	0.16278	1.48	0.15153	0.89
0.18393	5.71	0.1825	4.6	0.16344	1.59	0.15326	0.97
0.18418	6.18	0.1831	6.2	0.16423	1.47	0.15668	1.07
0.18449	6.84	0.1837	4.8	0.16515	1.70	0.15817	1.13
0.18482	7.16	0.1844	5.9	0.16613	1.64	0.15993	1.157
0.18511	10.1	0.1849	8.9	0.16719	1.88	0.16184	1.363
0.18540	9.13	0.1857	3.9	0.16822	1.94	0.16355	1.342
0.18605	2.64	0.1872	2.23	0.16988	1.95	0.16904	2.109
0.18737	2.04	0.1891	1.65	0.17062	2.14	0.17366	2.39
0.18899	1.70	0.1911	1.48	0.17151	2.36	0.17768	3.17
0.19020	1.60	0.1930	1.54	0.17240	1.97	0.18136	4.89
0.19117	1.47	0.1948	1.53	0.17338	1.987		
0.19236	1.30	0.1969	1.34	0.17438	2.40		
0.19396	1.34	0.1993	1.36	0.17536	2.58		

specific heat is displayed versus the relative temperature  $T/T_N$ . The squares denote the measurements on the sulphate and the triangles those on the chloride. The dashed curves denote the results for the  $s = \frac{1}{2}$  Ising model of s.c. structure obtained by Baker<sup>28</sup>). The width of the peak of the sulphate is fairly large compared to the temperature

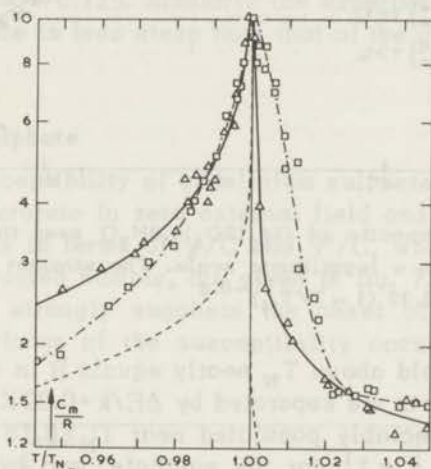


Fig. 5. The logarithm of the magnetic specific heat  $c_m/R$  is shown versus  $T/T_N$  for gadolinium sulphate ( $T_N = 0.1822$  K), and gadolinium trichloride hexahydrate ( $T_N = 0.1851$  K). The squares pertain to the sulphate, the triangles to the chloride. The dashed curves represent the Ising  $s = \frac{1}{2}$  s.c. result calculated by Baker<sup>28</sup>).

resolution so that a plot of the specific heat versus  $|1 - T/T_N|$  is feasible. The result is shown in fig. 6, which has logarithmic scales. The filled symbols denote the measurements below  $T_N$ , the open ones those above  $T_N$ . For  $10^{-2} < 1 - T/T_N < 10^{-1}$  the data may be described by the relation

$$c_m/R = B(1 - T/T_N)^{-\alpha'}$$

with  $B = 0.32$  and  $\alpha' = 0.60$ . Above  $T_N$  the curve levels off for  $T > 1.02 T_N$  so that an analysis cannot be made with confidence.

As to the overall behaviour of the singularities we may notice from fig. 5 the following points. a) The maxima of the peaks are almost equally high and rank among the highest values observed in magnetic systems. This result is established most unambiguously in the sulphate which has a relatively broad peak. b) For  $0.98 < T/T_N < 1$  the curves show a striking resemblance, whereas for  $1 < T/T_N < 1.02$  the curve of the chloride lies appreciably lower than that of the sulphate.

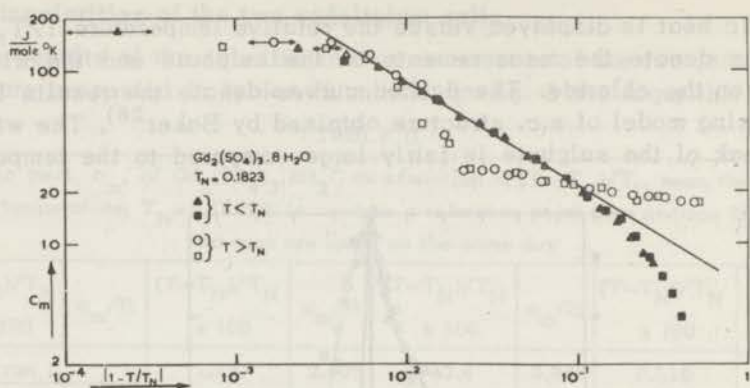


Fig. 6. Heat capacity of  $\text{Gd}_2(\text{SO}_4)_3 \cdot 8\text{H}_2\text{O}$  near the transition point, plotted on a logarithmic scale. The straight line corresponds to  $c_m/R = 0.32 (1 - T/T_N)^{-0.6}$ .

As the entropy yield above  $T_N$  nearly equals  $R \ln 4$  for both salts, and the lowest doublets are separated by  $\Delta E/k = 0.32\text{K}$ , only the lowest doublet will be appreciably populated near  $T_N = 0.18\text{K}$ . This doublet is characterized by  $s_z = \pm \frac{1}{2}$  for the sulphate, and by  $s_z = \pm \frac{7}{2}$  for the chloride. Near  $T_N$  the chloride may therefore be characterized by an effective spin  $\frac{1}{2}$  and strongly anisotropic  $g$ -values ( $g_{\parallel} \gg g_{\perp}$ ), which is reminiscent of the Ising  $s = \frac{1}{2}$  model. As we may notice from fig.5 the curve of the chloride is strongly asymmetric and shows a steep descent above  $T_N$ , which agrees qualitatively with the Ising model prediction.

Near  $T_N$ , for the lowest doublet, the sulphate has strongly anisotropic effective  $g$ -values ( $g_{\perp} \gg g_{\parallel}$ ) so that the dipolar interactions may be expressed by

$$H = - \sum_{\substack{ij \\ i < j}} 2 J_{ij}^{\text{dip}} (s_{ix} s_{jx} + s_{iy} s_{jy})$$

in a good approximation. In this formula  $J_{ij}^{\text{dip}}$  contains angular variables and the interaction has a long range. In the case  $J_{ij} = J$  for nearest neighbours only, the interaction may be called  $s = \frac{1}{2}$ -planar-Heisenberg interaction. The model using this interaction is also called XY model. Recently, for the XY model, Betts and Lee<sup>29)</sup> have derived the high-temperature specific-heat series of the f.c.c. lattice up to the ninth power in  $J/kT$ . Using a ratio-plot, the value of  $\alpha$  defined by the asymptotic relation

$$c/R \simeq A - B(1 - T_c/T)^{-\alpha}$$

was found to be  $-0.20 \pm 0.20$ . If  $\alpha$  is negative, the specific heat has a cusp near  $T_c$  and attains a finite maximum. Clearly near  $T_c$  the theoretical curve for the XY model is less steep than that for the Ising model, which has  $\alpha = +0.125$ . Similarly the experimental specific heat curve of the sulphate is less steep than that of the chloride.

## 4 Susceptibility

### 4.1 Gadolinium sulphate

The powder susceptibility of gadolinium sulphate was measured as a function of temperature in zero external field and at a frequency of 220 Hz. The results in terms of  $\chi'/C$  and  $\chi''/C$ , where  $C$  is the Curie constant for a powdered sample, are given in fig. 7. We conclude that the susceptibility strongly suggests the onset of antiferromagnetic ordering. The maximum of the susceptibility occurs at  $T = 0.1830$  K,

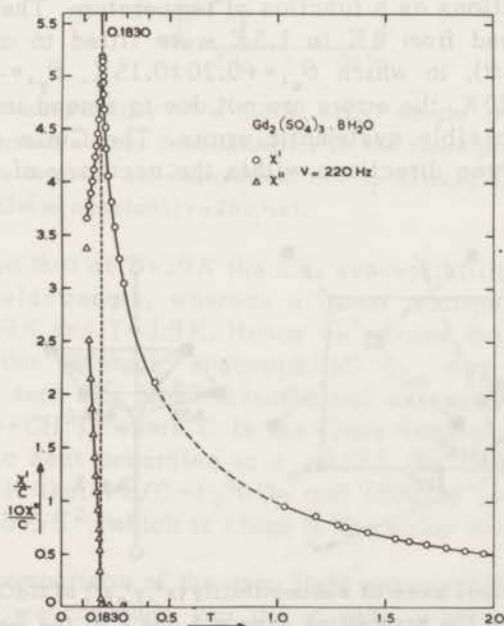


Fig. 7. A.c. susceptibility,  $\chi'$ , of powdered  $\text{Gd}_2(\text{SO}_4)_3 \cdot 8\text{H}_2\text{O}$ . The a.c. losses  $\chi''$  are indicated on a tenfold enlarged scale. Both  $\chi'$  and  $\chi''$  are divided by the Curie constant.

which is 0.4% higher than  $T_N$ . A further study of magnetic phenomena was not attempted in view of the scant knowledge about the crystal structure.

#### 4.2 Gadolinium trichloride

In this section we summarize the results of susceptibility measurements on the chloride, which were performed by Lubbers et al.<sup>30)</sup> in the temperature region between 0.1 and 4K a few years ago.

The sample was shaped in the form of a sphere. The original single crystals showed two large faces, the edges of which will be designed as  $a$  and  $c$  axes, the  $a$  axis being larger than the  $c$  axis. Presumably this identification of crystal axes is in accordance with Marezio e.a.<sup>9)</sup>, but differs from the notation of Dieke and Leopold<sup>31)</sup>. It was shown that the principal axes of the magnetic susceptibility in the ordered state, called  $x'$ ,  $y'$ ,  $z'$ , are as given in fig. 8. The  $y'$  axis coincides with the  $b$  axis, which is perpendicular to the  $ac$  plane; the accuracy of the determination of the direction  $x'$  or  $z'$  is about  $5^\circ$ .

The zero-field susceptibility ( $\nu=260$  Hz),  $\chi'$ , was measured in the  $x'$ ,  $y'$ , and  $z'$  directions as a function of temperature. The susceptibility data at 20K and from 4K to 1.5K were fitted to a Curie-Weiss relation  $\chi' = C/(T - \theta)$ , in which  $\theta_{x'} = +0.20 \pm 0.15$  K,  $\theta_{y'} = -0.10 \pm 0.10$  K and  $\theta_{z'} = -0.50 \pm 0.20$  K, the errors are not due to spread in the data but to estimates of possible systematic errors. The Curie constant was the same for the three directions within the accuracy of the measurements (5%).

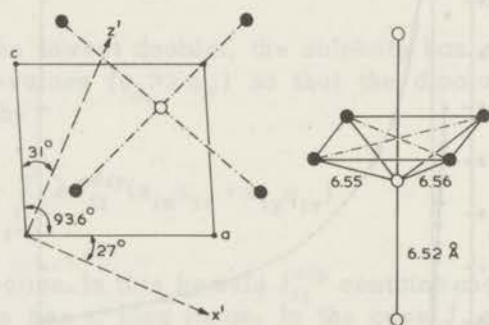


Fig. 8. Principal axes of susceptibility ( $x'$ ,  $y'$ ,  $z'$ ) of  $\text{GdCl}_3 \cdot 6\text{H}_2\text{O}$  with respect to the crystalline axes  $a$ ,  $b$  and  $c$  of the monoclinic unit cell. The  $y$  axis coincides with the  $b$  axis, which is perpendicular to the  $ac$  plane. The black and white circles denote the two crystallographically distinct Gd ions. The nearest Gd neighbours of one Gd ion are shown at right.

Lower temperatures were reached by adiabatic demagnetization of the sample from a fixed initial temperature (0.9 K) and from various field strengths. These measurements gave  $\chi_{x'}$ ,  $\chi_{y'}$ ,  $\chi_{z'}$  as functions of the temperature. The latter are shown in fig. 9. Particularly from the behaviour of  $\chi_{z'}$ , it may be seen that  $\text{GdCl}_3 \cdot 6\text{H}_2\text{O}$  becomes antiferromagnetic, while the temperature of the susceptibility maximum does not differ significantly from  $T_N$  as defined by the heat capacity singularity.

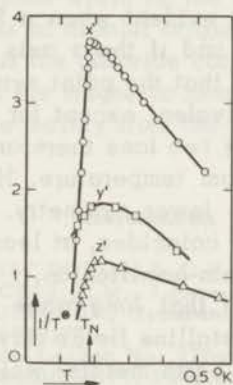


Fig. 9. Susceptibility of a  $\text{GdCl}_3 \cdot 6\text{H}_2\text{O}$  single crystal, ground into spherical shape. Susceptibility in the three principal directions as a function of temperature.  $1/T^*$  is defined as  $\chi'/C$ , where  $C$  is the Curie constant ( $\nu=260$  Hz).

It was found that at  $T=20$  K the a.c. susceptibility was independent of the d.c. field strength, whereas a linear relation of  $1/\chi$  vs.  $H^2$  was found at  $T=0.9$  K and  $T=3.8$  K. Hence we assume that at the two lower temperatures the adiabatic susceptibility  $\chi_{\text{ad}}$  was observed.  $\chi_{\text{ad}}$  is related to the zero d.c. field-isothermal susceptibility according to  $\chi_{\text{ad}}/\chi_{\text{is}} = b/(b+CH^2)$ , where  $C$  is the Curie constant and  $b$  is related to the specific heat according to  $c_m = b/T^2$ . We find from the data at 0.9 K and 3.8 K that  $\sqrt{b}/C = 1570$  Oe and 1600 Oe respectively, hence  $b/R = 0.242 \pm 0.005 \text{ K}^2$ , which is close to the value mentioned in section 3.2.

From the comparison of the zero field susceptibilities in  $x'$ ,  $y'$  and  $z'$  directions, we conclude that the  $x'$  axis is the preferred direction of the crystalline field, hence also of antiferromagnetic alignment. This would also follow from the positive value of  $\theta_{x'}$ , which presumably originates mainly from the crystalline electric field contribution,  $\theta_{x'} = -4b_2^0/k = +0.35$  K, but which may have in addition negative (anti-

ferromagnetic) contributions from dipolar interactions and possibly also exchange. Since the experimental data on  $\theta$  are not very accurate, the analysis of Levy<sup>21)</sup>, which starts from our measured  $\theta$ -values<sup>22)</sup>, may lead to quantitatively inaccurate conclusions, but we agree on the point that the crystalline field parameter  $b_2^0$  should refer to the  $x'$  axis and have a negative sign. The statement that the  $x'$  axis is the preferred axis at low temperature is supported by the data on transverse and longitudinal susceptibility, which show that a magnetic field in the  $y'$  or  $z'$  axis has a smaller effect on  $\chi$  than when the field is along the  $x'$  axis. This would be evident when a Stark level with predominantly  $s_z = \pm \frac{7}{2}$  were lowest and if the  $z$  axis would coincide with the  $x'$  axis. It may be remarked that the point symmetry of the Gd complex makes the two Gd ions equivalent except for a reflection with respect to the  $ac$  plane and that the two ions therefore have identical axes of the crystalline field at room temperature. However, deformations at low temperatures may give lower symmetry. It is plausible that the  $x', y', z'$  coordinate system coincides, at least approximately with the  $x, y, z$  coordinates of the spin-hamiltonian.

Furthermore, it is known that long-range magnetic interactions in conjunction with strong crystalline fields may lead to helical magnetic structures (e.g. in the rare earth metals) which differ from the simple axial spin alignment envisaged in the foregoing discussion.

## 5 Summary and conclusions

1. The gadolinium chloride hexahydrate and sulphate octohydrate become antiferromagnetic at respectively  $T_N = 0.185$  and  $T_N = 0.182 \pm 0.001$  K. Dysprosium ethylsulphate becomes ferromagnetic at  $T_c = 0.115 \pm 0.002$  K.

2. The heat capacity of the gadolinium salts is largely determined by Stark splittings. The behaviour of the dysprosium salt may be described largely by dipolar interactions between ions lying in a chain parallel to the  $c$  axis. The singularities of the three salts correspond to the onset of long-range order due to magnetic dipole coupling. A characteristic feature of these dipolar salts is the narrow specific heat peak, which on decreasing the temperature suddenly emerges from a region of weak temperature dependence.

3. Our data on Gd sulphate support the suggestion of Bogle *et al.*<sup>6)</sup> that the  $s_z = \pm \frac{1}{2}$  state is lowest, while the data on Gd chloride suggest that  $s_z = \pm \frac{7}{2}$  is lowest in the latter compound, which has been corroborated by the E.P.R. measurements of Meierling and Uhlmann<sup>23)</sup>.

4. The heat capacity of gadolinium sulphate above  $T_N$ , for instance in the region  $2T_N < T < 5T_N$ , is not correctly predicted by the sum of

calculated  $1/T^2$ -dependence of dipolar contributions and of a Schottky specific heat, even when the modification of the dipolar coupling by the Stark splitting is taken into account. The experimental results indicate that the series expansion of  $c_m$  in powers of  $1/T$  has some negative terms in case of dipolar interactions, in contrast to the case of exchange interactions.

5. At low  $T$  the heat capacity as a function of temperature rises very steeply in both salts. Since for  $T_N < T < 1.1T_N$  the heat capacity decreases sharply, the small width is the most characteristic aspect of the singularity, which is of dipolar origin.

6. The susceptibility of the chloride corresponds to the occurrence of a preferred direction of the magnetic moments along the  $x'$  axis, which is supposed to originate mainly from the crystalline field.

### References

1. GIAUQUE, W.F. and MACDOUGALL, D.P., *Phys. Rev.* 43(1933)768.
2. HEBB, W.H. and PURCELL, E.M., *J. chem. Phys.* 5(1937)338.
3. VAN DIJK, H. and AUER, W.U., *Commun. Kamerlingh Onnes Lab., Leiden No. 267b; Physica* 9(1942)785.
4. VAN DIJK, H., *Commun. Leiden No. 270a; Physica* 12(1946)371.
5. BOGLE, G.S. and SYMMONS, H.F., *Proc. phys. Soc. London A* 79(1962)775.
6. BOGLE, G.S. and TOUTENHOOFD, W., *Proc. phys. Soc. London A* 80(1962)230.
7. IVERANOVA, V.I., *Soviet Physics Cryst.* 9(1965)553.
8. ZACHARIASEN, W.J., *J. chem. Phys.* 3(1935)197.
9. MAREZIO, M., PLETTINGER, H.A. and ZACHARIASEN, W.H., *Acta Cryst.* 14(1961)234.
10. COOKE, A.H., EDMONDS, D.T., McKIM, F.R. and WOLF, W.P., *Proc. Roy. Soc. A* 252(1959)246.
11. MEYER, H. and SMITH, P.L., *J. Phys. Chem. Solids* 9(1959)285.
12. COOKE, A.H., McKIM, F.R., MEYER, H. and WOLF, W.P., *Phil. Mag.* 2(1957)928.
13. DANIELS, J.M., *Proc. phys. Soc. London A* 66(1953)673.
14. COOKE, A.H., EDMONDS, D.T., FINN, C.B. and WOLF, W.P., *J. Phys. Soc. Japan* 17 suppl. B1(1962)481.
15. KETELAAR, J.A.A., *Physica* 4(1937)619.
16. VAN VLECK, J.H., *J. chem. Phys.* 5(1937)320.
17. BROER, L.J.F. and GORTER, C.J., *Physica* 10(1943)621.
18. DE VRIES, A.J., Thesis, Leiden 1965, *Commun. Leiden, No. 356b; Physica* 36(1967)91.
19. DOMB, C., Ch. I in "Magnetism", Vol. IIA, eds. Rado, G.T. and Suhl, H., Ac. Press 1966 New York.
20. HELLWEGE, K.H., KÜCH, F., NIEMANN, K. and PFEFFER, W., *Z. Phys.* 162(1961)358.
21. LEVY, P.M., *J. Phys. Chem. Sol.* 25(1964)431.
22. DUFFY, W.T., LUBBERS, J., VAN KEMPEN, H., HASEDA, T. and MIEDEMA, A.R., *Proc. 8th Int. Conf. Low Temp. Phys., Butterworths, London* (1963).
23. MEIERLING, D. and ULLMANN, W., preprint; we thank the authors for communicating their results prior to publication.
24. WOLF, W.P., LEASK, M.J.M., MANGUM, B. and WYATT, A.F.G., *Proc. Int. Conf. Magnetism, J. phys. Soc. Jap.* 17 suppl. B1(1962)487.
25. AL'TSHULER, S.A. and KOZYREV, B.M., *Electron Paramagnetic Resonance* (translated from the Russian), Academic Press, New York (1964).
26. PARK, J.G., *Proc. Roy. Soc. A* 245(1958)118.

27. ONSAGER, L., Phys.Rev. 65(1944)117.
28. BAKER, G.A. Jr., Phys.Rev. 129(1961)99.
29. BETTS, D.D. and LEE, M.H., Phys.Rev.Letters 20(1968)1507.
30. LUBBERS, J., MIEDEMA, A.R. and HUIKAMP, W.J., Commun. Leiden No. 341b; Physica 31(1965)153.
31. DIEKE, G.H. and LEOPOLD, L., J.opt.Soc.Am. 47(1957)944.
32. WHEATLEY, J.C., Proc.int.Cal.Conf. Ann. Acad.sc. Fennicae, series A 210, Helsinki p. 15.  
HUDSON, R.P. and KAESER, R.S., Physics 3(1967)95.  
MESS, K.W., LUBBERS, J., NIESEN, L. and HUIKAMP, W.J., to be published in Physica.

### Samenvatting

Dit proefschrift beschrijft een onderzoek aan magnetische fase-overgangen in ionische kristallen. Gezien van theoretisch standpunt behoren ionische kristallen tot de relatief eenvoudige materialen a) daar de wisselwerking plaatsvindt tussen *gelokaliseerde* spins, in tegenstelling tot die tussen elektronen in een metaal of tot die tussen molekulen in een overgang tussen de vloeibare en gasvormige fase, en b) daar in die kristallen, waarin de wisselwerking voornamelijk van het "exchange" type is, deze in hoofdzaak plaatsvindt tussen *naasteburen*, waardoor de berekeningen aanzienlijk vereenvoudigd worden.

Gezien vanuit experimenteel standpunt zijn ionische kristallen aantrekkelijk voor het bestuderen van fase-overgangen, daar een groot aantal magnetische materialen kan worden gemaakt. Afhankelijk van de kristalstructuur kan de wisselwerking plaatsvinden of voornamelijk in ketens (refs. 1 en 2; hoofdstuk VI dysprosium ethylsulfaat), in een twee-dimensionale structuur (hoofdstuk III, 5.2,  $\text{CoCs}_3\text{Br}_5$ ; ref. 3), of in een drie-dimensionale structuur (talrijke voorbeelden, zie b.v. refs. 4 en 5;  $\text{CoCs}_3\text{Cl}_5$  in hoofdstuk III en b.v.  $\text{CuK}_2\text{Cl}_4 \cdot 2\text{H}_2\text{O}$  in hoofdstuk IV).

De experimenten zijn verricht in het temperatuurgebied rond 1 Kelvin. De thermische expansie effecten in dit temperatuurgebied zijn zeer klein vergeleken met de magnetische wisselwerking, zodat de magnetische fase-overgang in het algemeen niet gepaard gaat met een latente warmte. Een tweede voordeel is, dat de soortelijke warmte van het rooster zeer klein is ten opzichte van de soortelijke warmte van magnetische oorsprong, zodat slechts een kleine correctie op de gemeten totale soortelijke warmte behoeft te worden aangebracht. De experimentele opstelling wordt beschreven in hoofdstuk II.

In de laatste jaren zijn aanzienlijke vorderingen gemaakt in de theorie van fase-overgangen<sup>6,7</sup>). Voor een aantal thermodynamische eigenschappen van het Ising model met spin  $\frac{1}{2}$  zijn nauwkeurige numerieke resultaten verkregen zowel boven als beneden de kritische temperatuur (zie ook hoofdstuk I, 3.5). Voor het Heisenberg model zijn tot nu toe relatief weinig numerieke resultaten bereikt, daar de berekeningen moeilijker zijn. Voor de dipool-wisselwerking, die een lange dracht heeft, zijn zowel de theoretische als de experimentele resultaten schaars, zodat het veld van onderzoek nog open is.

In hoofdstuk I wordt een overzicht gegeven van fenomenologische en microscopische theoriën over fase-overgangen. In het bijzonder wordt de methode van analyse van eindige reeksen onder de loep genomen, die zijn afgeleid voor de susceptibiliteit en de soortelijke

warmte. Met een rekenprogramma gebaseerd op de analyse van deze reeksen met behulp van de "ratio" methode, zijn nieuwe resultaten in gesloten vorm verkregen, die de temperatuurafhankelijkheid van de beschouwde grootte beschrijven in het hele temperatuurgebied boven het kritische punt. Hiermee kunnen de experimentele resultaten op eenvoudige wijze worden vergeleken. Hoofdstuk I besluit met enkele beschouwingen over de afronding van de soortelijke-warmte curve, die in veel kristallen is waargenomen. Berekeningen gebaseerd op een eenvoudig model, waarin een Gaussische verdeling van overgangstemperaturen rond het kritische punt wordt aangenomen, tonen aan, dat de temperatuur waarbij de soortelijke-warmte curve het maximum bereikt, niet samenvalt met het kritische punt indien de soortelijke-warmte curve asymmetrisch is.

In hoofdstuk III worden de metingen geanalyseerd van de thermische eigenschappen van de kristallen  $\text{CoCs}_3\text{Cl}_5$  ( $T_N=0,527\text{K}$ ), and  $\text{CoCs}_3\text{Br}_5$  ( $T_N=0,282\text{K}$ ). Uit paramagnetische resonantiemetingen en calorische gegevens kan worden afgeleid dat  $\text{CoCs}_3\text{Cl}_5$  bij zeer lage temperaturen een goed voorbeeld is van een kubisch  $s=1/2$  Ising systeem. De piek in de soortelijke warmte wordt goed beschreven door een kubisch Ising model indien de kritische temperatuur gekozen wordt volgens de suggesties van hoofdstuk I. De eigenschappen van  $\text{CoCs}_3\text{Br}_5$  worden goed beschreven door een twee-dimensionaal Ising model. Karakteristieke trekken zijn de grote soortelijke warmte boven  $T_N$ , welke samenhangt met een aanzienlijke ordening op korte afstand, en een soortelijke warmte, die een logaritmische temperatuurafhankelijkheid vertoont bij het kritisch punt.

In hoofdstuk IV worden de soortelijke-warmte metingen beschreven van een tweetal isomorfe koperzouten, die een positieve "exchange" wisselwerking hebben, nl.  $\text{CuK}_2\text{Cl}_4 \cdot 2\text{H}_2\text{O}$  ( $T_c=0,88\text{K}$ ) en  $\text{Cu}(\text{NH}_4)_2\text{Br}_4 \cdot 2\text{H}_2\text{O}$  ( $T_c=1,74\text{K}$ ). Vroegere metingen aan het eerste zout hebben aangetoond dat het drie-dimensionale Heisenberg model met spin  $1/2$  van toepassing was. In dit hoofdstuk wordt aangetoond dat de calorische metingen aan  $\text{Cu}(\text{NH}_4)_2\text{Br}_4 \cdot 2\text{H}_2\text{O}$  goed beschreven worden door de spingolftheorie in het temperatuurgebied tot  $0,5T_c$ . Dit bevestigt de toepasbaarheid van het Heisenberg model met ruimtelijk gecentreerd kubisch rooster. Na het verschijnen van berekeningen voor de mate waarin de voorspellingen gemaakt voor een rooster met louter naaste-buur wisselwerking worden gewijzigd indien ook wisselwerking tussen tweede buren in aanmerking wordt genomen, werden de metingen opnieuw geanalyseerd. Voor een ruimtelijk gecentreerd kubisch rooster bedraagt de verhouding tussen tweede buur- en eerste buurkoppeling  $J_2/J_1 = +0,25 \pm 0,1$ , zodat de wisselwerking met de tweede

buren niet verwaarloosd mag worden. Van het zout  $\text{CuK}_2\text{Cl}_4 \cdot 2\text{H}_2\text{O}$  kon de piek in de soortelijke warmte worden gemeten tot  $|1 - T/T_c| = 10^{-3} T_c$ . De temperatuurafhankelijkheid aan beide zijden van de piek is logaritmisch en van gelijke amplitude.

In hoofdstuk V wordt de meting van de spontane magnetisatie besproken van de Heisenberg  $s=1/2$  ferromagneet  $\text{Cu}(\text{NH}_4)_2\text{Br}_4 \cdot 2\text{H}_2\text{O}$ . Resultaten zijn verkregen in het temperatuurgebied tussen  $0,05 T_c$  en  $0,997 T_c$ . Een kleine anisotropie energie werd gevonden, welke boven de kritische temperatuur nog niet tot nul is gereduceerd. Gezien de sterke spin-spin korrelatie wordt deze toegeschreven aan een kleine anisotropie term in de "exchange" koppeling tussen paren koperionen. De experimentele resultaten worden in het temperatuurgebied tot  $0,7 T_c$  goed beschreven met de spingolftheorie. Recente berekeningen met de Green's-functie methode stemmen met de meetresultaten overeen tot  $0,98 T_c$ . Dicht bij de kritische temperatuur,  $3 \cdot 10^{-3} < 1 - T/T_c < 10^{-1}$ , wordt de spontane magnetisatie beschreven door de relatie  $M(T)/M(0) = 1,33(1 - T/T_c)^{0,38}$ . De kritische isotherm wordt beschreven door  $H \sim M^\delta$ , waarbij  $\delta$  de lage waarde 3,9 heeft.

Tenslotte worden in hoofdstuk VI de soortelijke-warmte- en susceptibiliteitsmetingen besproken van drie zouten, waarbij de wisselwerking van dipolaire aard is. Gadoliniumsulfaat octohydraat  $\text{Gd}_2(\text{SO}_4)_3 \cdot 8\text{H}_2\text{O}$ , en gadoliniumtrichloride hexahydraat  $\text{GdCl}_3 \cdot 6\text{H}_2\text{O}$  worden antiferromagnetisch bij  $T_N = 0,182$  en  $0,185 \text{ K}$  respectievelijk. Dysprosium ethylsulfaat  $\text{Dy}(\text{C}_2\text{H}_5\text{SO}_4)_3 \cdot 9\text{H}_2\text{O}$  wordt ferromagnetisch bij  $T_c = 0,115 \text{ K}$ . De vrij grote soortelijke warmte van de gadoliniumzouten houdt verband met de bezettingstoename van de Kramers dubletten, die dicht bij elkaar liggen. Dysprosium ethylsulfaat gedraagt zich als een systeem van zwak gekoppelde lineaire ketens. In alle drie zouten zet de lange afstandsordening abrupt in, wat het best geïllustreerd wordt door de gadoliniumzouten. Opmerkelijk is verder het optreden van een rug in de soortelijke warmte curve juist boven de kritische temperatuur, welke beschreven kan worden door negatieve termen (in  $T^{-3}$  of in hogere orde van de inverse temperatuur) in de reeksontwikkeling van de soortelijke warmte bij hoge temperatuur.

Samenvattend kan de conclusie getrokken worden, dat de uitbreiding van de bekende technieken van calorimetrie en magnetisatiemeting naar temperaturen beneden 1 Kelvin, experimentele resultaten heeft opgeleverd, die direct kunnen worden vergeleken met numerieke resultaten van recent theoretisch onderzoek. Een dergelijke vergelijking is zinvol indien de magnetische materialen zorgvuldig gekozen worden met betrekking tot de toepasbaarheid van theoretische modellen voor de magnetische wisselwerking.

## Referenties

1. HASEDA, T., en MIEDEMA, A.R., *Physica* 27(1961)1102.
2. WITTEKOEK, S., Ac. proefschrift, Leiden, 1967.
3. BREED, D.J., *Physica* 37(1967)35.
4. KADANOFF, L.P., GÖTZE, W., HAMBLÉN, D., HECHT, R., LEWIS, E.A.S., PALCIAUSKAS, V.V., RAYL, M., SWIFT, J., ASPNES, D., en KANE, J., *Rev. Mod. Phys.*, 39(1967)395.
5. HELLER, P., *Rep. Progr. Phys.* 30, dl. II(1967)790.
6. DOMB, C., 'Magnetism' vol. IIA dl. I, uitg. RADO, G.T. en SUHL, H., Ac. Press New-York en Londen 1965.
7. FISHER, M.E., 'The theory of equilibrium critical phenomena', *Rep. Progr. Phys.* 30, dl. II(1967)615.
8. MIEDEMA, A.R., VAN KEMPEN, H., en HUISKAMP, W.J., *Physica* 29(1963) 1266; *Commun. of the Kamerlingh Onnes Lab.*, No. 336a.

### Curriculum vitae

Op verzoek van de faculteit der Wiskunde en Natuurwetenschappen volgt hier een overzicht van mijn studie.

Na het behalen van het Mulo-B diploma te Leeuwarden in 1955, heb ik de gymnasium afdeling gevolgd van het 2<sup>e</sup> Vrijzinnig-Christelijk-Lyceum te 's-Gravenhage. Het  $\beta$ -examen werd in 1958 afgelegd. De studie, voortgezet aan de Rijksuniversiteit te Leiden, resulteerde in 1961 in het behalen van het candidaatsexamen D' in de vakken natuurkunde, wiskunde en scheikunde. De tentamens voor theoretische natuurkunde en wiskunde werden afgelegd na het volgen van de colleges van de hoogleraren dr S.R. de Groot, dr P. Mazur, dr P.W. Kasteleijn, dr J.A.M. Cox en dr C. Visser.

In september 1963 trad ik toe tot de werkgroep adiabatistische demagnetisatie en kernfysica van het Kamerlingh Onnes Laboratorium, waarvan prof. dr C.J. Gorter de supervisie heeft, en de dagelijkse leiding berust bij dr W.J. Huiskamp. Prof. dr A.R. Miedema wijdde mij in in de experimentele technieken, en heeft tot januari 1965 op stimulerende wijze de experimenten geleid. Hierna werd ik in de gelegenheid gesteld het onderzoek voort te zetten. In mei 1965 legde ik het doctoraal examen gemengd theoretische- en experimentele natuurkunde af.

Sinds september 1964 heb ik een taak vervuld bij het natuurkundig praktikum. In januari 1965 verleende de stichting voor Fundamenteel Onderzoek der Materie, F.O.M., mij een kandidaats-assistentenschap in de werkgroep K IV, dat in juni werd omgezet in een medewerkerschap. Van eind 1964 tot december 1966 stonden drs. J.A. Roest en drs. H. W.J. Blöte mij terzijde bij de werkzaamheden, terwijl de heer R. Kuiken mij heeft geassisteerd in het eerste semester van 1967.

Garne wik ik besluiten met het vermelden van de vruchtbare discussies, die met prof. dr C.J. Gorter werden gevoerd, en zijn voortdurende belangstelling voor het onderzoek. Ook de stimulerende discussies en suggesties van dr W.J. Huiskamp over inhoud en vorm hebben veel bijgedragen tot het tot stand komen van dit proefschrift. Drs. C.A.W. Citteur ben ik erkentelijk voor het kritisch doorlezen van het eerste hoofdstuk. Door de collegiale medewerking van drs. K.W. Mess, drs. J.N. Haasbroek en drs. E. Lagendijk konden enkele bijzondere experimenten worden uitgevoerd. Met vrucht heb ik gebruik gemaakt van de diensten en faciliteiten voor de IBM 360-50 rekenmachine van het Rekencentrum van de Rijksuniversiteit te Leiden.

Door de goede verzorging van het technische en cryogene gedeelte van de apparatuur hebben de heren J. van Weesel, J. van der Waals en

T. Nieboer bijgedragen tot het welslagen van de experimenten. Het glastechnische gedeelte werd verzorgd door de heren C.J. van Klink en B. Kret, het elektronische gedeelte door de heer R. Hulstman. De tekeningen en het kaftontwerp werden gemaakt door de heer W.F. Tegelaar. Een groot gedeelte van het typewerk werd mij uit handen genomen door de administratieve staf.

Tenslotte wil ik mevrouw drs. F.E.M. Wielinga-Springer nog bedanken voor het corrigeren van de Engelse tekst.

